

SYNTHESIS AND SAR INVESTIGATION OF HAEMOZOIN-INHIBITING QUINAZOLINES ACTIVE AGAINST PLASMODIUM FALCIPARUM

The University of Cape Town

Department of Chemistry

August 2016



A dissertation submitted to the University of Cape Town in fulfilment for the degree of
Master of Science (M.Sc.)

by

Stefan Jason Benjamin

SUPERVISORS: Prof. T. J. Egan and Prof. R. Hunter

The copyright of this thesis vests in the author. No quotation from it or information derived from it is to be published without full acknowledgement of the source. The thesis is to be used for private study or non-commercial research purposes only.

Published by the University of Cape Town (UCT) in terms of the non-exclusive license granted to UCT by the author.

DECLARATION

SYNTHESIS AND SAR INVESTIGATION OF HAEMOZOIN- INHIBITING QUINAZOLINES ACTIVE AGAINST PLASMODIUM FALCIPARUM

I, Stefan Jason Benjamin, hereby declare the following:

1. That the above-titled thesis is my own work, both in concept and execution, apart from the normal guidance of my supervisors;
2. That in cases where others' work has been cited, this has been acknowledged and referenced;
3. That no part of this work has been, is being, or is to be submitted for another degree at this or any other university;
4. That I grant the University of Cape Town free license to reproduce this work, in whole or in part, for the purpose of research.

I hereby present this dissertation in fulfilment for the degree of Master of Science.

Stefan Jason Benjamin:

Signed by candidate

Witness:

Signature Removed

ABSTRACT

Malaria is a potentially fatal blood disease with most deaths caused by *Plasmodium falciparum*. It exists in 95 countries worldwide and puts nearly 3.2 billion people at risk of contracting the disease. Despite recent advances made in malaria eradication and control including by antimalarial drugs (the mainstay of malaria prophylaxis and disease treatment), the need for new antimalarials due to antimalarial drug resistance which is on the rise, means that malaria research remains an extremely important focus.

In this study, 21 derivatives of a biologically relevant scaffold, 2,4-diaminoquinazoline, based on hits found by high-throughput screening were rationally designed and synthesised using a three-step procedure. This involved chlorination of benzoylene urea (**1**), followed by two successive nucleophilic aromatic substitution reactions. The derivatives were purified by conventional methods before being fully characterised by NMR, HRMS and IR spectroscopy. The derivatives were then tested *in vitro* for β -haematin inhibition (β HI) using a NP-40 based assay and for aqueous solubility using turbidometry. The compounds were also tested for biological antimalarial activities in chloroquine sensitive (NF54) and chloroquine resistant (DD2) parasites. Cytotoxicity was tested in Chinese Hamster Ovarian cells.

Of the 21 synthesised quinazoline derivatives 15 were active with IC_{50} values below 1500 μ M for β HI and of the 15, ten compounds were similarly active with IC_{50} s below 1500 nM for antiplasmodial activity. Three compounds, **13** (NF54), **15** (NF54) and **10** (DD2) possessed potent activity below 120 nM against the indicated *Plasmodium* strains. Resistance and selectivity indices indicated that 2,4-diaminoquinazolines were not cross-resistant with chloroquine (CQ) and possess selective activity against *P. falciparum*. On the negative side, they possessed poor aqueous solubility, with the majority in the ranges 5-40 μ M. In terms of structure-activity relationships (SARs), the analysis showed that 2,4 substitutions to the

quinazoline scaffold in the forms of linear alkyl, secondary and less rigid amine groups, appear to diminish or even abolish activity, whereas substituents such as bulkier aromatics and cyclic alkyl groups, activated or inactivated π systems and combinations thereof, improve activity.

The results have shown that the 2,4-diaminoquinazoline scaffold exerts their activity in the form of haemozoin inhibition, decreasing haemozoin levels as well as increasing free haem in the malaria parasite at the IC_{50} , much like well-established β HI antimalarial, CQ. Furthermore, the quinazoline scaffold studied has shown excellent potential and scope for optimisation.

For Vincent and Avril Benjamin

ACKNOWLEDGEMENTS

A word of acknowledgement to those who have mentored, assisted and supported me throughout this journey of completing my Masters research and dissertation.

Prof. Timothy Egan – Thank you for giving me the opportunity to have been a part of your research group for the last few years, I am truly grateful for the mentoring and level of support you have provided me. I have enjoyed your passionate approach to teaching as well as your profound leadership ability.

Prof. Roger Hunter – I am without a doubt a better organic chemist than I was previously, thanks to your extensive and meaningful teaching style. You have certainly assisted in my improved ability to rationally think and apply myself in the laboratory.

The Haem Team and Hunter Group – Thank you for the stimulating working environments and the provided assistance in completing my research project.

Pete Roberts and the pharmacology unit and Medical School for NMR services and *in vitro* (antiplasmodial and cytotoxicity) testing respectively.

I am sincerely privileged to have the never-ending support of my family and friends. In particular, my parents, without whom I would never be where I am today. Thank you for giving me a solid platform from which I had the opportunity to complete my Masters. To Kim Jacobs and Matthew Williams, for your unfailing support, encouragement, companionship and much needed laughs, I say thank you.

National Institute of Allergy and Infectious Disease of the National Institutes of Health (R01AI110329) and the National Research Foundation (NRF) for funding the project.

ABBREVIATIONS

δ	chemical shift
ACT	artemisinin-based combination therapy
Ar	aromatic
AQ	amodiaquine
β HI	β -haematin inhibition
conc.	concentrated
CQ	chloroquine
CQR	chloroquine resistant
CQS	chloroquine sensitive
DCM	dichloromethane
d	doublet
ddd	doublet of doublet of doublets
DMSO	dimethylsulfoxide
DNA	deoxyribonucleic acid
ERG	electron releasing group
ESI	electron spray ionisation
EWG	electron withdrawing group
eq	equivalent
Fe(II)PPIX	ferrousprotoporphyrin IX / Haem
Fe(III)PPIX	ferriprotoporphyrin / Haematin
FV	food vacuole
Hb	haemoglobin
HDP	haem detoxification protein
HO-/H ₂ O-Fe(III)PPIX	aqua-ferriprotoporphyrin IX / Haematin
HPLC	high-performance liquid chromatography
HRP	histidine rich protein
HRMS	high resolution mass spectrometry
HTS	high throughput screening
HZ	haemozoin

ABBREVIATIONS

IC ₅₀	half maximal inhibitory concentration
IR	infrared
<i>J</i>	coupling constant
m	multiplet
<i>m/z</i>	mass/charge ratio
M.p.	melting point
NP-40	4-nonylphenyl-polyethylene glycol-40
<i>PfCRT</i>	<i>Plasmodium falciparum</i> chloroquine resistant transporter
<i>PfPgh1</i>	<i>Plasmodium falciparum</i> P-glycoprotein homologue 1
<i>PfPI3K</i>	<i>Plasmodium falciparum</i> phosphatidylinositol-3-kinases
<i>PfI</i>	<i>Plasmodium falciparum</i> inhibition
q	quartet
<i>R_f</i>	retention factor
RBC	red blood cell
s	singlet
SARs	structure-activity relationships
S _N Ar	nucleophilic aromatic substitution
TEM	transmission electron micrograph
THF	tetrahydrofuran
t	triplet
td	triplet of doublets
TLC	thin layer chromatography
VDW	van der Waals
UV	ultraviolet
WHO	World Health Organisation

TABLE OF CONTENTS

Declaration	i
Abstract	ii
Dedication	iv
Acknowledgements	v
Abbreviations	vi
Table of Contents	viii
Chapter 1 Introduction to Malaria	1-26
1.1 The history and global occurrence of malaria	2
1.2 <i>Plasmodium</i> , the parasitic protozoan	3
1.3 The life cycle of the parasite	4
1.4 Antimalarial drugs	5
1.5 Haem detoxification pathway by the <i>Plasmodium</i> spp.	8
1.6 Haemozoin formation	9
1.7 Inhibition of haemozoin formation by antimalarials	12
1.8 Antimalarial drug resistance	17
1.9 New scaffolds for malaria studies	19
1.9.1 High throughput screening (HTS)	20
1.10 Quinazoline – a pharmacologically relevant compound class	23
1.10.1 Retrosynthesis of 2,4-diaminoquinazoline	25
1.11 Aims and objectives	25
1.11.1 Aims	25
1.11.2 Objectives	26

Chapter 2	Synthesis of Quinazoline Derivatives	27-47
2.1	Synthesis of 2,4-dichloroquinazoline (2)	28
2.1.1	A proposed mechanism of formation of 2,4-dichloroquinazoline (2)	32
2.2	Synthesis of 2-chloroquinazoline-4-amine intermediates (3-8)	33
2.2.1	A proposed mechanism of formation and a proof of regioselectivity for the intermediates (3-8)	38
2.3	The synthesis of 2,4-diaminoquinazoline target compounds (9-22)	40
Chapter 3	Synthesis Rationalisation & Structure-Activity Relationships	48-59
3.1	Sub-structure activity study based on the parent compound (10)	49
3.2	Sub-structure activity study based on compound 13	51
3.3	β -haematin inhibition and comparison with antiplasmodial test results	54
3.4	Additional <i>in vitro</i> test results	56
3.5	Structure-activity relationships summary	58
Chapter 4	Conclusions and Future Work	60-64
4.1	Conclusions	61
4.2	Future work	62
Chapter 5	Experimental Methods	65-92
5.1	Physiochemical methods	66
5.1.1	β -haematin formation assay	66
5.1.2	Antimalarial assay	66

5.1.3	Cytotoxicity assay	67
5.1.4	Turbidometric assay	68
5.2	Synthesis	68
5.2.1	General	68
5.2.2	Precursor synthesis (2)	70
5.2.3	General Procedure for the synthesis of 2-chloro-quinazolin-4-amine intermediates (3-8)	71
5.2.4	General Procedure for the synthesis of 2,4-diaminoquinazoline final derivatives (9-22)	78
References		93-97
Supplementary Data (Appendix A)		98-100

CHAPTER 1

Introduction to Malaria

Stefan J. Benjamin

M.Sc. Dissertation

This chapter gives a brief overview of malaria, its historical background, global occurrence and pathology. It then discusses the relevant organism, *Plasmodium*, taking a brief look at the various stages of the life cycle. After which it focuses on the blood stage of the life cycle by discussing known blood stage inhibiting antimalarials, haemoglobin degradation by the parasite and haemozoin formation and inhibition of haemozoin by antimalarials. The concluding part of this chapter delves into antimalarial drug resistance, identification of new haemozoin inhibiting scaffolds for antimalarials and the scaffold of interest for this project, quinazoline. Finally, the aims and objectives of the project are discussed.

1.1 The history and global occurrence of malaria

The symptoms of malaria have been around for thousands of years. They were reported in ancient Chinese medical writings, *Nei Ching* (The Canon of Medicine), in 2700BC, in Egypt 3500–4000 years ago and Ancient Greece in 400BC.¹ While these reports well-documented the symptoms known today as malaria, it was only thousands of years later in 1880 that the malaria parasite was first identified by a French surgeon, Charles Louis Alphonse Laveran, in the blood of a soldier who suffered from the disease.² Seventeen years later a British officer in the Indian Medical Service, named Ronald Ross, first demonstrated that malaria parasites could be transmitted from infected patients to mosquitoes. Ross also later showed that mosquitoes could transmit malaria parasites from bird to bird.²

Until today, the scourge of malaria continues to wreak havoc across the globe. According to the World Health Organisation (WHO) in 2015, malaria had ongoing transmission in 95 countries, which put approximately 3.2 billion people at risk of contracting the blood disease. In 2015 malaria claimed the lives of an estimated 438 000 people, approximately 90% of these deaths occurring on the continent of Africa (Figure 1.1).³



Figure 1.1: Malaria distribution (dark grey regions) across the world.³

Although the facts are undeniably devastating, the WHO has documented a decrease in malaria incidence rates globally and within Africa (37% and 42% respectively), between the years 2000 and 2015. During the same time period, mortality rates diminished by 60% globally and by 66% within Africa. Currently in an effort to improve upon this situation, the WHO has developed the *Global Technical Strategy for Malaria 2016-2030* to address remaining challenges in global malaria control and elimination, by strategically providing a technical framework for all endemic countries as they work towards control and elimination.⁴ It should be noted that though the WHO has documented a decrease in Malaria, it still however remains a major concern.

1.2 *Plasmodium*, the parasitic protozoan

Due to the early breakthrough discoveries in the 19th century, malaria is now well understood to be an acute febrile blood disease. It is caused by a parasitic protozoan from the genus

Plasmodium, which is passed onto human beings by the initial host and transmission vector, the female *Anopheles* mosquito.^{4,5} There are approximately 200 known *Plasmodium* species, five of which cause malaria in humans and of the five, two species namely, *Plasmodium falciparum* and *Plasmodium vivax*, account for nearly 80% of malaria infections and deaths worldwide.^{6,7} *Plasmodium* is exclusively an obligate intracellular parasite that grows and replicates only within the host cells such as red blood and liver cells respectively, shown below.^{8,9}

1.3 The life cycle of the parasite

The parasite has a complex life cycle, illustrated in Figure 1.2, consisting of three stages, but symptoms of malaria only become obvious in the blood stage.¹⁰

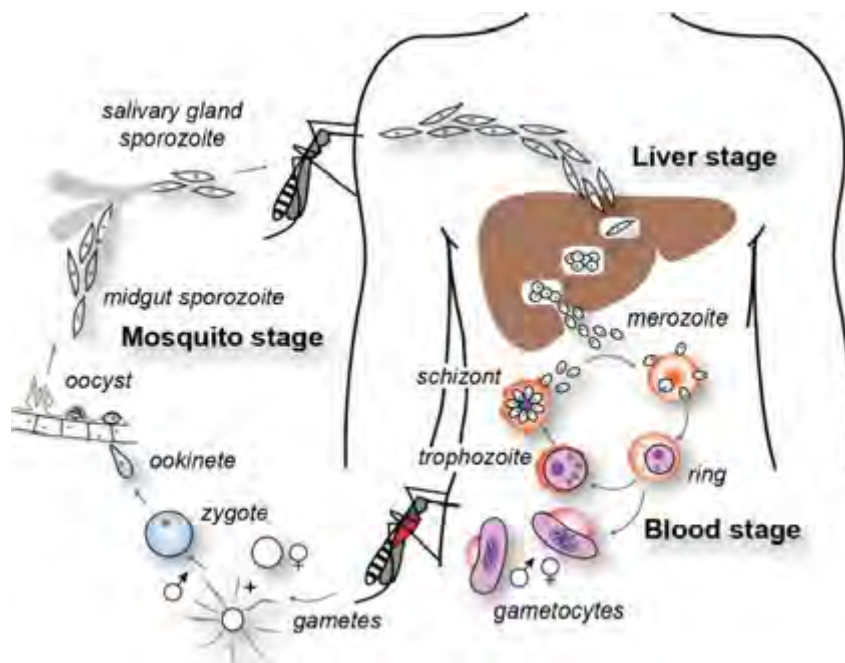


Figure 1.2: The life cycle of the malaria *Plasmodium* parasite. Copyright © 2012 Cowman *et al.*¹⁰

The infectious form of *Plasmodium* (sporozoites), which are located in infected female *Anopheles* mosquito's salivary glands, gains access to the human bloodstream while the mosquito feeds on the human host's blood, initiating human infection. The sporozoites immediately invade the liver of the host where asexual cell division occurs for approximately 14 days, which produces the haploid form of *Plasmodium* named merozoites (liver stage).

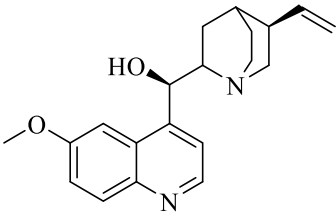
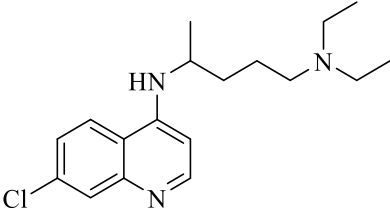
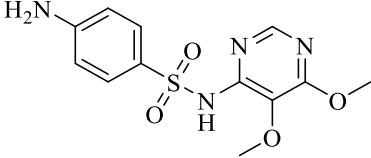
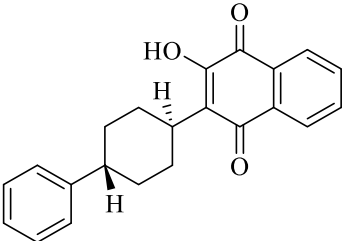
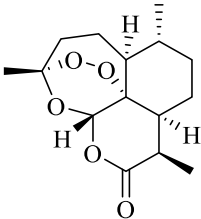
Upon lysis of the hepatocytes (liver cells), these haploid cells are released once more into the bloodstream of the host where red blood cell (RBC) invasion and infection occurs. During the asexual blood stage, the parasite undergoes a two-day cycle of morphological changes which include merozoite, ring, trophozoite and schizont stages.¹¹ Not all of the merozoites reproduce asexually but some further develop into female and male forms of the parasite called gametocytes. After the infected host is bitten by another mosquito, the mosquito ingests the gametocytes which undergo sexual reproduction within the mosquito to produce oocysts. These oocysts lyse and release sporozoites which migrate to the salivary glands, completing the parasitic life cycle.^{12,13}

While vector controls such as insecticide-treated mosquito nets and indoor residual spraying are effective measures for reducing the spread of parasites, alone they are not enough to prevent malaria. The backbone of malaria prophylaxis and disease treatment is through the use of antimalarial drugs.⁴

1.4 Antimalarial drugs

Currently, there are a broad variety of commercially available antimalarial drugs that act on different stages of the parasite life cycle; however, the majority of these drugs are active in the blood stage. The antimalarials are grouped into specific classes based on their molecular structures and modes of action. Table 1.1 summarises the classes of the most widely used blood stage inhibitors, giving an example of a commercially available antimalarial for each class.¹⁴

Table 1.1: Classes and examples of well-known blood stage inhibiting antimalarials

Class	Antimalarial
Aryl methanols	 <p>Quinine</p>
4-Aminoquinolines	 <p>Chloroquine</p>
Folate antagonists	 <p>Sulfadoxine</p>
Naphthoquinones	 <p>Atovaquone</p>
Endoperoxides	 <p>Artemisinin</p>

The mechanisms of malarial inhibition by a number of the blood stage acting drugs are not fully understood. Their actions, however, have been extensively studied and it is postulated

that many exert activity by means of either inhibition of nucleic acid synthesis, induction of oxidative stress or inhibition of the haem detoxification pathway.

The folate antagonist sulfadoxine is a nucleic acid synthesis inhibitor. It has been shown to disrupt dihydropteroate synthase, thus preventing the formation of dihydropteroate which is a critical molecule for the biosynthesis of folate, which in turn is essential for the biosynthesis of deoxyribonucleic acid (DNA). Like sulfadoxine, atovaquone also interrupts DNA biosynthesis by inhibiting the function of dihydroorotate dehydrogenase, via inhibition of cytochrome b_6 an enzyme used in electron transport, which consequently halts pyrimidine synthesis and hence DNA formation.^{14,15,16}

The mechanism of action is much less well understood for the endoperoxide, artemisinin. A prevailing hypothesis however, is that the antimalarial exerts activity in the form of radical activation of haem, Fe(II)PPIX, due to homolytic cleavage of the peroxide-bridge. The formation of highly energetic radical species may disrupt membrane function and the overall integrity of the parasite. Other theories relate to the ability of the compound to alkylate particular protein targets by primarily forming an epoxide at the peroxide bridge, supported by epoxides being well-known alkylating agents.^{14,15,16,17}

The majority of antimalarial drugs form part of the aryl methanol and 4-aminoquinoline drug classes which are known to act mainly on the haem disposal pathway of the parasite. These compounds inhibit the removal of toxic haem produced as a by-product of haemoglobin degradation by the parasite (discussed in section 1.5).^{14,15,16} The understanding of exactly how toxic haem species kill the parasite is still under scrutiny; however, there are two prevailing theories: (i) it produces reactive oxygen species, increasing oxidative stress which oxidises proteins and lipids and, (ii) due to its lipophilic nature it destabilises membranes making them more permeable.¹⁸

Of the classes of antimalarial drugs discussed, the last has historically been of most interest, since the majority of blood stage inhibiting drugs are understood to exert their potency in this fashion (inhibition of haem disposal). Therefore, in order to better understand the effects of these compounds in the blood stage, a closer look at the RBC is necessary.

1.5 Haem detoxification pathway by the *Plasmodium* spp.

Haemoglobin (Hb) is an iron (Fe)-containing metalloprotein in RBCs which is mostly used to carry oxygen from the lungs to tissues.¹⁹ However for human beings infected with *Plasmodium*, Hb now also becomes essential for parasite survival, with roughly 60 to 80% of the Hb in an infected RBC being consumed within the acidic food vacuole (FV) of *Plasmodium* - for nutritional purposes and to free up space in the RBC for the parasite to grow and hide from the host immune system.²⁰

Depending on the phase within the blood stage, the parasite will either engulf Hb, or have it transported by endocytotic vesicles into the specialised acidic compartment, the FV. Inside the FV, the parasite secretes various digestive enzymes, namely the metalloprotease facilysin, histo-aspartic protease, aspartic proteases plasmepsin I, II and IV, and cysteine proteases falcipain 1, 2 and 3. These enzymes facilitate the proteolysis of the globin portion of Hb into peptides which are later hydrolysed to amino acids for parasite consumption.^{21,22} Upon the degradation of Hb, however, the haem or ferrousprotoporphyrin IX (Fe(II)PPIX) prosthetic group is released as a by-product. It is spontaneously oxidised in the aqueous acidic oxygen-rich environment of the FV into haematin, also called aqua-ferriprotoporphyrin IX (HO-/H₂O-Fe(III)PPIX) or Fe(III)PPIX for short (Figure 1.4).^{20,23,24,25} Haematin represents a major danger to the parasite because it is lipid soluble and is capable of affecting membrane destruction by catalysing Fenton and Haber-Weiss reactions.¹⁸ This produces free radicals which increase oxidative stress in the parasite, evidently leading to its demise. So in what appears to be a

detoxification mechanism, *Plasmodium* very effectively sequesters approximately 95% of the Fe(III)PPIX by-product into a microcrystalline form of Fe(III)haem termed haemozoin (HZ), which is less toxic and is insoluble.^{18,23} An illustration of this process is shown in Figure 1.3.²⁰

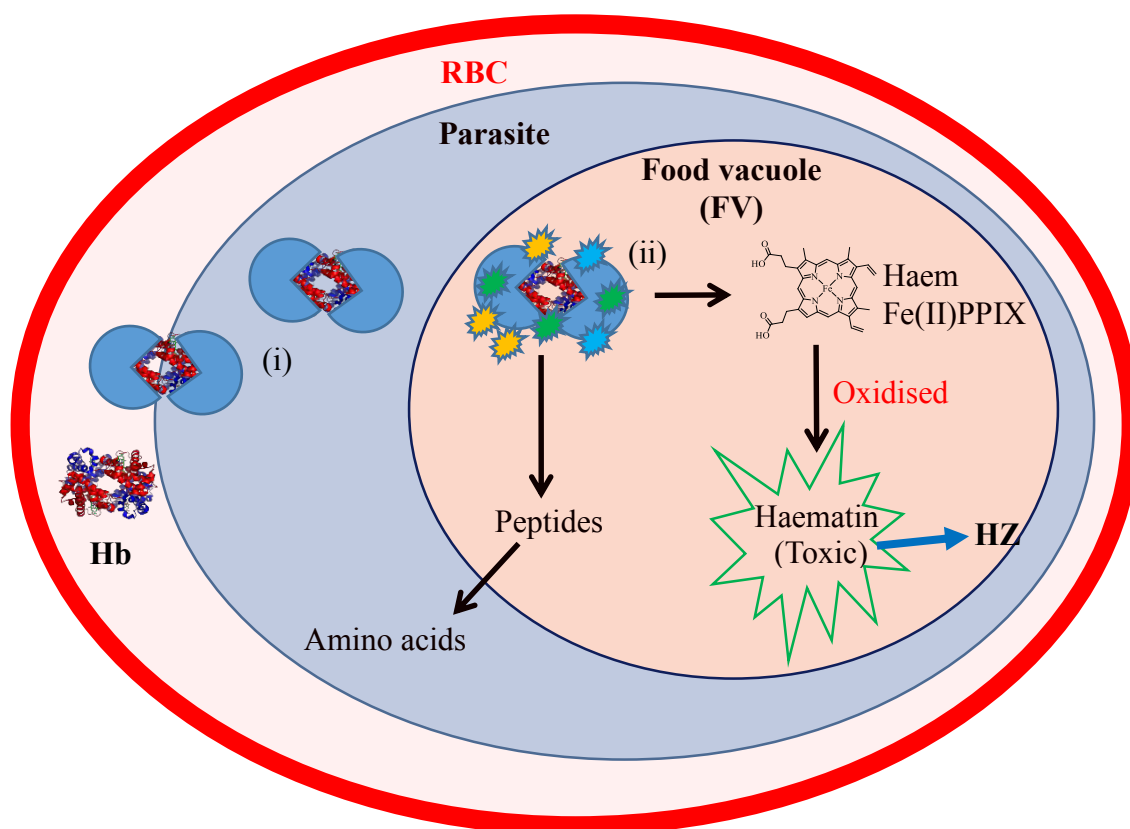


Figure 1.3: A summary of Hb degradation by the malaria parasite. (i) Endocytotic vesicle transportation of Hb into the acid food vacuole (FV). (ii) Proteolysis of Hb by digestive enzymes produces Fe(II)PPIX which is rapidly oxidised to HO-/H₂O-Fe(III)PPIX. (iii) Detoxification of HO-/H₂O-Fe(III)PPIX into haemozoin (HZ)²⁰

It is this process of HZ formation that aryl methanol and 4-aminoquinoline drugs target, which is discussed next.

1.6 Haemozoin formation

HZ (also referred to as malaria pigment) is an intracellular microcrystalline insoluble form of Fe(III)PPIX. It is made by the parasite to avert the toxic and damaging effects of haematin, discussed in subsection 1.5. It is well-known that approximately 5-10% of haematin is

detoxified within the parasite by neutralisation with histidine-rich proteins and degradation using reduced glutathione; however, approximately 90-95% of haematin has been shown to be sequestered into HZ by the *Plasmodium* species. HZ is formed by a unique reciprocal iron-oxygen coordinate bond, which links the central iron atom of haematin to the oxygen of the propionate moiety of an adjacent haematin molecule. Crystallisation is facilitated by π -stacking between porphyrin rings and hydrogen bonding between free propionic acid moieties, Figure 1.4.²⁶ In terms of external crystal morphology, they differ from organism to organism; however, usually taking the form of general rod-like shape with sizes within the range of 300 nm to 1 μm (Figure 1.4).²⁶

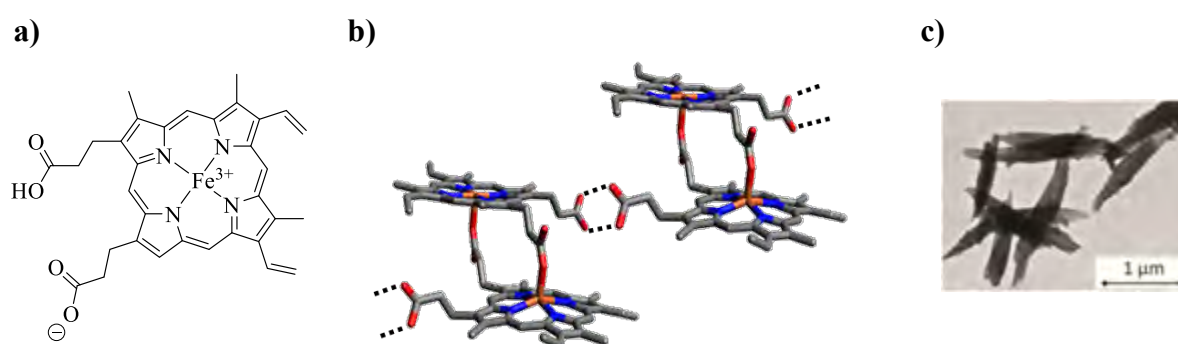


Figure 1.4: (a) The structure of haematin (Fe(III)PPIX) without axial water ligands, illustrating the propionate side chains. (b) A structure of HZ, indicating the iron-oxygen coordinate bond and H-bonding. (c) Transmission electron microscope image of synthetic HZ Copyright © 2013 Butykai *et al.*²⁶

The exact mechanism by which haematin is modified into less toxic HZ in order to avoid membrane lysis, lipid peroxidation and parasite death, is still incompletely understood. Initially haematin was believed to be detoxified into HZ completely by histidine-rich proteins (HRPs); however, it has since been shown that *Plasmodium* laboratory mutants lacking HRP I and II, could still effectively form HZ.²⁷ Now it is understood that there are species that actually lack orthologues to HRPs but still are capable of HZ formation. This brought about additional studies that led to the discovery of a potent haem detoxification protein (HDP) found in

P.falciparum (PfHDP) by Jani *et al.*²⁸ The group showed that the parasite secretes HDP into the cytosol of the infected RBC and subsequent endocytosis of the cytosol transports HDP to the FV, where it was shown that HDP is several times more effective in HZ formation than HRPs. Furthermore, recent studies by Chugh *et al.* and Nakatani *et al.* have indicated that within the FV HDP is functionally coupled with falcipain II and other proteases, and that HDP contains two identical haem binding sites which suggests that HDP may bind haem in a ratio of 2:1 (haem:HDP).^{29,30} HDP binding sites contain histidine residues and it has been shown that four of the nine residues of HDP are crucial for its function. Hist122 has been postulated to axially bind haem while Hist172 and Hist175 sit in the binding site and facilitate binding by correctly aligning both species.^{31,32} This has become a crucial factor in understanding HZ formation.

Alternatively, other experiments strongly support the hypotheses that HZ formation is lipid-driven as suggested by evidence shown of lipid bodies and phospholipid membranes in close proximity with HZ within the acidic food vacuole.^{27,33,34} Other evidence, has shown that lipids promote the formation of β -haematin (synthetic HZ), which is the synthetic, structural and chemical equivalent of HZ.^{33,35,36} Another particularly interesting result has shown that amphiphilic detergent molecules which spontaneously form micelles are capable of mediating β -haematin formation. Recently Sandlin and co-workers, have shown that multiple detergents such as Tween, NP-40, SDS, CHAPS and Triton promote β -haematin formation, albeit with different efficiencies. The detergent's ability to swiftly sequester haematin into the lipophilic core, allowing for crystal nucleation to occur, depends on the hydrophilic detergent chain size and length.³⁷ This result links to research which has shown that synthetic neutral lipid droplets and phospholipids have the ability to form emulsions that facilitate HZ formation.

The mechanism of HZ formation is still under debate. Furthermore, not only is it important in malaria studies, but HZ over the last several years has been discovered in numerous blood-

feeding organisms such as *Echinostoma trivolvis*, *Rhodnius prolixus*, *Haemoproteus columbae* and *Schistosoma mansoni*, which increases its relevance.³⁵

1.7 Inhibition of haemozoin formation by antimalarials

Cohen *et al.* and Macomber *et al.* suggested that haem was the target of antimalarials as early as the 1960s and since then one of the main aspects that has been studied has been drug-haematin (Fe(III)PPIX) interactions.^{38,39} Studies have now shown that some of the most well-known and highly active antimalarials (aryl methanols and 4-aminoquinolines) are understood to exert their activity by inhibiting the formation of HZ. These derivatives are of particular interest since some are partner drugs in artemisinin combination therapy (ACT). Furthermore new scaffolds that act in similar ways might not only lead directly to new drugs, but also help us to understand more about the mechanisms of inhibition, which if revealed might lead to major advances being made in the development of new drugs.^{14,35}

Egan *et al.* have shown using UV-visible spectroscopic titrations that the quinoline drugs associate with Fe(III)PPIX in 40-80% aqueous dimethyl sulfoxide (DMSO).^{40,41} Using chloroquine (CQ), quinine (QN), quinidine (QD), amodiaquine (AQ) and 9-epiquinine they were able to determine association constants ($\log K$) ranging from 4.00 – 5.50. UV-visible spectroscopic studies utilised the hypochromic effect for the Soret band of Fe(III)PPIX upon binding of antimalarial drugs to determine drug-Fe(III)PPIX association constants and stoichiometries. Further supporting evidence by Egan *et al.* showed the *in vitro* inhibition of β -haematin formation by the quinoline antimalarials, using a β -haematin inhibition (β HI) test assay. Both of the experiments demonstrated drug-Fe(III)PPIX interactions.⁴²

In 2008, the evidence of drug-Fe(III)PPIX interactions were reinforced by the determination of the first ever example of an X-ray crystal structure of Fe(III)PPIX with an antimalarial drug, shown by de Villiers *et al.* The group presented the halofantrine-Fe(III)PPIX X-ray crystal

structure, showing the deprotonated hydroxyl group of halofantrine coordinated to the iron centre of Fe(III)PPIX, while other π -stacking interactions were shown between the Fe(III)PPIX porphyrin ring and halofantrine aromatic system.^{43,44} Four years later, de Villiers *et al.*, determined additional X-ray crystal structures of QN and QD coordinated to Fe(III)PPIX (Figure 1.5).^{44,45}

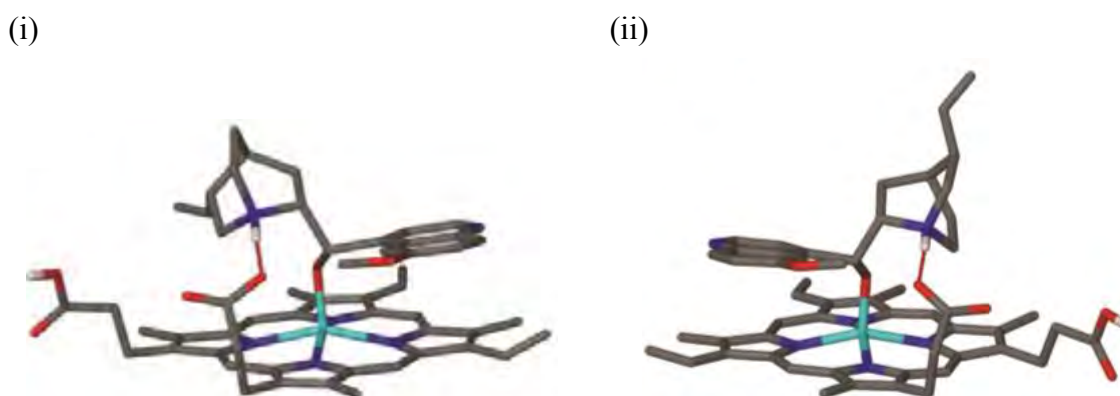


Figure 1.5: X-ray crystal structures of Fe(III)PPIX-antimalarial complexes. i) quinidine-Fe(III)PPIX and ii) quinine-Fe(III)PPIX. Copyright © 2012 K. A. de Villiers *et al.*⁴⁵

This work showed that a five coordinate complex formed involving the benzylic alkoxide of the compound and the iron core of Fe(III)PPIX, with π -stacking seen between the porphyrin system of Fe(III)PPIX and the quinoline moiety of each antimalarial.^{44,45}

While the evidence presented showed that quinoline and aryl methanol antimalarials interact with haem, the mechanism of inhibition of HZ is still under investigation. It has been speculated that the formation of a drug-Fe(III)PPIX complex prevents or delays the crystallisation of HZ.

Research investigations have also shown that CQ forms complexes with both monomeric Fe(III)PPIX and μ -oxo dimeric Fe(III)PPIX, and various conditions have been shown to influence dimerisation including pH, CQ concentration and lipids. Two models have been proposed for π - π complexes of CQ with the μ -oxo dimer (Fe-O-Fe bridge) Fe(III)PPIX species

(Figure 1.6). Model (ii) also postulates involvement of hydrogen bonding interactions between the protonated quinoline nitrogen atoms and μ -oxo bridge between the iron centres. While formation of the monomeric Fe(III)PPIX species is favoured at low pH and in 40% DMSO, CQ has been shown to shift the monomer-dimer equilibrium in favour of the dimer to produce equilibrium ratios of approximately 1:50 (monomer:dimer).⁴⁶

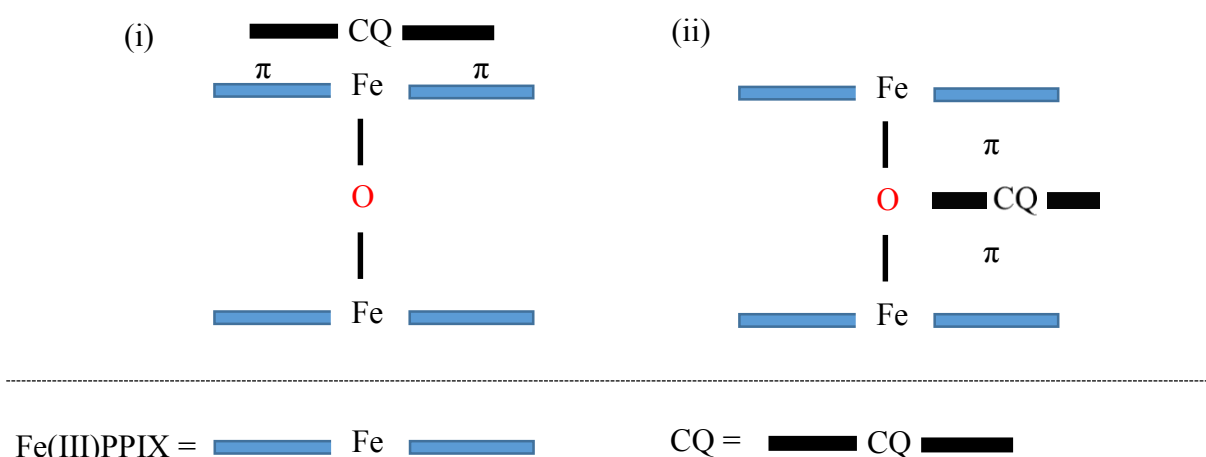


Figure 1.6: Two possible π - π interactions between CQ and the μ -oxo dimer of Fe(III)PPIX

Similarly early evidence have shown the significant complexation between QN and Fe(III)PPIX that acts differently to CQ-Fe(III)PPIX. Gorka *et al.* used magnetic susceptibility measurements to show that QN interacts predominantly with monomeric Fe(III)PPIX (through QN's oxygen atom of the hydroxyl group) and that the equilibrium shifts from the dimeric species to the monomeric, which was linked to antiparasmodial activity.^{46,47} The group conducted a structure activity series showing the importance of the hydroxyl group, rigid ring system and aliphatic nitrogen on the ability of QN to form monomeric complex species. Upon the removal of these structural features QN lost its ability to complex Fe(III)PPIX and as a result lost antiparasmodial activity.⁴⁷

Although the formation of drug-haematin complexes has not been directly shown to be responsible for HZ inhibition, their formation has lent support to the proposal that 4-aminoquinoline, aryl methanols and other antimalarials act by inhibiting HZ formation. An alternative hypothesis is that they inhibit the fastest-growing face of the HZ crystal. Which has recently become and currently is the favoured idea, which is discussed next.

In 2008, Weissbuch and Leiserowits described various types of antimalarials, such as quinolines, phenanthrene derivatives, and diethylaminoalkoxyxanthenes as HZ crystal capping agents and showed evidence of their capability to bind stereo-specifically to certain faces (001; 011; 100) of the crystal, subsequently inhibiting HZ formation and thus the growth of the parasite. An example of an inhibitor binding to the crystal is illustrated in Figure 1.7.⁴⁸

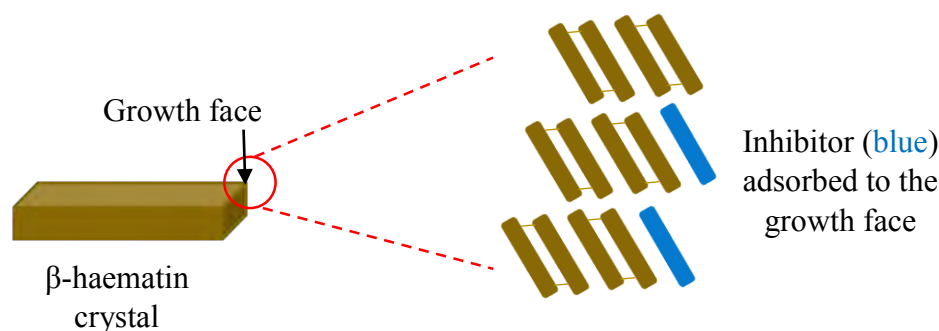


Figure 1.7: An illustration of how HZ inhibitors dock on a particular growing face of HZ.⁴⁹

In support of Weissbuch and Leiserowits' findings, Gildenhuis *et al.* investigated kinetic effects of CQ and QD on the formation of β -haematin using the Avrami equation and employing biomimetic lipid–water emulsion conditions. The decreased rate of β -haematin formation observed at low concentrations of both drugs was accounted for by supposing a mode of drug adsorption to sites on the fastest-growing face of β -haematin.⁴⁹

More recently, Olafson *et al.* used *in situ* atomic force microscopy to show that β -haematin crystallisation follows a classical mechanism in which layers are produced by 2-dimensional nucleation and growth from haematin in solution. Subsequently, four distinct classes of crystal

surface sites were identified (Figure 1.8) that are crucial for crystal growth (dimensional growth indicated in Figure 1.8 a) but could be blocked (c), demonstrated by the adsorption of CQ onto the surface, therefore slowing down the process of haem detoxification. CQ was shown to adsorb on the (100) face between the growth steps of the crystal (Figure 1.8).⁵⁰

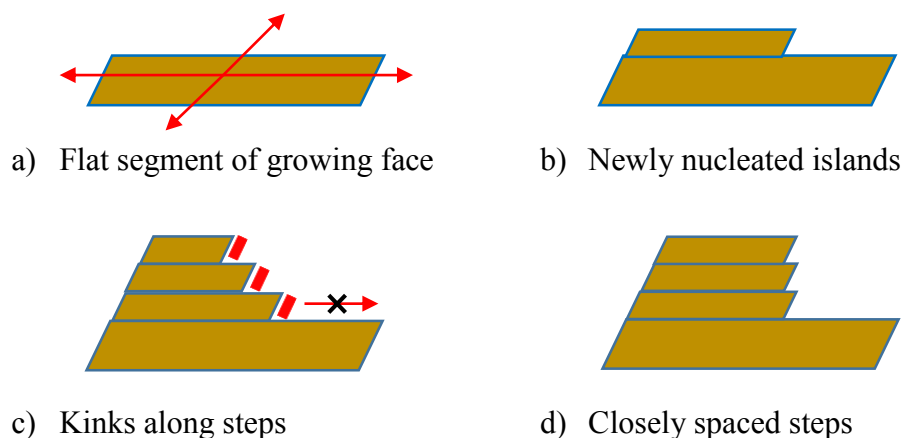


Figure 1.8: An illustration of the four distinct classes of HZ surface sites. c) Shows the inhibition of crystal nucleation and growth by an inhibitor (red).⁵⁰

In addition, the use of molecular docking simulations by Correa de Sousa *et al.*, using Molegro Virtual Docker (MVD) (version 2011.5.0), supplied further evidence of the ability of several AQ analogues to dock onto the HZ crystal.⁵¹ The group showed a relationship between binding strength and rotational freedom, demonstrating compounds with greater conformational freedom have a greater entropy loss upon binding, and therefore bind weakly.⁵²

These recent investigations indicate a paradigm shift towards drug-crystal docking as a favoured mode in the understanding of HZ inhibition. Understanding the details of the HZ inhibition mechanisms of antimalarials and of diverse new HZ-inhibiting scaffolds may thus lead to new antimalarial developments. This remains important given the documented reports over the last few decades concerning the worldwide rise in antimalarial drug resistance by *Plasmodium*, not only to quinoline and aryl methanol derivatives, but also recently to the potent

artemisinin derivatives. Resistance does not however appear to involve a change to the HZ formation target, thus this mechanism of action is still of relevance.

1.8 Antimalarial drug resistance

In 1967, the WHO defined drug resistance as, *“the ability of the parasite strain to survive or multiply despite the administration and absorption of a drug given in doses equal to or higher than those usually recommended but within the tolerance of the subject...”*.

The appearance of antimalarial drug resistance has been a major obstacle in the global control and elimination of malaria.

The 4-aminoquinoline, CQ, first made in the 1930s, became the most widely used antimalarial during the 1960s and 1970s, but today is not of clinical relevance due to CQ resistance by the parasite. CQ resistance was first seen in Thailand in 1957; it then spread through Southeast Asia and by the 1970s was being detected in Sub-Saharan Africa and South America. New antimalarials such as sulfadoxine, pyrimethamine and mefloquine have since been discovered in an effort to combat and control resistant strains; however, they too are losing or have lost efficacy due to increasing parasite resistance.⁵³

It was early on during the continuing search for new and safe therapies that the potent antimalarial drug, artemisinin, was discovered in China. This compound was extracted from the plant *Artemisia annua*, which had been used for hundreds of years in ancient Asian medicine to treat fevers. The discovery led to the synthesis of new antimalarial derivatives of artemisinin such as artesunate, artemether and arteether. For the last six years, the recommended first-line treatment by the WHO for malaria in vast parts of the world is artemisinin combination therapy (ACT) which combines one of the potent artemisinin derivatives with another antimalarial.⁵³ Current examples of ACT are: artesunate-mefloquine, artesunate-sulfadoxine/pyrimethamine, artemether-lumefantrine and artesunate-AQ.

Unfortunately in recent years, parasite resistance to the artemisinin derivatives has also been detected in five countries, namely: Cambodia, Lao Democratic Republic, Myanmar, Thailand and Vietnam, and is still continually spreading.^{4,3} At present, antimalarial drug resistance has been documented in various *Plasmodium* species, namely, *P. falciparum*, *P. vivax* and *P. malariae*, with *P. falciparum* acquiring resistance to nearly all commercially available drug-therapies, Figure 1.9.⁴

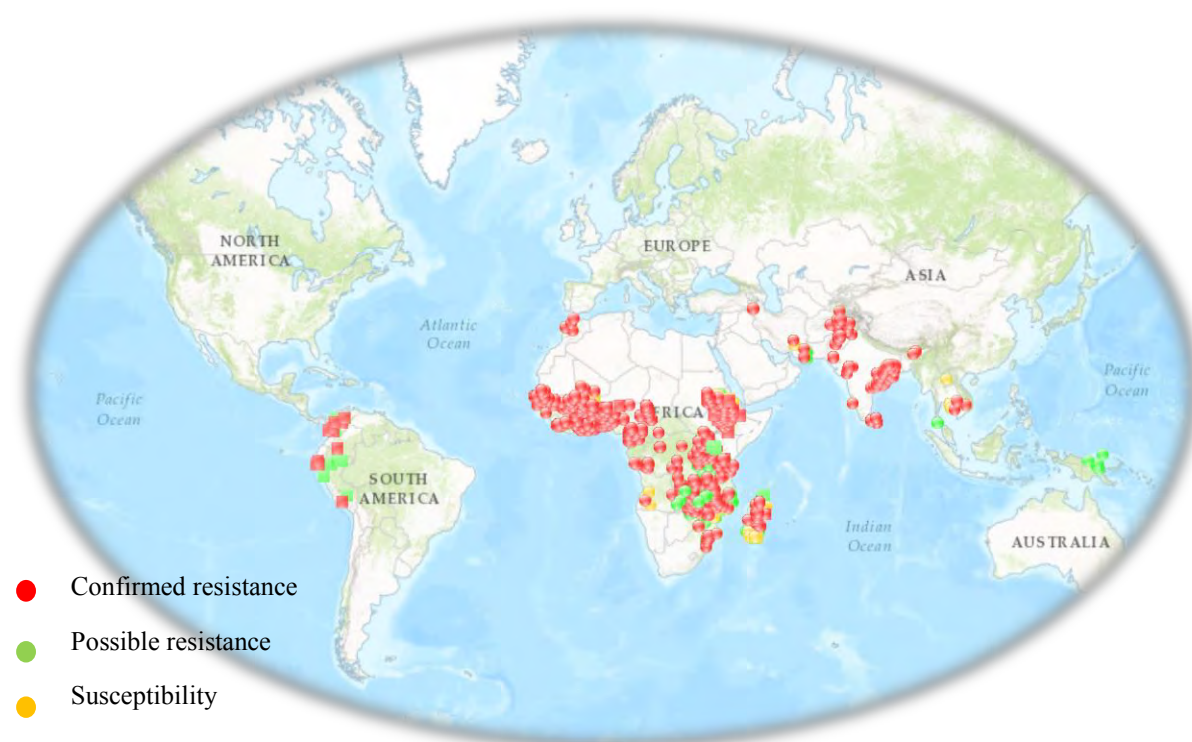


Figure 1.9: IR Mapper online user interface showing all antimalarial drugs resistance from all vector species across the globe recorded from 2005-2016.⁵⁴

There are two mutated genes associated with quinoline resistance in *P. falciparum*. The genes encode membrane carrier proteins called, *P. falciparum* P-glycoprotein homologue 1 (*PfPgh1*) and *P. falciparum* chloroquine-resistance transporter (*PfCRT*), with *PfCRT* being the main determinant of quinoline resistance.⁴⁴ These mutations in *PfCRT* allow the parasite to effectively remove CQ and other quinoline derivatives from the intracellular FV by efflux, thus rendering these antimalarials ineffective.^{55,56} It has been shown that a polymorphic change in

the transmembrane domain of *PfCRT* at position 76 is essential for CQ and quinoline resistance. This particular change in *PfCRT* substitutes the positively charged lysine residue for an uncharged threonine residue (K76T) and thus allows doubly protonated, positively charged CQ to travel down its electrochemical gradient and out of the acidic FV. It has been suggested that *P. falciparum* possesses these membrane transport proteins within the FV to effectively transport peptides and amino acids out of the FV.^{57,58}

With respect to artemisinin resistance by *P. falciparum*, research conducted by Mbengue *et al.* have provided recent cellular evidence that the artemisinin derivatives are effective inhibitors of *Plasmodium falciparum* phosphatidylinositol-3-kinases (*PfPI3K*). These are a collection of enzymes primarily understood to partake in general cellular functions such as growth, propagation, mobility and intracellular trafficking.^{59,60} These researchers demonstrated that the primary marker of artemisinin resistance, the C580Y *Plasmodium falciparum* Kelch23 (*PfKelch13*) mutation, is capable of limiting proteolysis of *PfPI3K*, resulting in amplified levels of this kinase, resulting in resistance.⁶⁰

These briefly discussed mechanisms of quinoline and artemisinin resistance, although still under much scrutiny, remain the most plausible within the literature at the moment.

The ever-emerging resistance towards these antimalarials has led many in the field to turn their attention to identifying new antimalarial compounds that may be used to study malaria in all aspects and lighten the burden of the disease.

1.9 New scaffolds for malaria studies

For decades the scientific community have been searching for novel antimalarials, especially potential scaffolds for antimalarials that are structurally different from the well-known classes. In 1997, Riscoe and co-workers identified a structurally unique class of potential antimalarial derivatives by having revealed that 2,3,4,5,6-pentahydroxyxanthone (X5) inhibited the *in vitro*

growth of *P.falciparum* (CQS and multi-drug resistant strains).⁶¹ Over the next few years, this group demonstrated important structure-activity relationships (SARs) for a library of approximately 50 isomeric hydroxyxanthenes, inspired by X5, and showed that these compounds exerted their primary antimalarial activity during the erythrocytic cycle of the parasite, and that they are β -haematin inhibitors. This important research investigation and SARs gave rise to a number of new antimalarial agents.⁶²

Investigations in the 1980s by Fujioka *et al.* identified potent acridine alkaloids extracted from the *Glycosmis*, *Citrus* or *Severinia* plants, which showed *in vitro* and *in vivo* activity against rodent malaria.⁶³ This was not the first known acridine derivative that showed potent antimalarial activity, since during the 1930s, quinacrine became a medically approved antimalarial drug.⁶⁴ It was much later that further SAR investigations of these scaffolds led to the evaluation and lead optimisation of dual-functioning antimalarial acridones (in 2009).⁶⁵

Although SAR investigations and natural product extraction screenings, are useful methods for the identification of new antimalarial scaffolds, over the last 16 years high-throughput screening (HTS) has become one of the topmost tools for the identification of new compounds.

1.9.1 High throughput screening

HTS is a very well-established approach to drug discovery that is used widely by pharmaceutical industries across the world. Using robotic automation and data processing, HTS is a time and cost effective way to assay libraries of millions of molecular compounds to assess activities against particular species. The results of these experiments used for drug discovery, usually identify 'hit' scaffolds of interest, which may be used as a starting point for new compound design.

There have been multiple HTS campaigns focused on β HI for new antimalarial scaffolds conducted over several years. In 2000, Kurosawa *et al.* used a haematin crystallisation assay to screen for scaffolds that had better activity than CQ, but were not of the quinoline class. This investigation screened over 100000 compounds from several sources (SPECS, Roche cocktails, NCC, combinatorial chemistry libraries and microbial broths), which resulted in various scaffolds for potential optimisation namely, triarylcarbinol, benzophenone and hydrazine derivatives.⁶⁶ In 2009, a similar HTS study by Rush *et al.* utilised a colorimetric assay established by Ncokazi and Egan, for the primary screening of approximately 16000 compounds which gave rise to various pyrimidine chemotypes.^{42,67} Furthermore, additional large phenotypic HTS studies conducted by Gamo *et al.* and Guiguemde *et al.* in 2010, screened over approximately 2 million and 300000 compounds respectively, large portions of which came from GlaxoSmithKline's chemical library.^{68,69} The screens again utilised antiplasmodial assays for inhibitors of *P. falciparum* (not target specific) in an effort to find potential antimalarial pharmacophores.^{68,69}

The results of a HTS study conducted by Sandlin *et al.* was used in this project to identify a new scaffold for β HI and *Plasmodium falciparum* inhibition. The Egan group (University of Cape Town), in collaboration with the Wright group (Vanderbilt University), have screened 144330 compounds from the Vanderbilt University Institute of Chemical Biology (VICB) library, using two assays, a primary screen to detect β HI and a secondary screen to detect inhibition of *Plasmodium falciparum* growth. This was used to identify hit scaffolds that may be of interest.⁷⁰

The full library was tested in a 4-nonylphenyl-polyethylene glycol P-40 (Nonidet P-40/NP-40) β -haematin formation assay (see experimental methods) which led to the identification of 729 compounds displaying $\geq 80\%$ β -haematin inhibitory activity. Therefore only potent β -haematin inhibitors were determined and this smaller quantity of compounds was suitable for subsequent

dose-response experiments. Random selections were then made of the initial 729 compounds and tested in the β HI assay at a concentration of 0.5-110 μ M, which identified false positives and assessed the strength of specific compounds against β -haematin formation. 530 compounds that exhibited IC_{50} values ≤ 27 μ M against the formation of β -haematin were established as hits, having smaller IC_{50} values than CQ (53.0 μ M). The 530 identified compounds were then tested in a subsequent screen at a concentration of 23 μ M to determine if they were or were not active against *P. falciparum*. Compounds that displayed $\geq 90\%$ inhibition of growth against *P. falciparum* were considered to be hits. The final batch of 171 compounds that inhibited the formation and growth of both β -haematin and *P. falciparum* was subjected to further analysis. Of these 171 compounds, 73 showed activity at ≤ 5 μ M against *P. falciparum*. Dose-response testing in the multidrug resistant C234 strain identified a further 21 compounds with nanomolar activity against *P. falciparum* and it was consequently from this last batch that the molecular parent molecule and proposed scaffold were selected for this project (Figure 1.10).⁷⁰

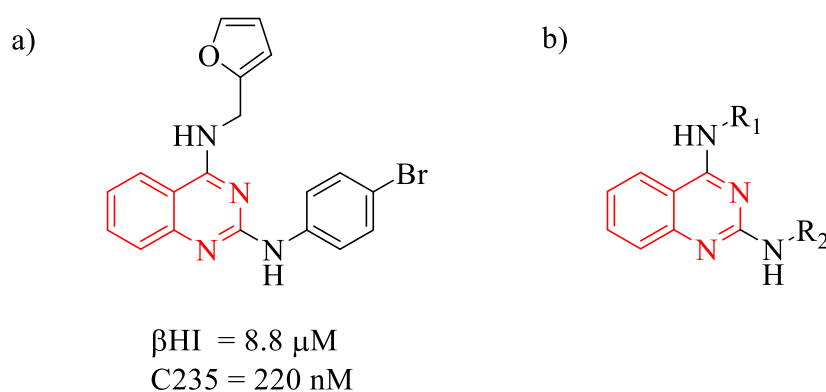


Figure 1.10: a) One of the most active screened compounds, with β -haematin inhibition (β HI) and *P. falciparum* (C235) activity IC_{50} values shown. b) The proposed synthetic scaffold for the project based on the chemotype in a).

Figure 1.10 shows the parent molecule, N^2 -(4-bromophenyl)- N^4 -(furan-2-ylmethyl)quinazoline-2,4-diamine (a), as well as the proposed synthetic scaffold, 2,4-diaminoquinazoline (b), for this project. The quinazoline structural motif is shown in red.

1.10 Quinazoline – a pharmacologically relevant compound class

Quinazoline, named for being an aza derivative of the well-known quinoline, is an organic compound that possesses two fused six-membered ring systems, benzene and pyrimidine. This scaffold was first synthesised in 1895 by the German chemist August Bischler, although Griess had reported the first derivative of quinazoline, 2-cyano-3,4-dihydro-4-oxoquinazoline in 1869.⁷¹

Presently, substituted quinazoline derivatives have been shown to be extremely pharmacologically active and relevant, with there being several commercially available drugs for the treatment of cancer, microbial, viral, protozoal and fungal infections, inflammation, muscle stiffness, tuberculosis, depression, convulsions and many more indications (Figure 1.11).^{72,73}

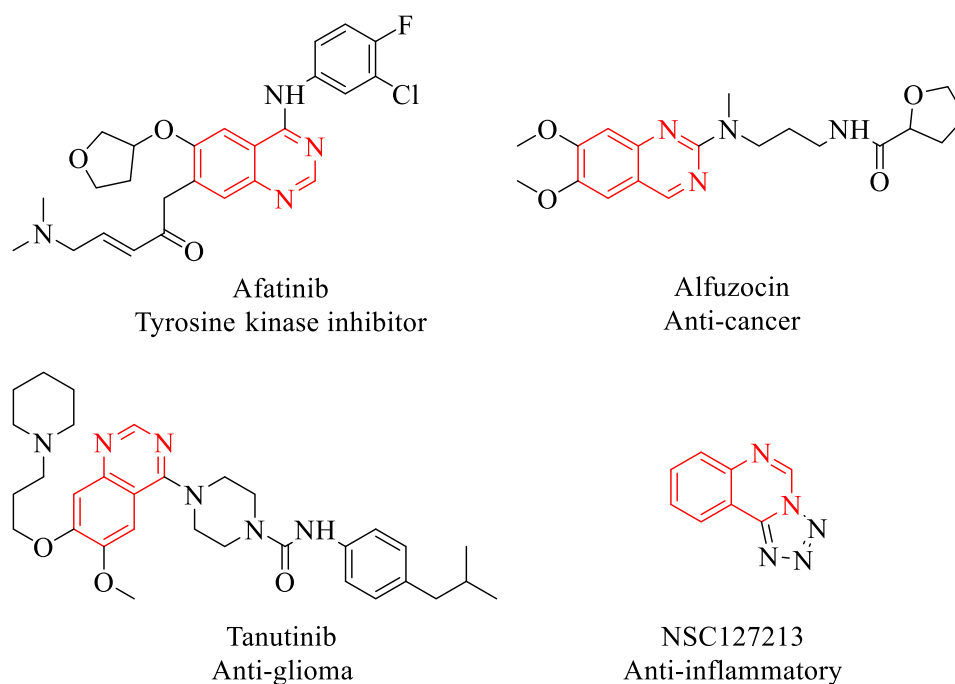


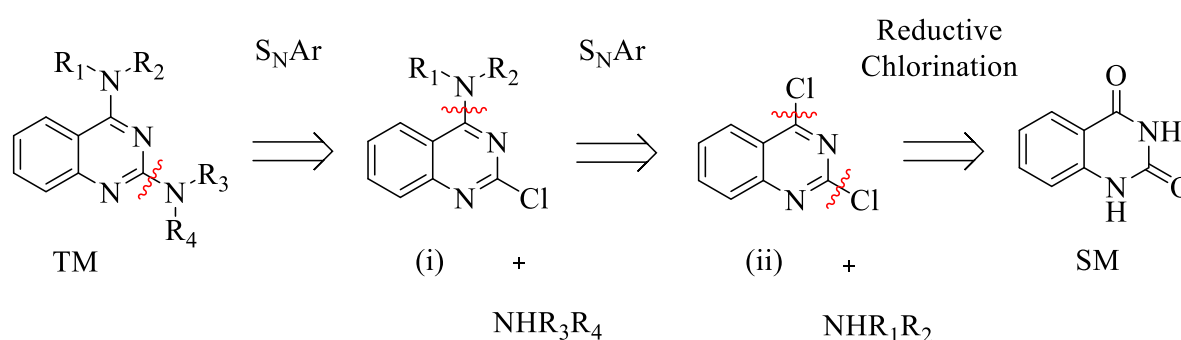
Figure 1.11: Some examples of commercially available quinazoline derivatives used as drugs in a variety of diseases/conditions.

There are numerous reported methods to synthesise quinazolines, including: Niementowski's synthesis of quinazolines using anthranilic acid with formamide, Diels-Alder synthesis involving the coupling of an imine to an electron rich alkene, one pot palladium-catalysed synthesis by McGowan *et al.* using an imidamide with halo-aryls and benzaldehyde, zinc-catalysed five-step synthesis of various imidazole-quinazoline derivatives and aza-Wittig synthesis by He *et al.* using azides and triphenylphosphine in toluene.^{74,75,76,77}

There is thus an extensive body of research related to the synthesis and biological testing of quinazoline derivatives, but to the best of our knowledge none involving the synthesis of 2,4-diaminoquinazolines as potential antimalarials. This consequently presented an opportunity to investigate this unexplored area.

1.10.1 Retrosynthesis of 2,4-diaminoquinazoline

A three-step synthesis was envisaged as illustrated in the retrosynthetic analysis shown in Scheme 1.1.



Scheme 1.1: Envisaged retrosynthesis of the target molecules

In the forward synthesis, reductive chlorination of benzoylene urea (SM) by phosphoryl oxychloride (POCl_3) results in the formation of the precursor, 2,4-dichloroquinazoline (ii). Using (ii) in a series of nucleophilic aromatic substitution ($\text{S}_{\text{N}}\text{Ar}$) reactions would result in the synthesis of various required mono-substituted quinazoline intermediates (i), which upon further $\text{S}_{\text{N}}\text{Ar}$ reaction would give rise to the final target compounds (TM). Further discussion and details can be found within Chapter 2.

1.11 Aims and Objectives

1.11.1 Aims

The aims of this research study were to synthesise a series of 2,4-diaminoquinazolines and investigate their *in vitro* antimalarial activity in order to discover structure-activity relationships in their antimalarial activity and to evaluate their potential for further optimisation and development as antimalarials.

1.11.2 Objectives

The specific objectives required to attain the proposed aims were to:

1. Synthesise derivatives of 2,4-diaminoquinazoline.
2. Purify the derivatives by flash column chromatography or recrystallisation and quantify their purity using high performance liquid chromatography ($\geq 95\%$).
3. Fully characterise them using high resolution mass spectrometry (HRMS), nuclear magnetic resonance (NMR) and infrared spectroscopy (IR)
4. Determine the β HI IC_{50} s of the derivatives using a NP-40 detergent mediated assay, as well as their Pf IC_{50} s, against chloroquine-sensitive NF54 parasites.
5. Conduct additional *in vitro* tests on compounds that possess Pf (NF54) IC_{50} s < 1000 nM, including:
 - a. cytotoxicity in a mammalian cell line,
 - b. Pf IC_{50} s in the CQ-resistant strain DD2,
 - c. aqueous solubility using turbidometry.
6. Assess structure-activity relationships (SARs).

CHAPTER 2

Synthesis of Quinazoline Derivatives

Stefan J. Benjamin

M.Sc. Dissertation

The synthesis of the target scaffold derivatives mentioned in Chapter 1, namely 2,4-diaminoquinazolines, was accomplished using a three-step synthetic procedure involving chlorination and nucleophilic aromatic substitution reactions. The general procedure for their synthesis is presented below, as well as a detailed example for one of them, followed by a summary of all the compounds synthesised. The numbering system of the compounds prepared is based on structural consistency, rather than strictly adhering to a IUPAC designation in which the IUPAC numbering of the quinazoline ring itself is adopted as shown in Figure 2.1.

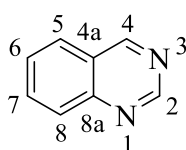
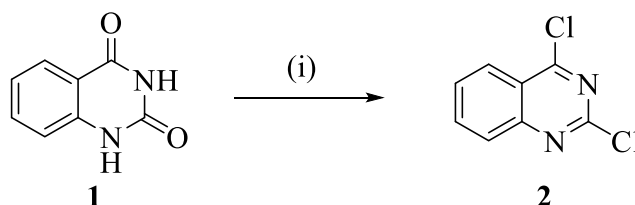


Figure 2.1: IUPAC numbering of the quinazoline ring

2.1 Synthesis of 2,4-dichloroquinazoline (**2**)

The synthesis of 2,4-dichloroquinazoline, **2**, was successfully performed according to the general procedure reported by Cho *et al.*, using triethylamine (Et_3N) instead of *N,N*-diethylaniline as a base (Scheme 2.1).⁷⁸ The starting material, benzoylene urea, **1**, was refluxed with phosphoryl oxychloride (POCl_3) and Et_3N for 18 hours under nitrogen atmosphere. This resulted in both amide functionalities being converted into their imidoyl chlorides as in **2**.



Scheme 2.1: (i) POCl_3 (10 eq), rt, 30 min; Et_3N , rt to 106 °C, 18 h

A large excess of POCl_3 (10 eq) was needed to form the dichlorinated product, as using insufficient equivalents resulted in monochlorination according to nuclear magnetic resonance (NMR) spectroscopy. Upon reaction completion, the excess POCl_3 was carefully quenched using a saturated solution of sodium carbonate (Na_2CO_3) and the solution then subjected to a conventional extraction and purification using column chromatography. Recrystallisation from boiling methanol (MeOH) gave **2** in a yield of 87%, whose melting point agreed well with that of the literature, m.p. 117-118 °C (Lit ⁷⁹: 118-120 °C).

Spectroscopic characterisation was as follows. Firstly, the infrared (IR) spectrum in Figure 2.2 indicated the loss of both $\text{C}=\text{O}$ as well as NH stretching frequencies as expected (*).

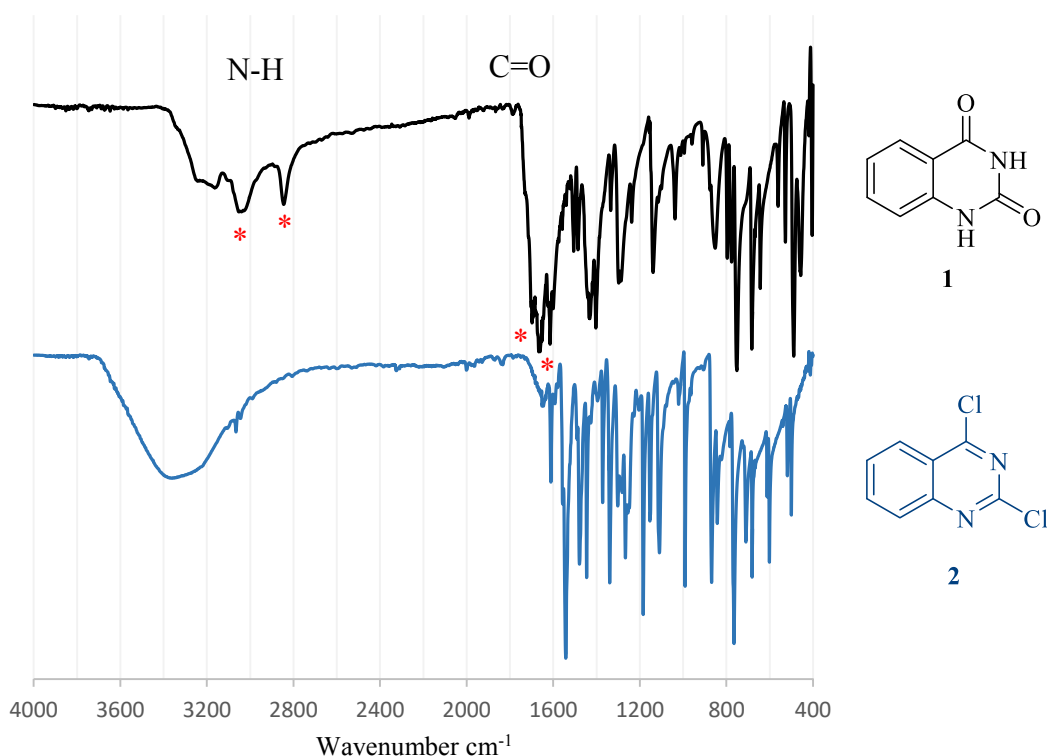


Figure 2.2: IR spectra of compounds **1** and **2**

The ^1H NMR spectra of starting material **1** and product **2** are shown in Figure 2.3:

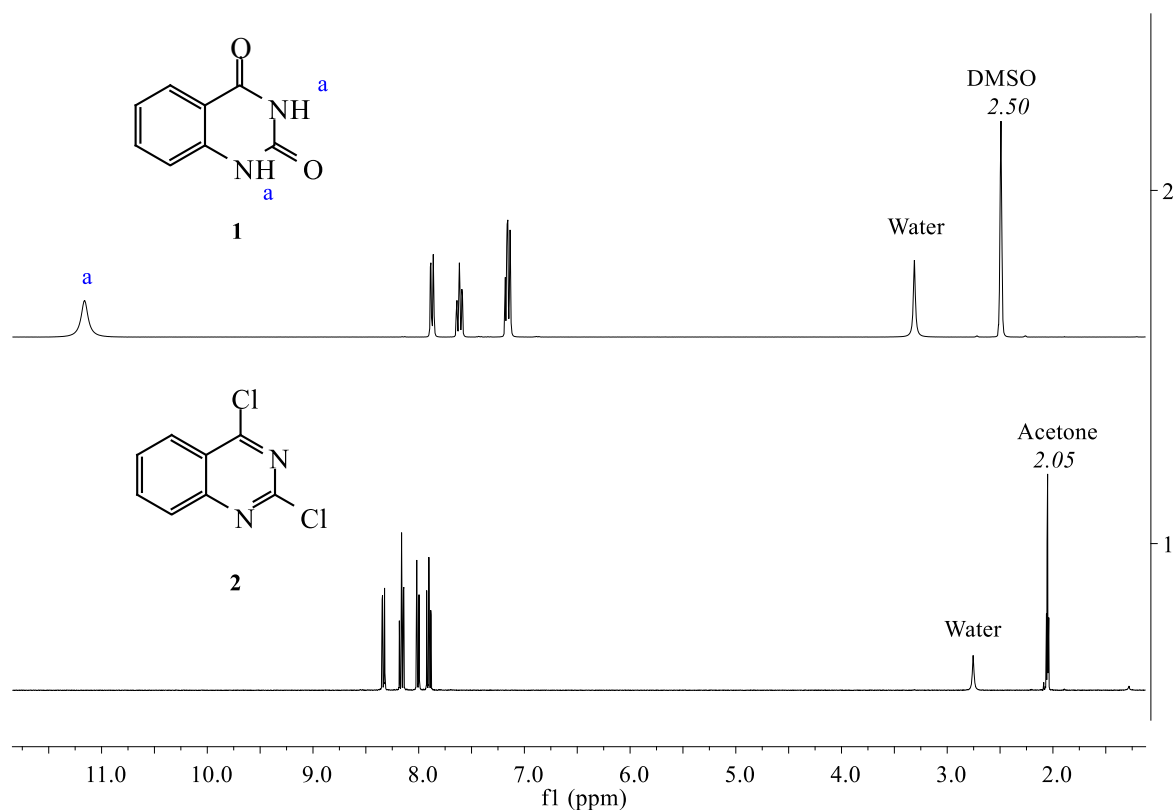


Figure 2.3: ^1H NMR spectra of compounds **1** & **2**, illustrating a key structural change (a)

In the ^1H NMR spectrum of **2** the loss of the amide hydrogen resonances (a) were noted, together with a deshielding of the aromatic resonances due to the ring becoming π -deficient. The data agreed with that of Cho.⁷⁸ Similarly, ^{13}C NMR spectroscopy could also be used to corroborate the structure. As seen in Figure 2.4, the ^{13}C spectrum showed the anticipated eight singlets. However, unequivocal assignments were not made for individual carbons in view of their similarity, but rather assigned as either CH or quaternary carbons based on relative relaxation (NOE) effects. Indeed, this was a recurring theme throughout the library. The details of the assignments may be seen within the experimental methods section.

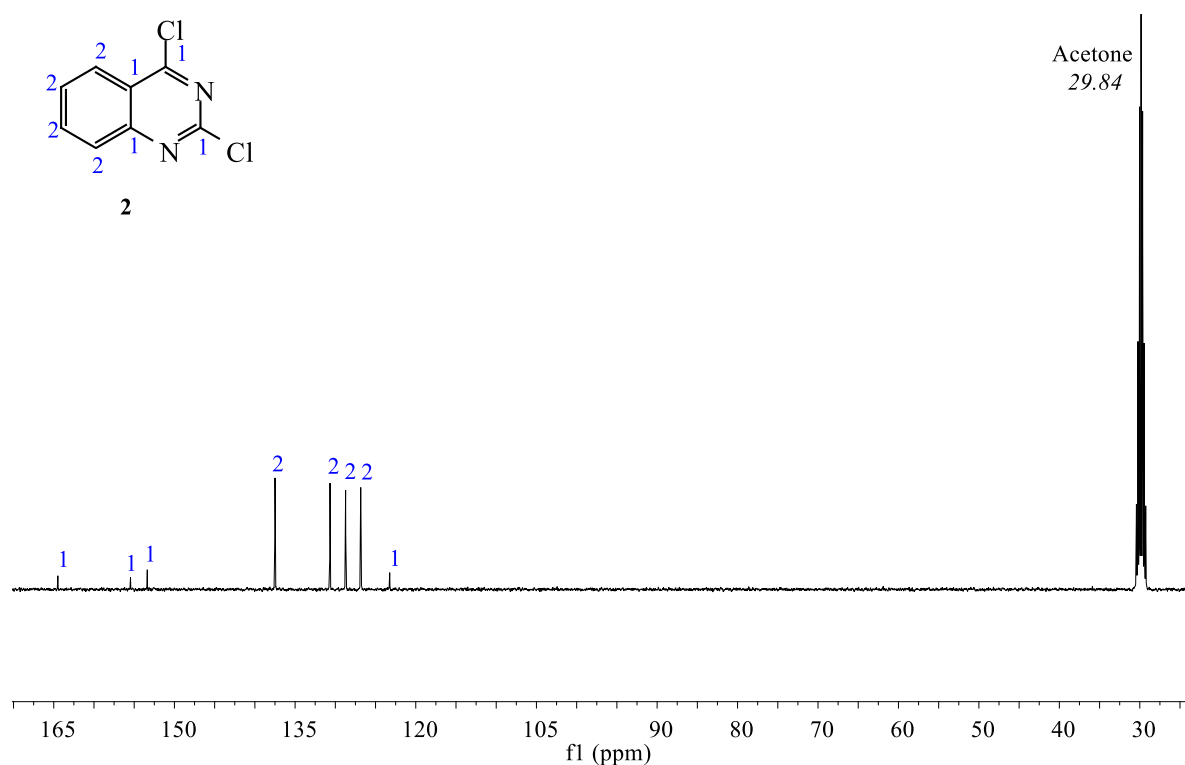


Figure 2.4: ^{13}C NMR spectrum of compound **2** illustrating the correct number of carbon count quaternary (1) and tertiary (2) signals

Finally, a high resolution mass spectrum (HRMS) was recorded using a Waters Synapt G2 electron spray ionisation (ESI) instrument with an observed mass of 198.9822 which was in good agreement with the calculated value of 198.9830 for $\text{C}_8\text{H}_5\text{Cl}_2\text{N}_2$ $[\text{M}+\text{H}]^+$.

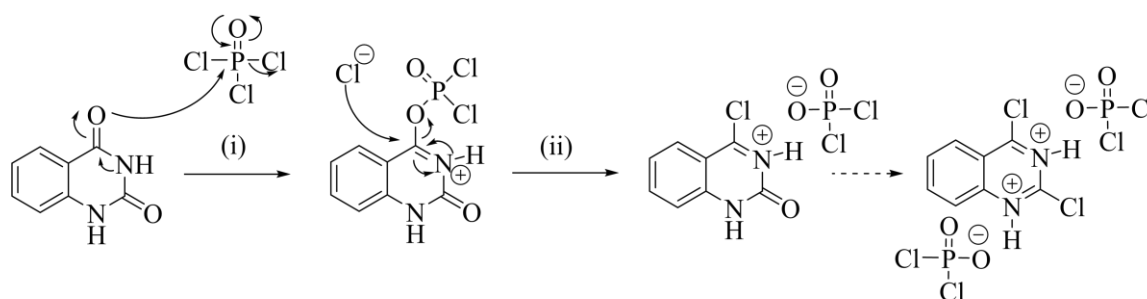
The HRMS results indicated that the $[\text{M}+\text{H}]^+$ ion was the dominant species, which was not surprising in view of the presence of protonatable nitrogen atoms in the structure, where the calculated and observed masses agreed well within an acceptable error (25 parts per 10 000). Collectively, the data proved the successful synthesis of compound **2**.

For biological evaluation, all the compounds synthesised needed to be $\geq 95\%$ pure, in which purification was achieved using flash-column chromatography and recrystallisation

techniques. Measurement of purity was determined using HPLC conducted using a Agilent 1220 LC system V. In this manner HPLC purity of **2** was determined to be 99%.

2.1.1 A proposed mechanism of formation of 2,4-dichloroquinazoline (**2**)

The proposed mechanism for formation of the monochlorinated intermediate on route to **2** is shown in Scheme 2.2. It is understood that the same mechanism would take place at both carbonyl groups, but for simplicity only one is shown.



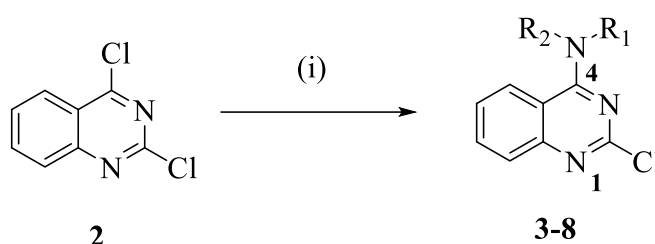
Scheme 2.2: Proposed half synthesis of 2,4-dichloroquinazoline, **2**.

The step labelled (i), shows the attack of the nucleophilic oxygen on the electrophilic phosphorus centre of POCl₃. This allows for the S_NAc-like expulsion of the chloride ion which in turn nucleophilically attacks the resultant iminium species (ii), with expulsion of a dichlorophosphate leaving group. The same process then repeats at the other carbonyl functionality to afford the dichlorinated species, 2,4-dichloroquinazoline, shown in the scheme as a bis-salt, which is neutralised on work-up with base (aq. Na₂CO₃), ultimately to afford unprotonated **2**.

Once synthesised, **2** was then used in a series of nucleophilic aromatic substitution reactions to afford various intermediate compounds that are discussed in the next section.

2.2 Synthesis of 2-chloroquinazoline-4-amine intermediates (3-8)

The synthesis of mono-substituted 2-chloroquinazoline-4-amine intermediates, **3-8**, was successfully performed, according to the general methodology reported by Odingo *et al.*⁸⁰ by way of nucleophilic aromatic substitution (S_NAr). Scheme 2.3 represents the general case using 1-1.7 equivalents of the desired amine and Et_3N as base (to neutralise HCl produced) which were refluxed at 60 °C with **2** for 3-6 hours.

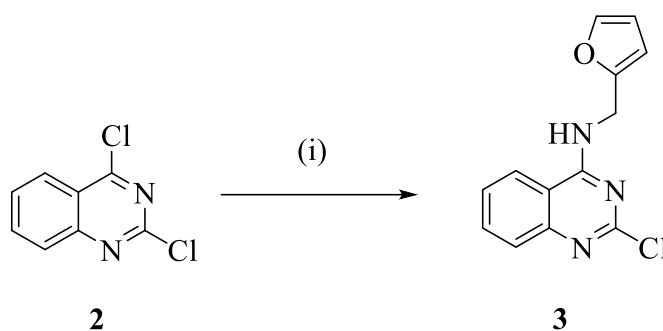


Scheme 2.3: (i) R_1R_2NH (1-1.7 eq), THF, Et_3N , reflux 3-6 h

Under these conditions, regioselective substitution at C-4 occurred to afford derivatives **3-8**. The explanation and proof of regioselectivity will be covered later in section 2.2.1, since this is an extremely important aspect of the work.

The reactions were quenched with ice water before being neutralised with a saturated solution of Na_2CO_3 , to remove any HCl salts that may have formed. After extraction with $CHCl_3$ and concentration under high vacuum, the intermediates were purified by flash column chromatography and recrystallised to afford the pure samples as confirmed by HPLC.

By way of example, details are given for substitution with furfurylamine (furan-2-ylmethanamine), Scheme 2.4.



Scheme 2.4: (i) Furan-2-ylmethanamine (1.1 eq), THF, Et₃N, reflux 6 h

Following work-up, substituted quinazoline **3** was obtained after chromatography and recrystallisation from boiling MeOH in a yield of 50%, whose melting point was sharp (m.p. 158-159 °C). Although not a new compound, its melting point was not cited in the literature.

As an example, the spectroscopic characterisation is presented here which includes the NMR spectroscopic and HRMS results, highlighting characteristic features that prove the synthesis of compound **3**. Similar logical rationalisations were used for all intermediates, **3-8**.

The ¹H NMR spectrum of **3**, Figure 2.5, showed the presence of both furan resonance peaks, as well as those of the quinazoline fragment in the correct relative integration. Notably, the furan H-**c** resonances were observed upfield at around 6.4 ppm, while the furan H-**c*** resonance appeared more downfield as a result of its α-relationship to oxygen. A downfield triplet for the NH hydrogen at δ = 9.2 ppm, coupling to an upfield methylene as a doublet (δ = 4.7 ppm), confirmed substitution.

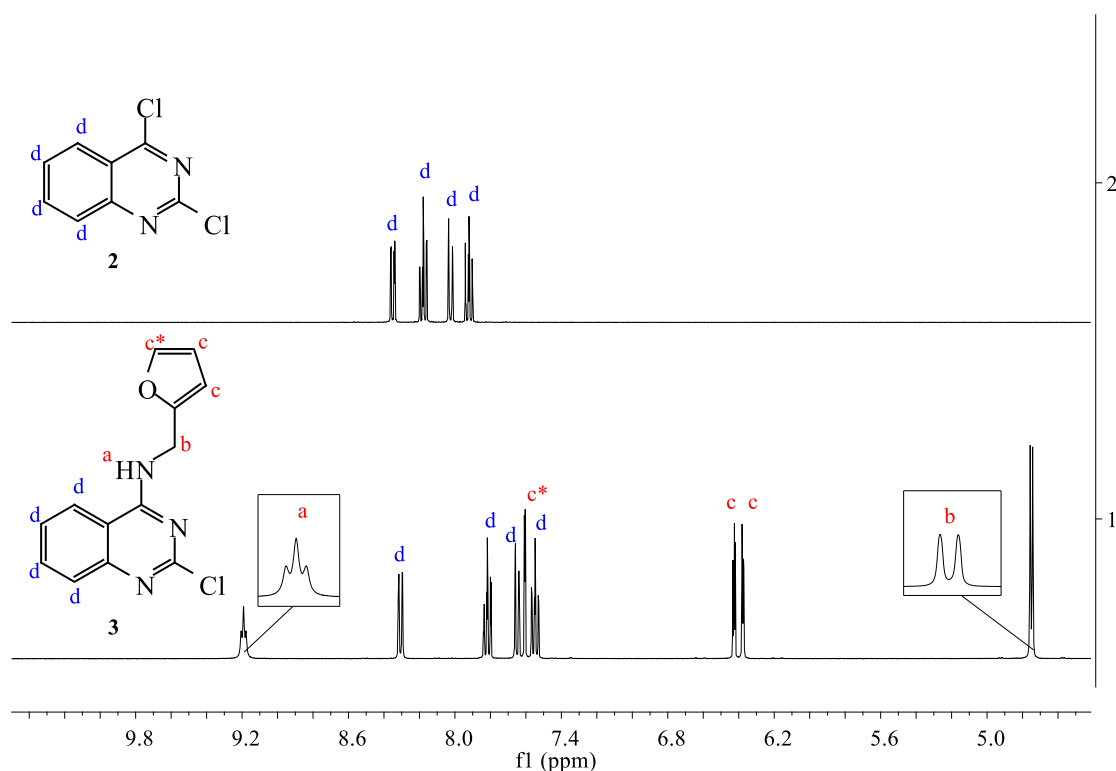


Figure 2.5: ^1H NMR spectra of compounds **2** & **3**

The ^1H NMR spectroscopic chemical shifts agreed with those of the literature presented by Odingo *et al.*⁸⁰ As before, ^{13}C NMR spectroscopy could also be used to corroborate the structure.

As seen in Figure 2.6, the spectrum showed the anticipated thirteen singlets. However, specific assignments were not attempted; rather peaks are divided as before between quaternary (1) and non-quaternary (2) carbon atoms, although the two upfield CH carbons at around 110 ppm can be safely assigned to the furan ring C-2*, as confirmed by HSQC. The two types (quaternary or non-quaternary) were assigned on the basis of relative relaxation effects (NOE). Indeed, this was a recurring theme throughout the library.

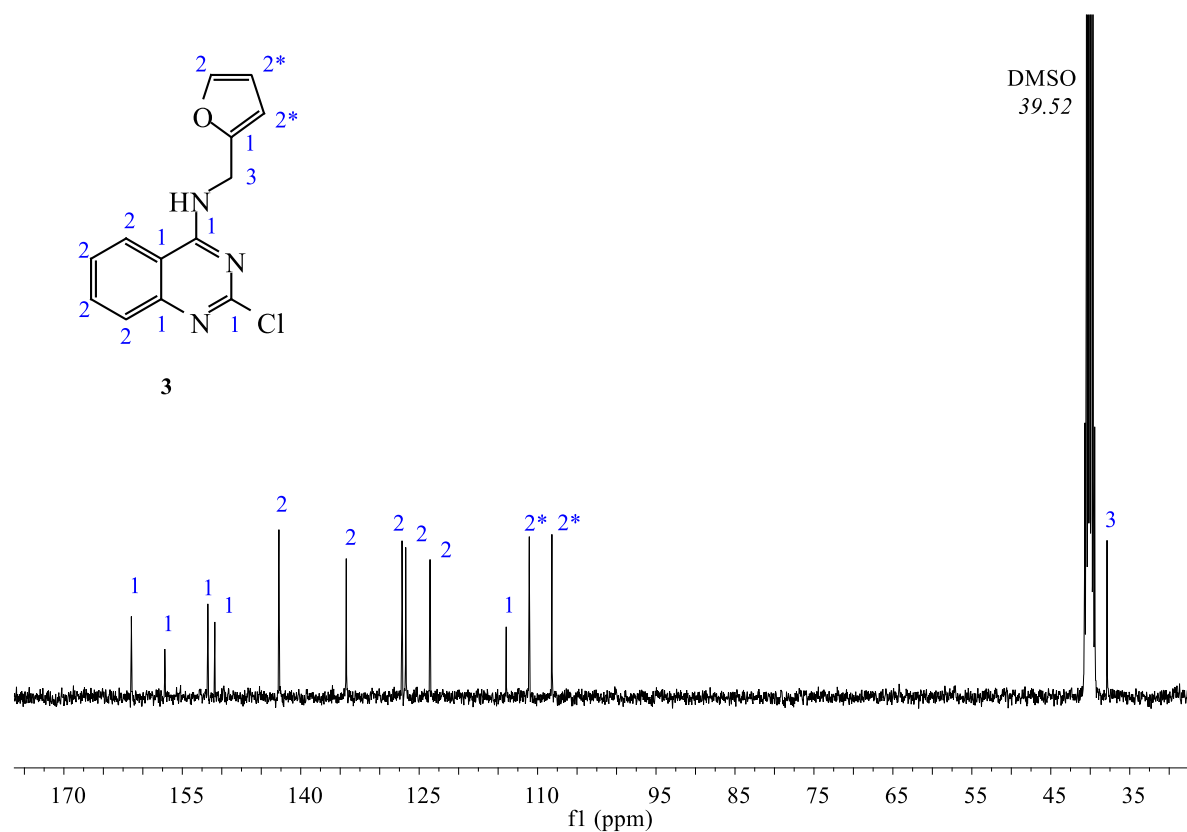
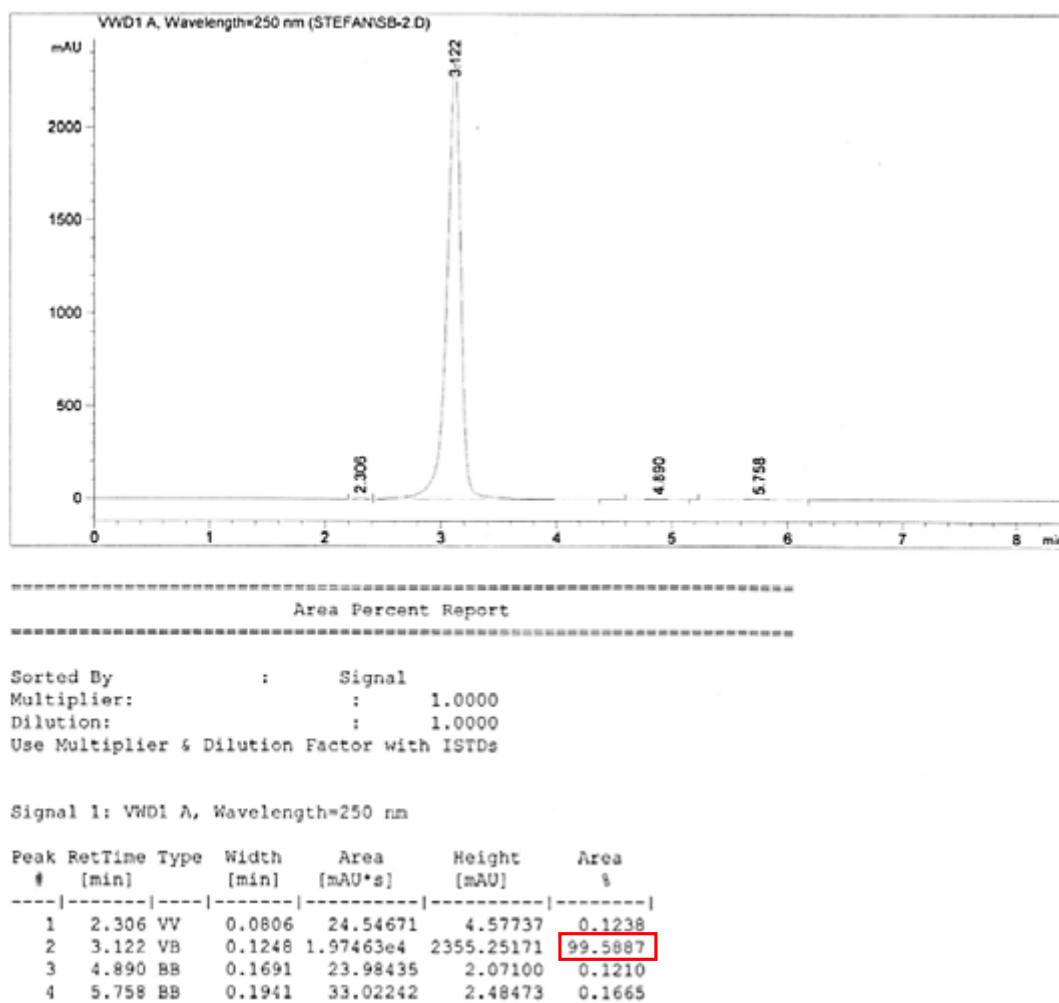


Figure 2.6: ¹³C NMR spectrum of compound **3** illustrating the correct carbon atom count and the expected signal intensities

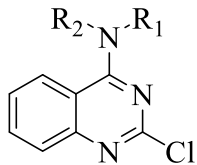
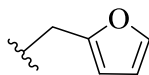
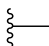

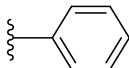
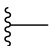
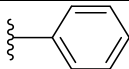
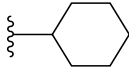
Finally, a HRMS was recorded using a Synapt G2 instrument in which a $[M+H]^+$ peak was obtained with an observed mass of 260.0538 which was in good agreement with the calculated value of 260.0591 for $C_{13}H_{11}ClN_3O$ $[M+H]^+$.

Collectively, the data proved the successful synthesis of compound **3** at the required purity (99.6 %) as shown by the HPLC trace (Figure 2.7).

**Figure 2.7:** HPLC trace for compound 3

The same characterisation methods and similar rationalisations were used for all the 2-chloroquinazoline-4-amine intermediates synthesised (**3-8**). Their structures are shown in Table 2.1.

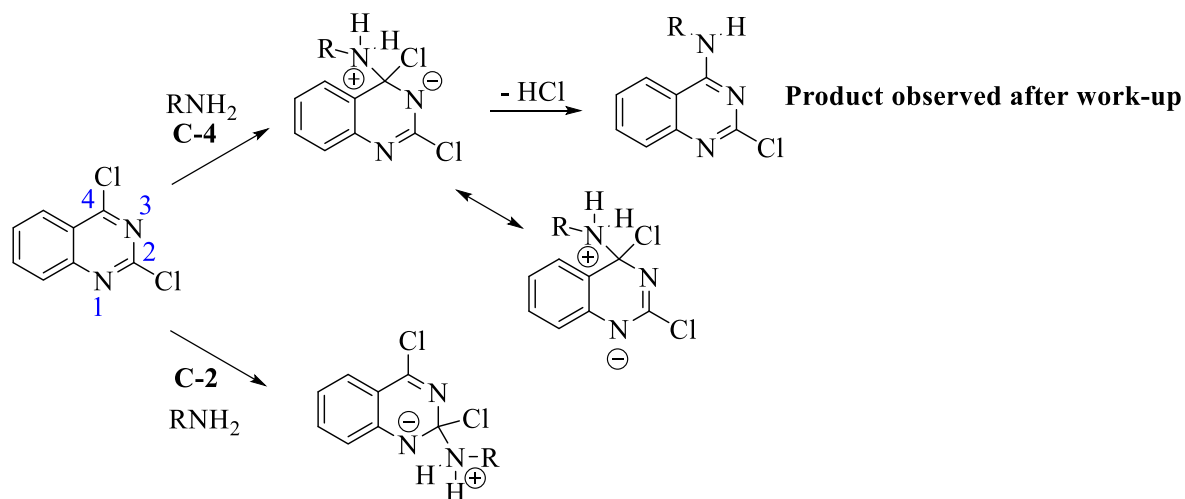
Table 2.1: The 2-chloroquinazoline-4-amine intermediates (**3-8**)

Scaffold			
Compound	R ₁	R ₂	Yield
3	-H		50%
4	-H		89%
5	-H		75%
6	-H		89%
7			66%
8	-H		96%

2.2.1 A proposed mechanism of formation and a proof of regioselectivity for the intermediates (**3-8**)

Literature reports on the synthesis of products **3-8** via S_NAr with various primary and secondary amine derivatives indicate that the reaction is regioselective for the 4-position (see Figure 2.1).⁸¹ Hence, in this project 4-regioselectivity was expected. Although no explanation in the literature could be found to rationalise this important outcome, one based on a resonance argument is shown in Scheme 2.5 using a generalised primary amine involving the classical addition/elimination sequence. Resonance theory suggests that substitution at C-4 provides a more stabilised intermediate than that from substitution at C-2. This is because the intermediate

Meisenheimer-type amidine anion (N^-) can delocalise directly into the amidine imine bond ($C=N$) only in the C-4 case, as shown in the scheme.



Scheme 2.5: Resonance argument for C-4 regioselectivity

In view of the difficulties in unambiguously assigning regioselectivity using NMR spectroscopy data, it was decided to prove the regioselectivity at C-4 for one particular amine (cyclohexylamine) used in this project by using X-Ray crystallography. To this end, crystals were grown of compound **8**, from MeOH and sent for X-ray analysis at The University of Cape Town's Chemistry Department Crystallography Unit. The results may be seen in Figure 2.8

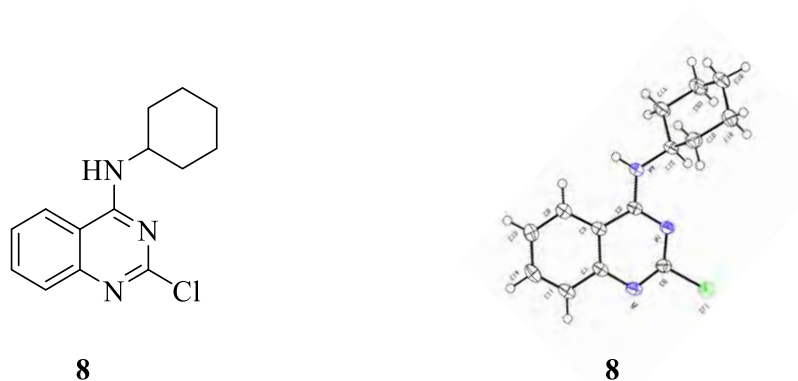


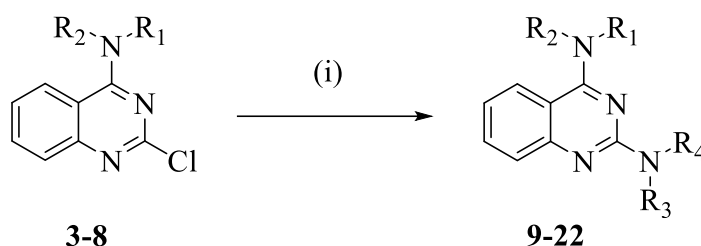
Figure 2.8: X-ray structure for 2-chloro-*N*-cyclohexylquinazolin-4-amine, **8**

The X-Ray structure unambiguously proved a C-4 regioselective substitution. Compound **8** was shown to crystallise in the Monoclinic C2/c space group, with, $a=30.523$ (5) $b=6.798$ (12) $c=19.261$ (3) $\alpha=90$ $\beta=128$ $\gamma=90$. The full details are provided in Appendix A.

In concluding this subsection, the synthesis of six 2-chloroquinazoline-4-amine products (**3-8**) were successful, and these were then used in a second substitution to afford the final library members as discussed in the next section.

2.3 The synthesis of 2,4-diaminoquinazoline target compounds (9-22)

The synthesis of 2,4-diaminoquinazoline target compounds, **9-22** were successfully performed according to the general methodology reported by van Horn *et al.*, making use of isopropanol (*i*-PrOH) as solvent as opposed to ethanol as suggested by further literature evidence.^{82,95,96,82,97} Scheme 2.6 represents the general approach used for the synthesis of these compounds, using the previously synthesised intermediates, **3-8**, and 1-2 equivalents of the desired amine derivative. The mixtures were allowed to react for 15-24 hours in a sealed tube at 150 °C.

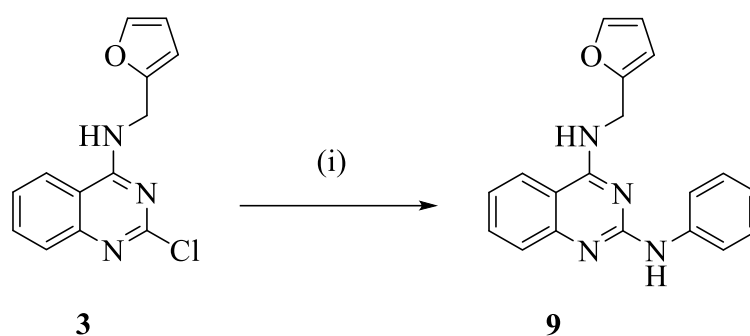


Scheme 2.6: (i) R₃R₄NH (1-2 eq) , *i*-PrOH, 15-24 h, 150 °C

Once the reaction was deemed complete by TLC, the vessel was cooled to ambient temperature after which it was neutralised with 1M sodium hydroxide (NaOH) solution and the organic product extracted into dichloromethane (DCM)/ ethyl acetate (EtOAc), 50:50. The organic phases were then concentrated under high vacuum to reveal the crude product. The compounds

were purified by flash column chromatography and recrystallised from boiling MeOH to afford pure samples as confirmed by HPLC ($\geq 95\%$). A full characterisation of these compounds using NMR and HRMS confirmed the identity of the products.

Scheme 2.7, represents an example of one of the target molecules synthesised, namely *N*⁴-(furan-2-ylmethyl)-*N*²-phenylquinazoline-2,4-diamine, **9**. Characterisation of this compound serves as an example illustrating the logic used for the characterisation of all final compounds.



Scheme 2.7: (i) Phenylamine (1.2 eq) , *i*-PrOH, 18h, 150 °C

For the synthesis of compound **9**, the desired amine utilised was phenylamine (aniline). The reaction followed that of the general procedure and required 18 hours to achieve full conversion. After completion, as judged by TLC analysis indicating a spot-to-spot conversion, a normal workup, extraction and purification by flash column chromatography was conducted. Multiple recrystallisations to a constant melting point from boiling MeOH, gave **9** in an overall yield of 36% with a m.p. of 103-104 °C. The low overall yield could be attributed to losses encountered in there crystallisation steps.

The spectroscopic characterisation follows. New ¹H NMR spectroscopy resonances were noted for **9**, indicated in red as ‘e’, ‘f’, ‘f’ and ‘f’ in Figure 2.9, revealing the introduction of the new phenyl ring. Those for the starting material in the reaction, compound **3**, are shown in blue for comparison. In addition, signals for the furan-2-ylmethanamine substituent at C-4 showed

that this still remained attached (resonances **a**, **b** and **c** / **c***), in which the signals correctly integrated for the 6 hydrogen atoms present (three aromatic Hs, one amine H and two methylene Hs). Signal '**a**' represents the amino hydrogen of the amine at C-4, which was expected (as before) as a triplet. However, in this case the NH signal could be seen as a broad triplet (seen in the enlarged signal '**a**'). Finally, the quinazoline ring hydrogens could also be seen as the **d** signals. Notably, the introduction of the second amine (aromatic) into the molecule resulted in resonances being more spread out due to the impact of shielding and deshielding effects.

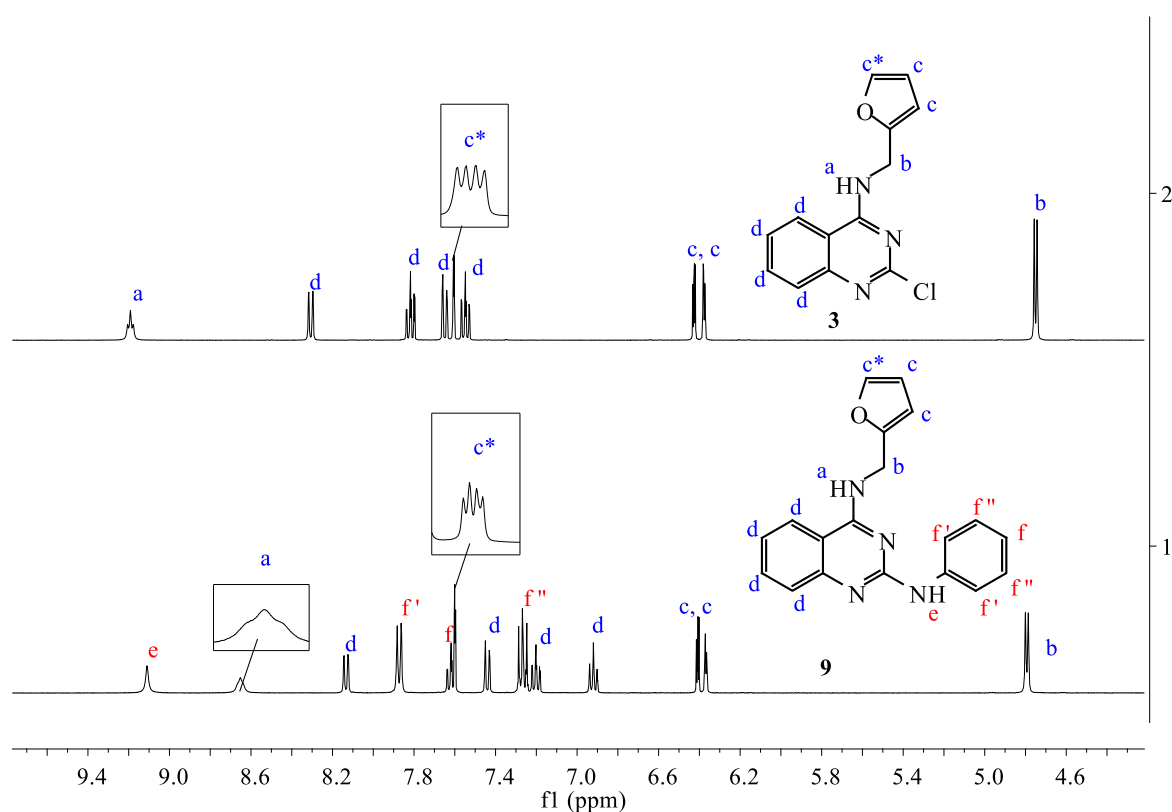


Figure 2.9: ¹H NMR spectra of compounds **3** & **9**

Overall, the ¹H NMR data shown agreed with the literature presented by van Horn *et al.*⁸² Similarly, ¹³C NMR spectroscopy could also be used to corroborate the structure. As seen in Figure 2.10, the spectrum showed the anticipated seventeen singlets for C₁₉H₁₆N₄O, taking into

account the C2-symmetry of the new aniline phenyl ring. As before, no attempt was made to categorically assign individual carbon atoms; just to distinguish CH carbons from quaternary ones. Since the phenyl hydrogens of the newly introduced aniline moiety could be identified in the ^1H spectrum, HSQC allowed them to be identified in the ^{13}C spectrum as shown in Figure 2.11.

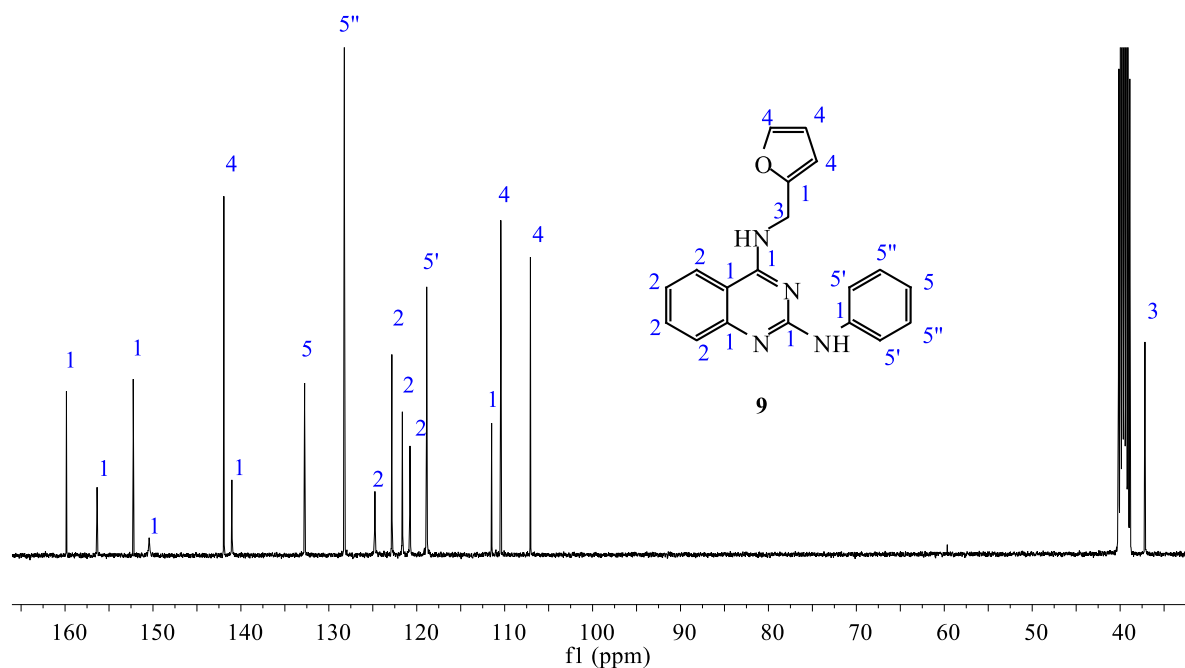


Figure 2.10: ^{13}C NMR spectrum of compound **9**

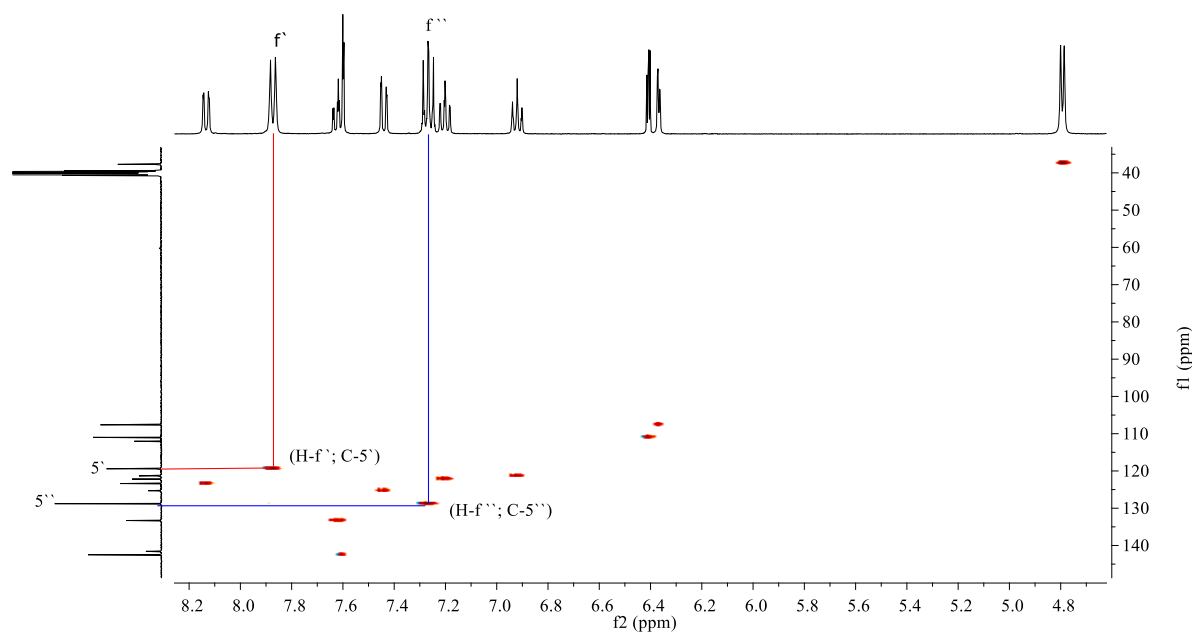


Figure 2.11: Heteronuclear single quantum coherence (HSQC) spectroscopy for compound **9**

For simplicity, only two HSQC signals have been labelled in Figure 2.11, so as to illustrate an example of carbon atom identification and less so the entire assignment. The full assignment may be seen in the experimental methods section.

Finally, a HRMS was recorded using a Synapt G2 instrument, with an observed mass of 317.1393 being obtained which is in good agreement with the calculated value of 317.1402 for $\text{C}_{19}\text{H}_{17}\text{N}_4\text{O} [\text{M}+\text{H}]^+$.

Collectively, the various data proved the successful synthesis of compound **9** at the required purity (97.6%) shown by the HPLC trace (Figure 2.12).

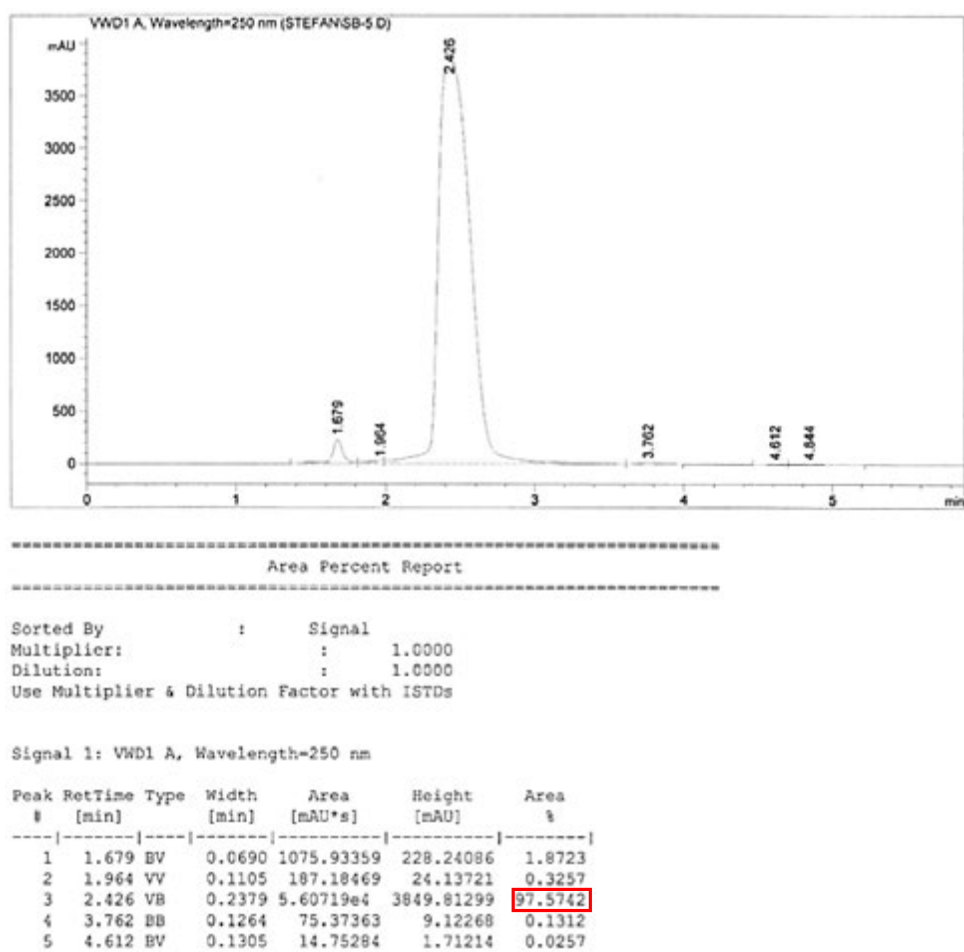
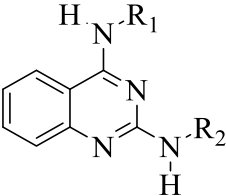
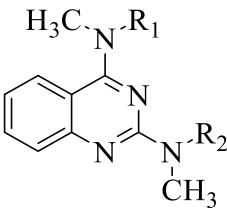
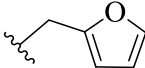
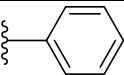
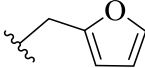
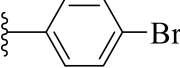
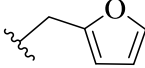
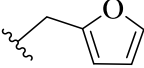
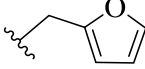
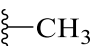


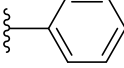
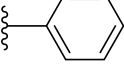
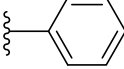
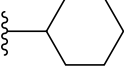


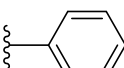
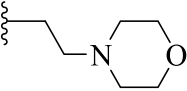
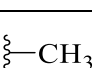

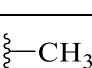
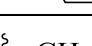
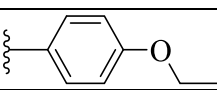
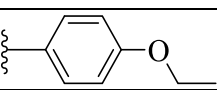
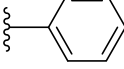
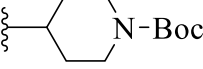
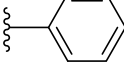
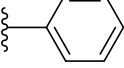


Figure 2.12: HPLC trace of compound 9

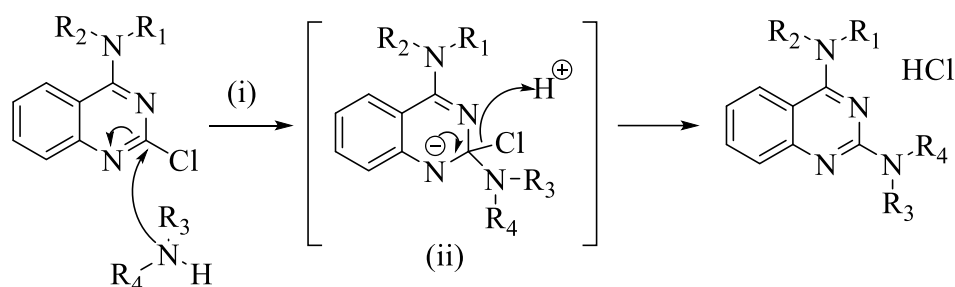
The same characterisation methods and similar rationalisations were used for all the 2,4-diaminoquinazoline target compounds synthesised (**9-22**). Their structures are shown in Table 2.2.

Table 2.2: The 2,4-diaminoquinazoline final compounds (**9-22**)

Scaffold	<div style="display: flex; justify-content: space-around; align-items: center;"> <div style="text-align: center;">  <p>9-21</p> </div> <div style="text-align: center;">  <p>22</p> </div> </div>		
	R ₁	R ₂	Yield
9			36%
10			78%
11			66%
12			51%
13			82%
14			52%
15			72%
16			69%
17			71%
18			64%
19			92%
20			64%
21			85%
22			73%

*The yields calculated here are for the final step of the synthesis and not a cumulative step-wise yield.

The mechanism of the second substitution is expected to follow the S_NAr pathway shown previously and is depicted in Scheme 2.8, with the expected addition (i) and elimination (ii) steps.



Scheme 2.8: The proposed S_NAr mechanism showing the formation of the final target molecules

In conclusion synthesis of the target scaffold derivatives were successfully accomplished using a three-step synthetic procedure, which involved chlorination and nucleophilic aromatic substitution reactions. All of the compounds synthesised (Table 2.1 and 2.2) were fully characterised by NMR spectroscopic analysis including 1H , ^{13}C , Cosy and HSQC experiments. HRMS and IR spectra, together with melting point determinations were used to complete the characterisations.

For biological evaluation all the compounds synthesised needed to be $\geq 95\%$ pure. Purification of these compounds was successfully achieved using flash-column chromatography and recrystallisation techniques. Measurement of purity was determined using HPLC conducted using a Agilent 1220 LC system V and individual purities are quoted in the experimental methods chapter. These biological evaluations will be described in the next chapter.

CHAPTER 3

Rationalisation and Structure-Activity Relationships

Stefan J. Benjamin

M.Sc. Dissertation

This chapter discusses the reasoning behind the selection of the quinazoline derivatives synthesised and takes a detailed look at various *in vitro* and biological test results, identifying SARs for this scaffold.

3.1 Sub-structure activity study based on the parent compound (10)

As discussed in Chapter 1, HTS identified the parent quinazoline derivative (**10**) for this project (Figure 3.1). This figure also illustrates the initial sub-structure study conducted to identify specific structural features of **10** giving rise to its promising antiplasmodial activity. This was done in order to make rational synthetic modifications to the scaffold.

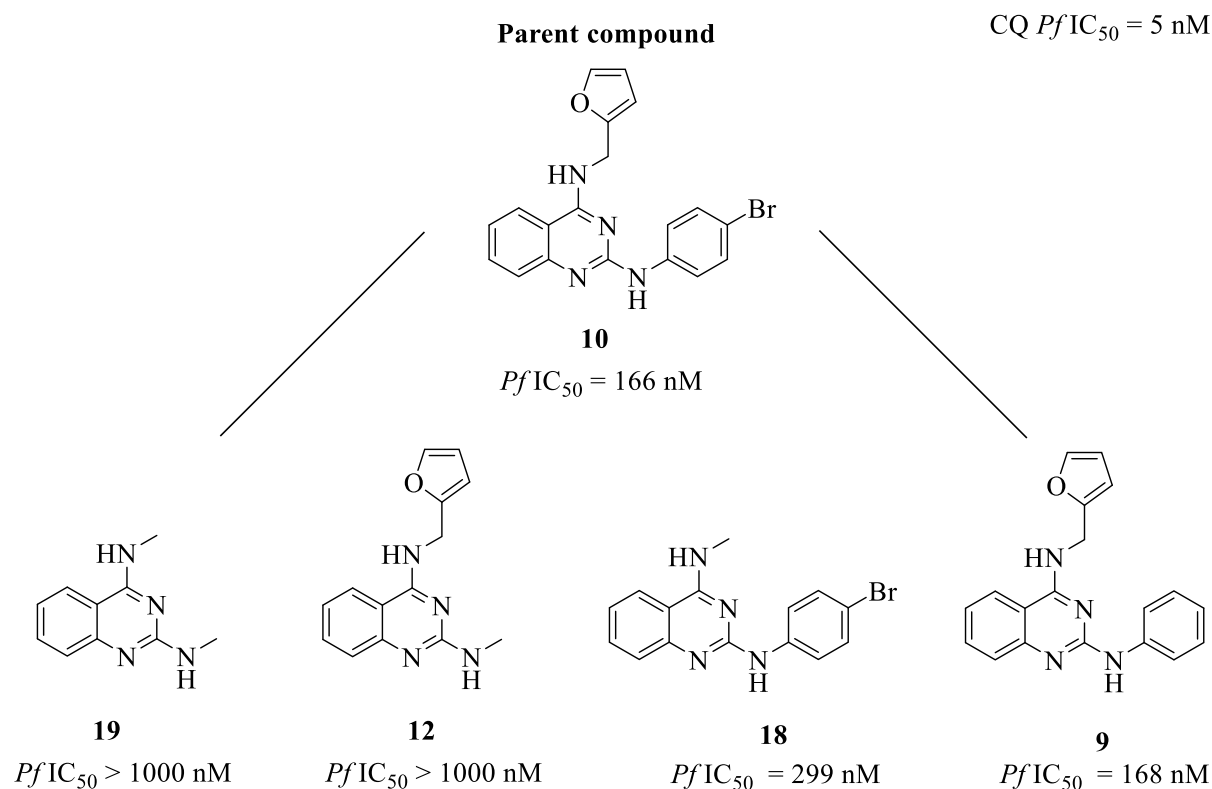
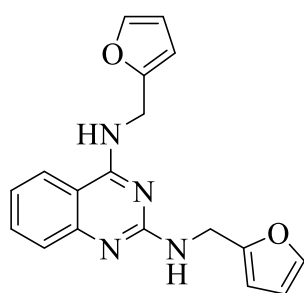


Figure 3.1: Sub-structure activity study based on the parent molecule with NF54 *Plasmodium falciparum* 50% inhibitory concentrations ($PfIC_{50}$ s) shown.

The sub-structure study showed that the activity of **10** depended primarily on the presence of the 4-bromoaniline group, since replacing this substituent with a methyl amine group completely abolished antiparasmodial activity (**12**), whereas removal of only furan-2-ylmethanamine (**18**) reduced, but did not eliminate activity. This suggests that furan-2-ylmethanamine may not be essential for activity. Removal of both aromatic substituents (4-bromoaniline and furan-2-ylmethanamine) completely abolished activity as expected (**19**). The bromo group did not appear to be essential to the activity of **10**, since its replacement with a hydrogen atom (**9**) had no effect on the activity.

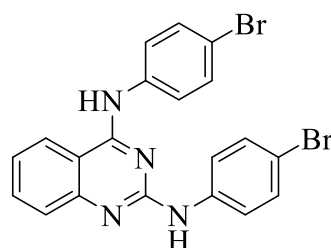
Based on the above findings showing the importance of the 4-bromoaniline or aniline groups for activity, the synthesis of a doubly substituted 4-bromoaniline moiety was considered to test whether this would have enhanced the overall activity, while a doubly substituted furan-2-ylmethanamine moiety was tested to confirm whether this molecular feature indeed has little role in activity, giving rise to a weakly active or completely inactive derivative (Figure 3.2).

CQ $PfIC_{50} = 5$ nM



11

$PfIC_{50} = 786$ nM



13

$PfIC_{50} = 80$ nM

Figure 3.2: Doubly substituted substituents of the parent molecule

Synthesised compounds **11** and **13** confirmed the importance of the 4-bromoaniline moiety, since **13** had drastically improved activity with an IC_{50} of 80 nM. The lack of potency of the furan-2-ylmethanamine moiety in antiparasitic activity was confirmed by compound **11** which had a very high IC_{50} of 786 nM. **13**, was thus the most active compound synthesised in the first round of SAR investigations, which consequently led to a second structure activity study in an effort to determine what features of **13**, brought about its strong activity.

3.2 Sub-structure activity study based on compound 13

It was expected that a sub-structure activity study based on **13** could possibly have led to rapid improvement in the activity of the series, as well as further enhance understanding of the SARs of the scaffold. Thus the compounds shown in Figure 3.3 were tested. Here the role of aromaticity in **13**, was assessed.

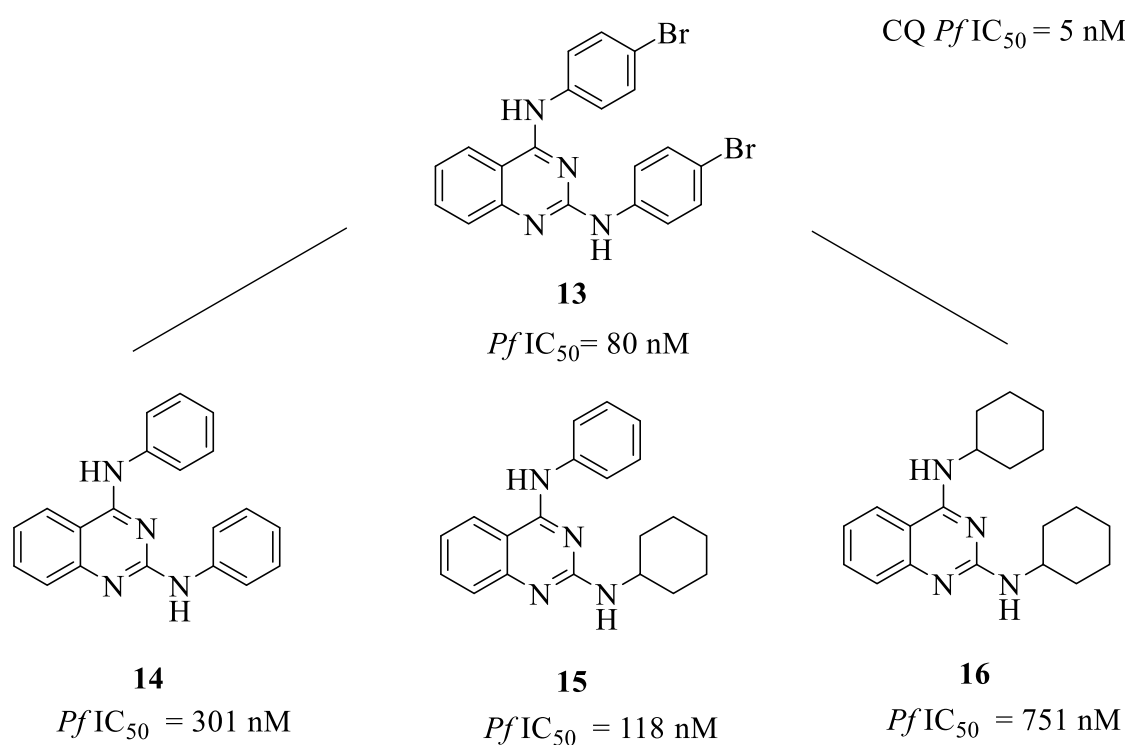


Figure 3.3: Structural influences in the activity of **13** against NF54 *Plasmodium falciparum*

Upon removal of both bromine atoms, compound **14** lost substantial activity (301 nM), which led to the hypothesis that electronic effects of the bromine atoms on the aromatic ring systems influence activity to some extent. The results also clearly indicated that removal of the aromaticity of both substituents greatly diminished activity (**16**) and that a balance between aromaticity and non-aromaticity was required for good activity as seen in compound **15** with an activity value of 118 nM. This suggested that derivatives related to **14** and **15**, might maintain or even improve activity. Thus further questions related to electronics effects and nitrogen H-bonding capability on activities were explored. This led to the next set of derivatives presented in Figure 3.4.

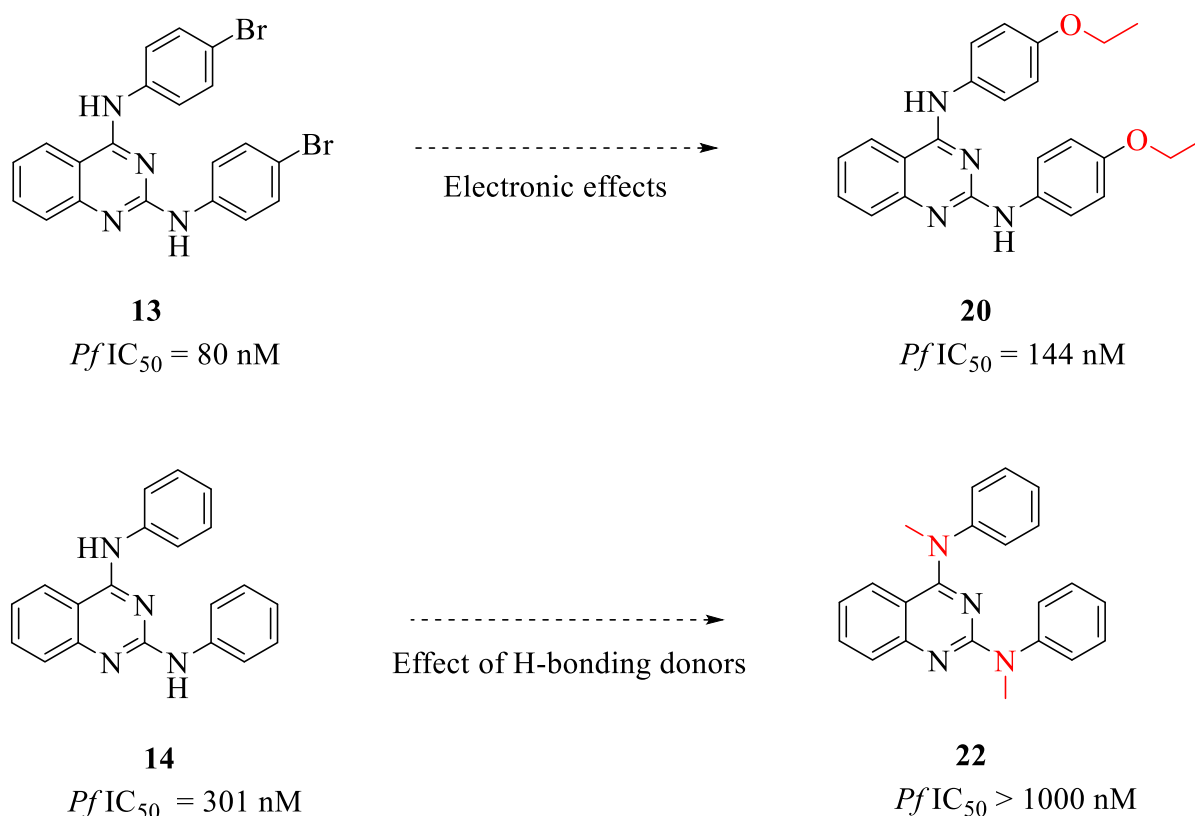


Figure 3.4: The impact of aromatic electronics and nitrogen hydrogen-bonding capacity on the antiplasmodial activities against NF54 *P.falciparum*

Results presented in Figure 3.4, suggested that changing from the electron withdrawing bromine substituents which is less releasing (Br is able to back donate through the π system) to electron releasing ethoxy groups had no major impact on the activity of the derivatives. It was tentatively proposed that these features may allow the aromatic rings to π -stack with Fe(III)PPIX, thus inhibiting the formation of HZ, which may be how the compounds exert activity. The ability to π -stack with Fe(III)PPIX may however be reduced upon methylation of the exo-quinazoline nitrogen atoms which seem to be needed to lock the π -stacked rings in place with strong hydrogen bonding interactions. These thoughts were later supported by the ability of the compounds to inhibit the formation of β -haematin, using an NP-40 β HI assay. Finally, a derivative was made in an effort to improve aq. solubility and hence activity, as it was noted in the laboratory that majority of the compounds synthesised were not soluble in aq. solution and hence activity might be expected to improve by increasing the aq. solubility of these derivatives. The ethylmorpholine group shown in Figure 3.5 was investigated.

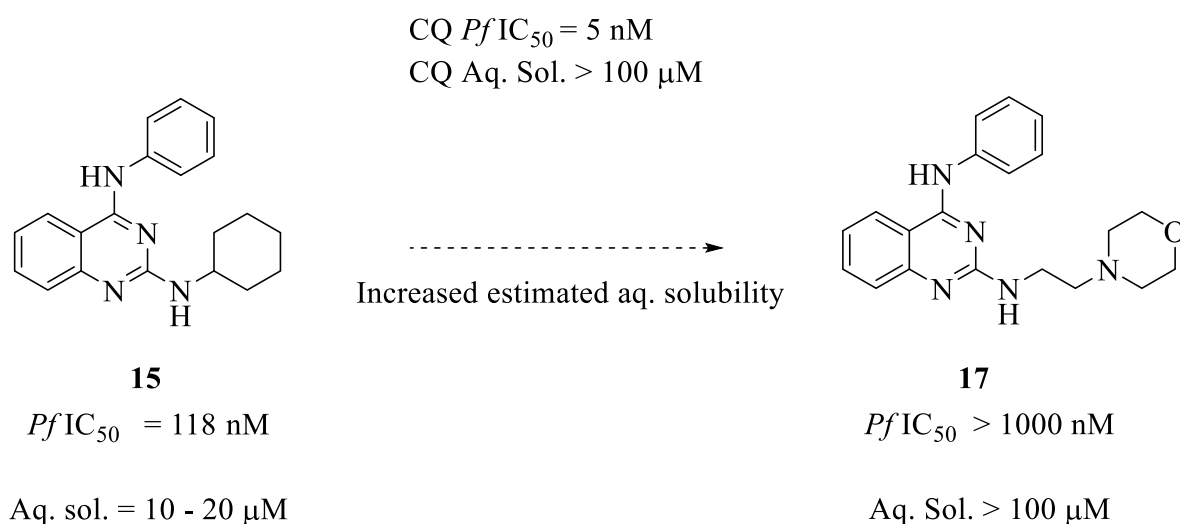


Figure 3.5: Influence of solubility and activity of an ethylmorpholine group on quinazoline derivative **15**

Aqueous solubilities were determined using a turbidometric 96-well plate assay.^{83,84} The loss of activity in going from compound **15** to **17** (Figure 3.5), probably does not arise from its

increased aqueous solubility, but rather from the flexible ethyl linker of the ethylmorpholine group. Loss of conformational freedom upon interaction with the drug target may be expected to result in an entropic penalty that impairs its activity.

3.3 β -haematin inhibition and comparison with antiplasmodial test results

Having investigated SARs against *P. falciparum*, all compounds were tested for β HI. As described in Chapter 1, β -haematin is the synthetic, structural and chemical. Equivalent of HZ, a microcrystalline form of Fe(III)PPIX made by the parasite to avert the toxic effects of haematin. The β -haematin inhibitory effects of quinazoline derivatives were tested using a NP-40 detergent-mediated assay (see experimental methods).⁸⁵

The β HI IC₅₀ and NF54 *Pf*IC₅₀ results for the entire library of compounds is presented in Table 3.1. The activity cut off concentrations were set at ≥ 1500 μ M and ≥ 1500 nM for β HI and *Pf*I respectively.

Table 3.1: β HI & *Pf*IC₅₀ results with standard errors (n=3)

Compounds	β HI (μ M)	<i>Pf</i> I (nM)
2	>1500	>1500
3	>1500	>1500
4	>1500	>1500
5	74 \pm 5	>1500
6	522 \pm ND	>1500
7	1249 \pm ND	>1500
8	145 \pm ND	>1500
9	23 \pm 2	168 \pm 30
10	15 \pm 3	166 \pm 40
11	115 \pm 7	786 \pm 96
12	264 \pm ND	1053 \pm 50
13	20 \pm 2	80 \pm 2
14	39 \pm 3	301 \pm 26
15	26 \pm 3	118 \pm 26
16	>1500	751 \pm 32
17	>1500	1201 \pm 11
18	25 \pm 3	299 \pm 40
19	>1500	>1500
20	536 \pm ND	144 \pm 3
21	166 \pm 14	166 \pm 6
22	735 \pm ND	>1500
AQ*	17 \pm 2	7 \pm 3

*AQ – Amodiaquine⁸⁶

Parent compound (**10**)

Of the 21 synthesised quinazoline derivatives, 15 were active below 1500 μM for βHI and of the 15, ten compounds were correspondingly active below 1500 nM for *PfI*, while the precursor (**2**) and all the intermediates (**3-8**) were inactive against *PfI* at the cut-off as illustrated in Scheme 3.1. These results strongly suggested that the quinazoline derivatives exert activity by HZ inhibition. Indeed, parasite activity was found to be correlated with βHI (Figure 3.6). A plot of $1/\beta\text{HI IC}_{50}$ vs $1/\text{PfI IC}_{50}$ gave an R^2 value of 0.72, with the exclusion of two clear outliers, **20** and **21**.

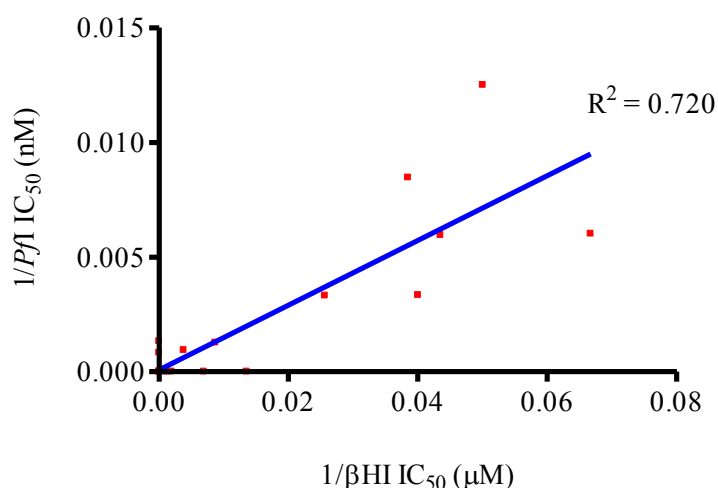


Figure 3.6: A linear regression plot ($R^2 = 0.72$) of the correlation between $1/\beta\text{HI}$ vs $1/\text{PfI IC}_{50}$ values for the entire library of compounds excluding **20** & **21**. All values greater than the cut off of 1500 $\mu\text{M/nM}$ were taken as zero.

Further evidence directly supported this mode of action, at least in the case of the most active derivative (**13**). This compound caused a dose-dependent decrease in HZ and an increase in free haem, similar to that of the well-established HZ inhibiting antimalarial CQ, described by Combrinck *et al.*⁸⁷ (The data in Figure 3.7 were kindly provided by Roxanne Openshaw, unpublished research).

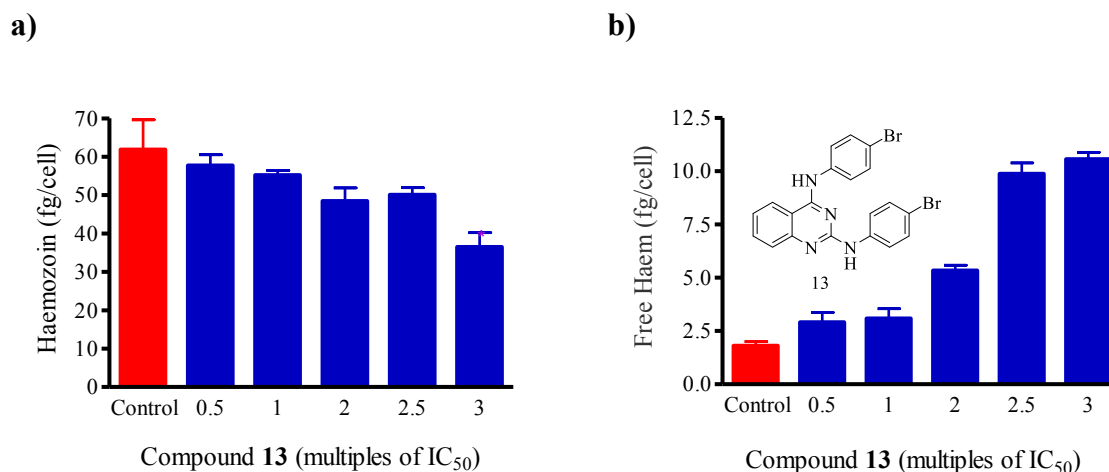


Figure 3.7: Bar charts indicating biological results for, a) HZ and b) free haem. Control (no drug)

3.4 Additional *in vitro* test results

Given the fact that ten of the 21 derivatives had *PfI* activities less than 1000 nM, with two exhibiting values below 100 nM, the series could be considered interesting for further development. Consequently, further questions were investigated relating to: a) cross resistance in *Plasmodium falciparum* with CQ, since it could be argued that 2,4-diaminoquinazolines are similar to 4-aminoquinoline antimalarials and b) cytotoxicity, since activity against *P. falciparum* could be non-specific.

Therefore a selection of the most active compounds against the parasite were tested for activity against a chloroquine resistant (CQR) strain, DD2, as well as for cytotoxicity against Chinese hamster ovarian (CHO) cell lines. Selectivity and resistance indices are reported in Table 3.2.

Table 3.2: *Pf* DD2 and Cytotoxicity CHO for a selection of the most active *Pf* NF54

Comp.	<i>Pf</i> NF54 (nM)	<i>Pf</i> DD2 (nM)	Resistance Index IC ₅₀ DD2/ IC ₅₀ NF54	Cytotoxicity, CHO (μM)	Selectivity Index IC ₅₀ CHO/IC ₅₀ NF54	Est. Aq. Sol. (μM)
9	168 ± 30	198 ± 36	1.2	15.4 ± 1.7	91	5-10
10	166 ± 40	90 ± 16	0.5	5.3 ± 0.8	32	5-10
11	786 ± 96	1277 ± 437	1.6	20.0 ± 0.2	25	20-40
13	80 ± 2	233 ± 8	2.9	4.8 ± 0.2	60	1-5
14	301 ± 26	416 ± 66	1.4	4.4 ± 0.5	15	5-10
15	118 ± 26	299 ± 63	2.5	6.4 ± 1.3	54	10-20
16	751 ± 32	830 ± 381	1.1	6.2 ± 0.8	8	10-20
18	299 ± 40	209 ± 55	0.7	5.2 ± 0.3	17	10-20
CQ	5 ± 0.2	152 ± 30	25.5	10	1670	>>100

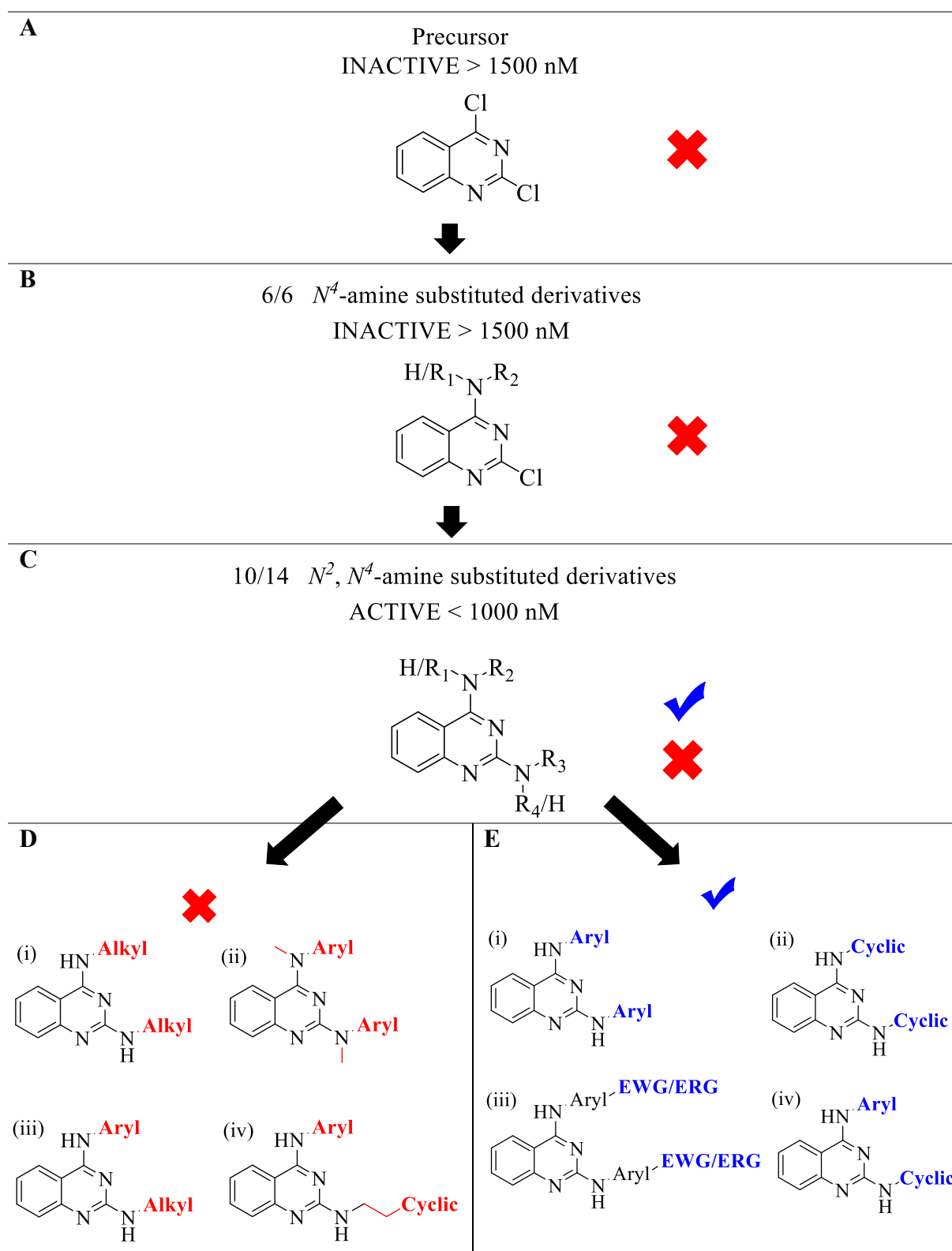
Results clearly showed that the compounds tested were not cross-resistant with CQ, since they displayed low resistance indices in the range 0.5-2.5 compared to 25.5 for CQ. Although most compounds showed a marginal loss in activity in DD2 parasites, compound **10** showed an good activity increase from 166 nM to 90 nM. The results confirmed that the 2,4-diaminoquinazoline scaffold is sufficiently structurally distinct from CQ to make it unsusceptible to CQ resistance pathways.

The results further showed that 2,4-diaminoquinazolines are not merely cytotoxic, since they possess selective activity against *P. falciparum*. The general consensus for a positive (i.e. not cytotoxic) result requires a selectivity index greater than 100 as seen for the case of CQ (1670). The lower this ratio is, the more cytotoxic a compound is. Here, although not meeting the requirements for a drug, the most active compounds were 30-60 times more active against malaria parasites than mammalian cells.

Finally, aqueous solubility ranges shown were also determined (Table 3.2). These revealed that these compounds have very poor aqueous solubility in comparison to CQ. This would be an area to focus on in event of the further development of this series as potential clinical candidates.

3.5 Structure-activity relationships summary

Scheme 3.1 represents, a graphic summary of the major SAR features of the quinazoline series.



Scheme 3.1: SAR summary for *Pf1* results, representing levels of structural design A – E. Here alkyl refers to non-cyclic groups.

For several structural designs presented in Scheme 3.1, it may be seen with reference to panel **D** that 2,4 substituents on the quinazoline scaffold in the form of non-cyclic alkyl amines (i), tertiary amines (ii) and less rigid amines (iv), appear to diminish activity, whereas panel **E** highlights the facts that bulkier aromatic and cyclic (i, ii), activated or inactivated π systems (iii) and combinations thereof (iv), give rise to active quinazolines.

Collectively, these results indicate that 2,4-diaminoquinazolines are indeed biologically relevant and show great potential for future work related to optimisation for antimalarial purposes. There is considerable scope for further modification of the scaffold that could improve solubility, cytotoxicity and activity in the quest for the next generation of potent antimalarials.

CHAPTER 4

Conclusions and Future Work

Stefan J. Benjamin

M.Sc. Dissertation

4.1 Conclusions

The aims of this research study were to gain insights into the biological activity of the 2,4-diaminoquinazolines, to discover structure-activity relationships in their antimalarial activity and to evaluate their potential for further investigation as potential new antimalarials worthy of further optimisation.

These aims were achieved by synthesising derivatives of the scaffold and studying *in vitro* β -haematin inhibition, *P. falciparum* IC₅₀s in CQ sensitive (NF54) and CQ resistant (DD2) parasites, aqueous solubilities, mammalian cytotoxicities in CHO cells and SARs.

In conclusion, this study has shown that the 2,4-diaminoquinazoline scaffold possesses potent antiplasmodial activity by inhibiting the formation of HZ within the blood stage of the parasite life cycle. This was shown by the correlation between β HI and *Pf* IC₅₀ values for the entire library of compounds, excluding two outliers (**20**, **21**), and by the dose-dependent decrease in HZ and increase in free haem, similar to that of well-established HZ inhibiting antimalarial CQ in the case of **13**.

Furthermore, this investigation has shown that 2,4-diaminoquinazoline derivatives have several attributes making them suitable for potential future development: firstly, they can be made in a three-step, cost-effective synthetic procedure which has obvious commercial benefit; secondly, the scaffold has been shown not to be cross-resistant with CQ and that strong activities possessed are selective in killing *Plasmodium falciparum*; lastly, the scaffold possesses additional sites that are amenable to variation. These can therefore be exploited to improve aqueous solubility and *in vitro* activities.

The SAR analysis showed that 2,4-disubstitutions to the quinazoline scaffold in the forms of linear alkyl, secondary and less rigid amine groups, appeared to diminish or even abolish activity, whereas 2,4-disubstitutions such as bulkier aromatics and cyclic alkyl groups,

activated or inactivated π systems and combinations thereof, improved activity for the scaffold studied. C-4 monosubstitutions of bulkier aromatics and cyclic alkyl groups, activated or inactivated π systems and combinations thereof, however appeared to diminish or even abolish activity. As a result, sites of activity modulation for the scaffold have been identified on the pyrimidine ring as a result of SAR analysis (Figure 4.1).

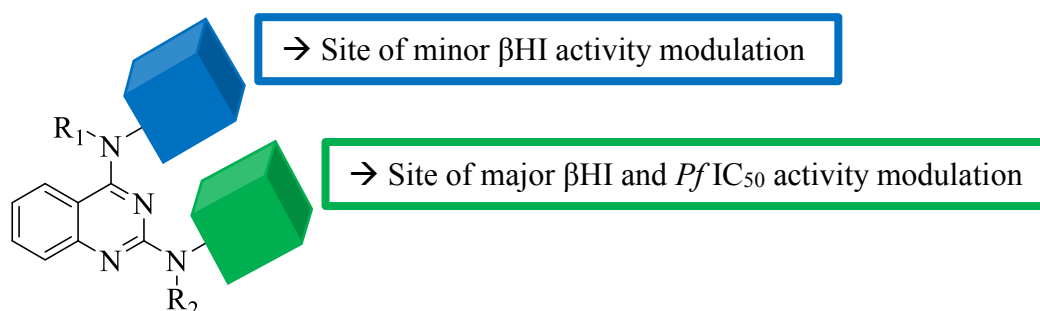


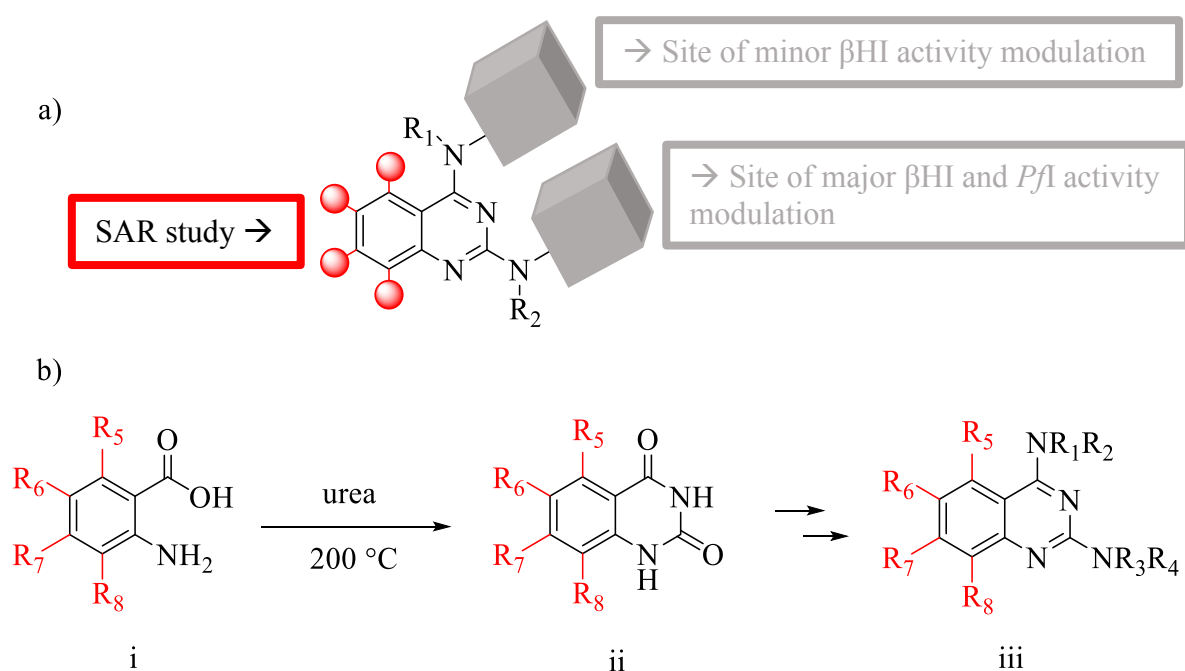
Figure 4.1: 2,4-diaminoquinazoline sites of modulation for β HI and Pf IC₅₀ on the pyrimidine ring

4.2 Future work

While this research study has uncovered the possible mode of 2,4-diaminoquinazoline antimalarial activity and has shown the scaffold's potential to be a serious candidate worth future optimisation, there remains important evidence that is lacking and improvements that need to be made.

Computer modelling simulations may be used to support the mode of inhibition discovered in this project and to determine the mechanism of HZ inhibition by 2,4-diaminoquinazolines. These simulations would aim to illustrate regions of the HZ inhibiting scaffold that interact with the fastest-growing faces of the HZ crystal by estimating favourable binding-energies associated with these interactions.

Furthermore, Scheme 4.1 illustrates regions that can be explored to improve aqueous solubility and *in vitro* activity against *P. falciparum* (a), as well as a proposed route for the synthesis of these derivatives (b).



Scheme 4.1: a) Proposed regions for structural change and b) the synthesis of derivatised 2,4-diaminoquinazoline

The proposed structural derivatisation adds one additional step to the general synthesis of the 2,4-diaminoquinazoline derivatives (iii), making use of cheap commercially available starting compounds, urea and 2-aminobenzoic acid derivatives (i). There are > 60 derivatives of 2-aminobenzoic acid commercially available from Sigma-Aldrich. Of these, there are numerous derivatives that may be used to explore hydrophilicity by introducing polar functional derivatives to the quinazoline framework such as alcohols, carboxylic acids, amides and amines. Some examples are 2-aminobenzene-1,4-dicarboxylic acid, 2,3-diaminobenzoic acid, 2-amino-3-formylbenzoic acid, 2-amino-3-hydroxybenzoic acid, methyl 2-amino-3-carboxybenzoate, 2-amino-3-methoxybenzoic acid and 4,6-bianthranilic acid.

In vitro activities may also be influenced by introducing the above functional groups, bearing in mind that certain criteria increase druglikeness. Derivatives that possess molecular masses less than 500 g/mol, no more than five H-bond donors, no more than ten H-bond acceptors and a partition coefficient (logP) less than 5, are said to increase druglikeness by generally showing better pharmacokinetics (adsorption, distribution, metabolism and excretion) in the human body.⁸⁸

With great scope for future work optimisation coupled with good results presented in this research investigation, 2,4-diaminoquinazoline is a promising scaffold for antimalarial drug discovery.

CHAPTER 5

Experimental Methods

Stefan J. Benjamin

M.Sc. Dissertation

5.1 Physiochemical methods

5.1.1 β -Haematin formation assay⁸⁵

The compound tested or the control (AQ) were made up in DMSO to a final concentration of 20 mM, after which 20 μ L of the required test compound or control was added to column 12. To every well in columns 1-11, 100 μ L of a solution containing water, NP-40 (305.5 μ M) and DMSO at a v/v ratio of 70/20/10 was added. Then, 140 μ L and 40 μ L of water and NP-40 (305.5 μ M) were added to column 12 respectively. A serial dilution of the test compound was then performed across the plate from column 12 through to 1, serially diluting 100 μ L increments and discarding the increment from column 2, to keep column 1 blank. 178 μ L of a haemin solution (25 mM) made in DMSO was added to 20 mL acetate buffer (1M, pH 4.7), then 100 μ L of this solution was added to every well on the plate, before the plate was then set to incubated for approximately 5 hours at 37 °C.

After incubation, 32 μ L of a pyridine solution (20% water, 20% acetone, 10% 2M HEPES & 50% pyridine) and 60 μ L acetone were added to every well on the plate. The plate was then measured at 405 nm (SpectraMax M5 plate reader) and analysed using a sigmoidal dose response curve on Prism Graph Pad v4.0 to extract the IC₅₀ via non-linear least squares fitting.

5.1.2 Antimalarial assay

The screening of the test compounds was conducted in triplicate to accurately determine the *in vitro* antiplasmodial activity against a chloroquine sensitive (CQS) strain of *P. falciparum* (NF54) and against the chloroquine resistant (CQR) strain of *P. falciparum* (DD2). Continuous *in vitro* cultures of asexual erythrocyte stages of *P. falciparum* were preserved using an improved technique of Trager and Jensen (Trager and Jensen, 2005), while a quantitative evaluation of antiplasmodial action *in vitro* was determined through the lactate dehydrogenase assay by means of a revised procedure as reported by Makler *et al.*^{89,90} A 20 mg/ml stock

solution of the test compounds was prepared in 100% DMSO and sonicated to improve solubility; however, compounds not completely dissolved were tested as a suspension. A full dose-response was completed for all samples to define the concentration preventing 50% of parasite growth (IC_{50} value), with sodium artesunate and CQ used as reference drugs in every test performed. The samples were tested at an initial conc. of 100 ng/mL, which was then serially diluted two-fold in complete medium to provide ten concentrations (lowest conc. 0.2 ng/mL). Note, the highest conc. of solvent that the parasites were exposed to had no quantifiable consequence on the parasite viability. The data were analysed and the IC_{50} values obtained by plotting a nonlinear dose response curve using Graph Pad Prism v4.0 software.

5.1.3 Cytotoxicity assay

The resulting method was used to test the quinazoline derivatives for *in vitro* cytotoxicity in Chinese Hamster Ovarian (CHO) cells, making use of 3-(4,5-dimethylthiazol-2-yl)-2,5-diphenyltetrazoliumbromide assay reported by Mosman *et al.* and Rubinstein *et al.*^{91,92}

A 2 mg/ml stock solution of the test samples (tested in triplicate) were prepared in 10% MeOH or 10% DMSO and were tested as a suspension if not properly dissolved, with emetine used as the reference drug in all experiments. The primary concentration of emetine (100 µg/ml), was serially diluted in complete medium (ten-fold) to provide six concentrations, the lowest being 0.001 µg/ml. Identical dilution procedures were used to test all compounds. The highest conc. of solvent to which the cells were exposed to had no quantifiable consequence on the cell viability. The 50% inhibitory concentration (IC_{50}) values were obtained from full dose-response plots, using a non-linear plot fitting analysis via GraphPad Prism v.4 software.

5.1.4 Turbidometric assay

The procedure was taken from Bevan *et al.* and Alsenz *et al.* and has been described briefly below.^{83,84}

The assay was done using a 96-well plate method which involved dissolving the test compound in a solvent (usually DMSO) that it was soluble in and then making a serial dilution across a ‘pre-dilution’ 96-well plate. Aliquots of this solution were added to pH 7.4 phosphate buffered saline (PBS) (aqueous solution) to obtain a further serial dilution from which successive concentrations were determined. The assay-plate was then left to incubate for 2 hours at ambient temperature. The estimated aqueous solubility of the test compound was determined from the concentration value above which the test compound precipitated from solution and hence caused turbidity. The measure of turbidity was determined using a UV-visible absorbance of the suspension at a wavelength of 620 nm. For this project the compounds aqueous solubilities were determined with reference to two controls, hydrocortisone (aq. soluble) and reserpine (aq. insoluble).

5.2 Synthesis

5.2.1 General

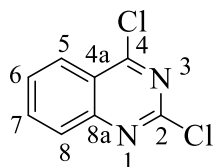
All chemicals and solvents were bought from Sigma-Aldrich or Fluka and unless otherwise specified, were used as received. Tetrahydrofuran (THF) and DCM were freshly distilled under nitrogen atmosphere, dried over sodium wire with benzophenone and phosphorus pentoxide respectively. Reactions were monitored using TLC pre-coated silica-gel 60 F₂₅₄ (0.2 mm) mounted on aluminium-backed plates, commercially available from Merck. Compounds were detected using a UV light with an absorption of 254 nm and stained for visible detection using either iodine filings, ninhydrin or anisaldehyde. Purification procedures involved the use of

flash column chromatography and single or double solvent recrystallisation techniques, using a Biotage Isolera Four EXP and analytical reagent grade solvents respectively.

Characterisation procedures comprised: the determination of the melting points of the compounds using a Reichert-Jung Thermovar hot stage microscope; IR spectra recorded on a Bruker Tensor 27 FT-IR spectrometer; NMR spectra recorded on Bruker Ultrashield 400 Plus (for ^1H , $^{13}\text{C}_{\text{stan}}$, HSQC and COSY). The NMR spec solvents used were deuterated acetone (d -(CD_3) $_2\text{CO}$), deuterated dimethyl sulfoxide (d -(CD_3) $_2\text{S=O}$) and deuterated chloroform (CDCl_3) with reference peaks occurring at 2.05, 2.50 and 7.26 ppm in the ^1H NMR and 29.84, 39.52 and 77.16 ppm in the ^{13}C NMR spectra respectively.⁹³ All chemical shifts are stated in ppm and coupling numbers in hertz (Hz); HPLC was conducted using a Agilent 1220 LC system V; HRMS (*ESI*) was conducted at the University of Stellenbosch, Central Analytical facilities (CAF) using a Waters Synapt G2 instrument.

5.2.2 Precursor synthesis

2,4-dichloroquinazoline (**2**)^{78,94}



Et₃N (1.4 mL, 10 mmol) was added to a suspension of benzoylene urea **1** (0.82 g, 5.1 mmol) in POCl₃ (9.2 mL, 51 mmol) under inert conditions and set to reflux at 106 °C for approximately 18 h. The reaction was monitored using TLC (MeOH/DCM, 1:99, R_f = 0.85) until the presence of the starting material diminished, indicating the completion of the reaction. After completion, the reaction mixture was diluted with DCM (80 mL) and poured over crushed ice, after which the slurry was neutralised using a saturated solution of Na₂CO₃ (approx. 30 mL) and allowed to stir for 1 h. The aqueous layer was extracted several times with DCM, after which all the DCM fractions were pooled, dried over sodium sulfate (Na₂SO₄) and the organic fraction concentrated under vacuum. The crude material was purified using flash column chromatography (MeOH/DCM 1:99, R_f = 0.85), followed by recrystallisation from boiling MeOH to obtain compound **2** as a white solid (0.87 g, 87%), m.p. 117-118 °C (Lit ⁷⁹: 118-120 °C). ¹H NMR (400 MHz, Acetone) δ_H 8.33 (1H, ddd, *J* 8.4, 1.4, 0.7 Hz, H-5), 8.16 (1H, td, *J* 8.4, 1.4 Hz, H-7), 8.01 (1H, ddd, *J* 8.4, 1.4, 0.7 Hz, H-8), 7.90 (1H, td, *J* 8.4, 1.4 Hz, H-6); ¹³C NMR (101 MHz, Acetone) δ_C 164.5 (C-q), 155.5 (C-q), 153.4 (C-q), 137.5 (C-H), 130.7 (C-H), 128.7 (C-H), 126.8 (C-H), 123.2 (C-q); HRMS (ESI) *m/z*: Found 198.9822. Calculated 198.9830, C₈H₅Cl₂N₂ [M+H]⁺; HPLC purity: 99%.

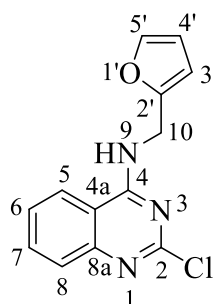
5.2.3 General Procedure for the synthesis of 2-chloro-quinazolin-4-amine intermediates (3-8)^{80,82,95,96,97}

The following is a general procedure for the synthesis of intermediates (3-8) was followed unless otherwise stated in the specific intermediate experimental details.

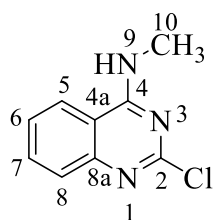
The 2-chloro-quinazolin-4-amine intermediates were synthesised on a 0.50-1.0 g scale by reacting the preferred amine derivatives (1.1-1.7 eq) with dichloroquinazoline (**2**, 1.0 eq) and Et₃N (1.5-2 eq) in THF (10-15 ml) for 3-12 h at 60 °C.

As previously mentioned in sub-section 5.2.1, TLC was used to monitor the reaction progress in combination with UV (254 nm) absorption and staining using iodine, ninhydrin or anisaldehyde.

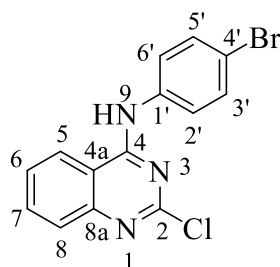
Upon reaction completion, the reaction vessel was allowed to cool to room temperature before the reaction contents were diluted in EtOAc and DCM (50:50), after which the contents were neutralised with a saturated solution of Na₂CO₃ and left to stir for several minutes. The aqueous and organic layers were separated and the former washed multiple times with DCM, after which the DCM fractions were pooled and concentrated under high vacuum. Chromatography of the residue followed by recrystallisation from boiling MeOH or DCM, produced solid products that were characterised and evaluated for analytical purity.

2-Chloro-*N*-(furan-2-ylmethyl) quinazolin-4-amine (3)

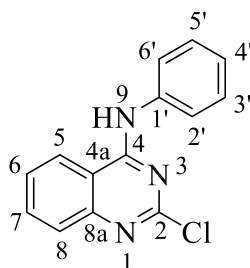
Furfurylamine (0.16 mL, 1.8 mmol, 1.1 eq) and Et₃N (0.36 mL, 2.5 mmol, 1.5 eq) were added to a suspension of **2** (0.34 g, 1.7 mmol) for the synthesis of **3**. Compound **3** was purified by recrystallisation from boiling MeOH and obtained as a white solid (0.33 g, 50%), m.p. 158–159 °C, *R_f* = 0.2 (EtOAc/hexane, 20:80). ¹H NMR (400 MHz, DMSO) δ_H 9.18 (1H, t, *J* 5.5 Hz, H-9), 8.30 (1H, ddd, *J* 8.4, 1.2, 0.5 Hz, H-5), 7.81 (1H, td, *J* 8.4, 1.2 Hz, H-7), 7.63 (1H, ddd, *J* 8.4, 1.2, 0.5 Hz, H-8), 7.60 (1H, dd, *J* 1.8, 0.9 Hz, H-5'), 7.54 (1H, td, *J* 8.4, 1.2 Hz, H-6), 6.42 (1H, dd, *J* 3.2, 1.8 Hz, H-4'), 6.37 (1H, dd, *J* 3.2, 0.9 Hz, H-3'), 4.74 (2H, d, *J* 5.5 Hz, H-10); ¹³C NMR (101 MHz, DMSO) δ_C 160.9 (C-q), 156.7 (C-q), 151.2 (C-q), 150.3 (C-q), 142.2 (C-5'), 133.7 (C-7), 126.6 (C-8), 126.2 (C-6), 123.1 (C-5), 113.4 (C-q), 110.5 (C-4'), 107.7 (C-3'), 37.3 (C-10); HRMS (ESI) *m/z*: Found 260.0538. Calculated 260.0591, C₁₃H₁₁ClN₃O [M+H]⁺; HPLC purity: 99%.

2-Chloro-*N*-methylquinazolin-4-amine (4)

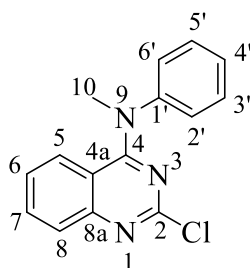
33% Methylamine in ethanol (0.25 mL, 1.8 mmol, 1.1 eq) and Et₃N (0.36 mL, 2.5 mmol, 1.5 eq) were added to a suspension of **2** (0.30 g, 1.5 mmol) for the synthesis of **4**. Compound **4** was purified by recrystallisation from boiling MeOH and obtained as a white solid (0.26 g, 89%), m.p. 207-208 °C, R_f = 0.1 (EtOAc/hexane, 10:90). ¹H NMR (400 MHz, DMSO) δ_H 8.74 (1H, q, *J* 4.3 Hz, H-9), 8.18 (1H, ddd, *J* 8.4, 1.3, 0.5 Hz, H-5), 7.77 (1H, td, *J* 8.4, 1.3 Hz, H-7), 7.61 (1H, ddd, *J* 8.4, 1.3, 0.5 Hz, H-8), 7.52 (1H, td, *J* 8.4, 1.3 Hz, H-6), 3.00 (3H, d, *J* 4.3 Hz, H-10); ¹³C NMR (101 MHz, DMSO) δ_C 161.5 (C-q), 157.0 (C-q), 150.0 (C-q), 133.4 (C-7), 126.6 (C-8), 126.0 (C-6), 122.8 (C-5), 113.6 (C-q), 27.9 (C-10); HRMS (ESI) *m/z*: Found 194.0477. Calculated 194.0485, C₉H₉ClN₃ [M+H]⁺; HPLC purity: 98%.

***N*-(4-Bromophenyl)-2-chloroquinazolin-4-amine (5)**

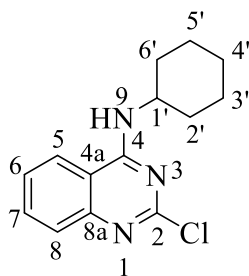
4-Bromoaniline (0.50 g, 2.9 mmol, 1.4 eq) and Et₃N (0.51 mL, 3.5 mmol, 1.7 eq) were added to a suspension of **2** (0.40 g, 2.0 mmol) for the synthesis of **5**. Compound **5** was purified by recrystallisation from boiling MeOH and obtained as a white solid (0.51 g, 75%), m.p. 167-168 °C, R_f = 0.3 (EtOAc/hexane, 30:70). ¹H NMR (400 MHz, DMSO) δ_H 10.21 (1H, s, H-9), 8.55 (1H, ddd, *J* 8.4, 1.2, 0.5 Hz, H-5), 7.89 (1H, td, *J* 8.4, 1.2 Hz, H-7), 7.82 – 7.76 (2H, m, H-3', 5'), 7.72 (1H, ddd, *J* 8.4, 1.2, 0.5 Hz, H-8), 7.65 (1H, td, *J* 8.4, 1.2 Hz, H-6), 7.63 – 7.59 (2H, m, H-2', 6'); ¹³C NMR (101 MHz, DMSO) δ_C 159.2 (C-q), 155.9 (C-q), 150.8 (C-q), 137.6 (C-q), 134.1 (C-7), 131.4 (C-2', 6'), 126.9 (C-8), 126.6 (C-6), 124.6 (C-3', 5'), 123.4 (C-5), 116.5 (C-q), 113.7 (C-q); HRMS (ESI) *m/z*: Found 333.9713. Calculated 333.9747, C₁₄H₁₀BrClN₃ [M+H]⁺; HPLC purity: 99%.

2-Chloro-*N*-phenylquinazolin-4-amine (6)

Aniline (0.26 mL, 2.8 mmol, 1.1 eq) and Et₃N (0.53 mL, 3.8 mmol, 1.5 eq) were added to a suspension of **2** (0.50 g, 2.5 mmol) for the synthesis of **6**. Compound **6** was purified by recrystallisation from boiling DCM and obtained as a white solid (0.57 g, 89%), m.p. 187-188 °C, *R*_f = 0.3 (EtOAc/hexane, 30:70). ¹H NMR (400 MHz, DMSO) δ_H 10.16 (1H, s, H-9), 8.57 (1H, ddd, *J* 8.4, 1.2, 0.5 Hz, H-5), 7.87 (1H, td, *J* 8.4, 1.2 Hz, H-7), 7.82 – 7.75 (2H, m, H-2', 6'), 7.71 (1H, ddd, *J* 8.4, 1.2, 0.5 Hz, H-8), 7.64 (1H, td, *J* 8.4, 1.2 Hz, H-6), 7.48 – 7.39 (2H, m, H-3', 5'), 7.22 – 7.18 (1H, m, H-4'); ¹³C NMR (101 MHz, DMSO) δ_C 159.4 (C-q), 156.2 (C-q), 150.8 (C-q), 138.2 (C-q), 134.0 (C-7), 128.6 (C-3', 5'), 126.8 (C-8), 126.5 (C-6), 124.7 (C-4'), 123.4 (C-5), 122.9 (C-2', 6'), 113.7 (C-q); HRMS (ESI) *m/z*: Found 256.0633. Calculated 256.0642, C₁₄H₁₁ClN₃ [M+H]⁺; HPLC purity: 100%.

2-Chloro-*N*-methyl-*N*-phenylquinazolin-4-amine (7)

N-methylaniline (0.30 mL, 2.8 mmol, 1.1 eq) and Et₃N (0.53 mL, 3.8 mmol, 1.5 eq) were added to a suspension of **2** (0.50 g, 2.5 mmol) for the synthesis of **7**. Compound **7** was purified by recrystallisation from boiling MeOH and obtained as a white solid (0.46 g, 66%), m.p. 189-190 °C, *R*_f = 0.7 (EtOAc/hexane, 30:70). ¹H NMR (400 MHz, DMSO) δ_H 7.73 – 7.60 (2H, m, H-5, 7), 7.51 – 7.47 (2H, m, H-2', 6'), 7.44 – 7.38 (1H, m, H-4'), 7.38 – 7.34 (2H, m, H-3', 5'), 7.08 (1H, ddd, *J* 8.4, 1.2, 0.5 Hz, H-8), 6.86 (1H, td, *J* 8.4, 1.2 Hz, H-6), 3.58 (3H, s, H-10); ¹³C NMR (101 MHz, DMSO) δ_C 162.0 (C-q), 155.3 (C-q), 152.3 (C-q), 146.4 (C-q), 132.6 (C-7), 129.8 (C-3', 5'), 127.1 (C-8), 126.9 (C-6), 125.8 (C-2', 6'), 125.6 (C-5), 124.7 (C-4'), 114.2 (C-q), 42.0 (C-10); HRMS (ESI) *m/z*: Found 270.0798. Calculated 270.0798, C₁₅H₁₃ClN₃ [M+H]⁺; HPLC purity: 99%.

2-Chloro-*N*-cyclohexylquinazolin-4-amine (8)

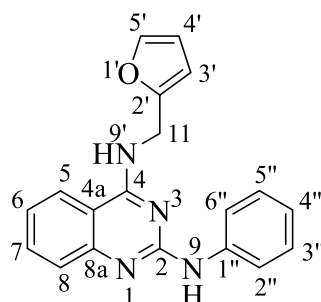
Cyclohexylamine (0.31 mL, 2.8 mmol, 1.1 eq) and Et₃N (0.53 mL, 3.8 mmol, 1.5 eq) were added to a suspension of **2** (0.50 g, 2.5 mmol) for the synthesis of **8**. Compound **8** was purified by recrystallisation from boiling MeOH and obtained as a white solid (0.63 g, 96%), m.p. 154–155 °C, *R*_f = 0.4 (EtOAc/hexane, 30:70). ¹H NMR (400 MHz, DMSO) δ_H 8.33 (1H, ddd, *J* 8.4, 1.3, 0.4 Hz, H-5), 8.30 (1H, d, *J* 7.8, Hz, H-9), 7.75 (1H, td, *J* 8.4, 1.3 Hz, H-7), 7.58 (1H, ddd, *J* 8.4, 1.3, 0.4 Hz, H-8), 7.49 (1H, td, *J* 8.4, 1.3 Hz, H-6), 4.16 – 4.04 (1H, m, H-1'), 1.99 – 1.03 (8H, m, H-2', 3', 5', 6'), 1.68 – 1.57 (1H, m, H-4'), 1.23 – 1.03 (1H, m, H-4'); ¹³C NMR (101 MHz, DMSO) δ_C 160.1 (C-q), 157.0 (C-q), 150.3 (C-q), 133.4 (C-7), 126.5 (C-8), 125.7 (C-6), 123.3 (C-5), 113.4 (C-q), 49.7 (C-q), 31.7 (CH₂ × 2), 25.2 (CH₂), 24.8 (CH₂ × 2); HRMS (ESI) *m/z*: Found 262.1102. Calculated 262.1111, C₁₄H₁₇ClN₃ [M+H]⁺; HPLC purity: 99%.

5.2.4 General Procedure for the synthesis of 2,4-diaminoquinazoline final derivatives (9-22)^{80,82,96,98}

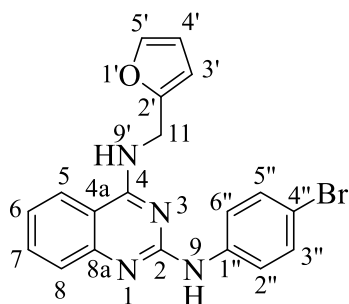
The following is a general procedure for the synthesis of the final compounds (9-22) and was followed unless otherwise stated in the specific experimental details.

The quinazoline-2,4-diamine final compounds (9-22) were synthesised on a 0.05 – 0.30 g scale by reacting the required 2-chloro-quinazolin-4-amine intermediate (1 eq) with the desired amine compound (1 - 2 eq) in a sealed tube overnight at a temperature of 150 °C in isopropanol (2-5 mL). TLC was used to monitor the reactions in combination with UV (254 nm) absorption and staining using iodine, ninhydrin or anisaldehyde.

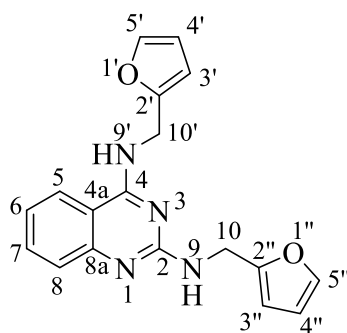
Upon reaction completion, the reaction contents were allowed to cool to ambient temperature before being diluted with EtOAc, after which they were neutralised with a solution of NaOH (1 M, 3-4 ml), which was allowed to stir for several minutes. The aqueous and organic layers were separated and the former washed multiple times with EtOAc, after which the EtOAc fractions were pooled and concentrated under high vacuum. Chromatography of the residue, followed by recrystallization from boiling MeOH or DCM, produced solid products that were characterised and evaluated for their analytical purity.

***N*⁴-(Furan-2-ylmethyl)-*N*²-phenylquinazoline-2,4-diamine (**9**)**

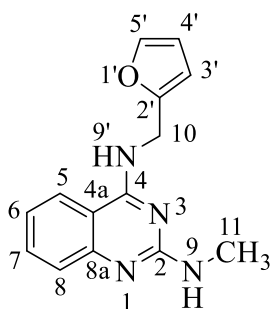
Phenylamine (0.11 mL, 1.2 mmol, 1.2 eq) was reacted with compound **3** (0.26 g, 1.0 mmol) for the synthesis of **9**. Compound **9** was purified by recrystallisation from boiling MeOH and obtained as a white solid (0.11 g, 36%) m.p. 103-104 °C, R_f = 0.4 (EtOAc/hexane, 30:70). ¹H NMR (400 MHz, DMSO) δ_H 9.10 (1H, s, H-9), 8.64 (1H, t, J 5.6 Hz, H-9'), 8.12 (1H, dd, J 8.4, 1.0 Hz, H-5), 7.86 (2H, dd, J 8.6, 1.0 Hz, H-2'', 6''), 7.62 (1H, td, J 8.4, 1.0 Hz, H-7), 7.59 (1H, dd, J 1.8, 0.8 Hz, H-5'), 7.43 (1H, dd, J 8.4, 1.0 Hz, H-8), 7.29 – 7.23 (2H, m, H-3'', 5''), 7.19 (1H, td, J 8.4, 1.0 Hz, H-6), 6.95 – 6.86 (1H, m, H-4''), 6.40 (1H, dd, J 3.2, 1.8 Hz, H-4'), 6.36 (1H, dd, J 3.2, 0.8 Hz, H-3'), 4.78 (2H, d, J 5.6 Hz, H-11); ¹³C NMR (101 MHz, DMSO) δ_C 159.8 (C-q), 156.4 (C-q), 152.3 (C-q), 150.4 (C-q), 141.9 (C-5'), 141.0 (C-q), 132.8 (C-7), 128.2 (C-2'', 6''), 124.8 (C-8), 122.8 (C-5), 121.6 (C-6), 120.8 (C-4''), 118.9 (C-3'', 5''), 111.5 (C-q), 110.4 (C-4'), 107.1 (C-3'), 37.2 (C-11); HRMS (ESI) m/z : Found 317.1393. Calculated 317.1402, C₁₉H₁₇N₄O [M+H]⁺; HPLC purity: 97%.

***N*²-(4-Bromophenyl)-*N*⁴-(furan-2-ylmethyl)quinazoline-2,4-diamine (**10**)**

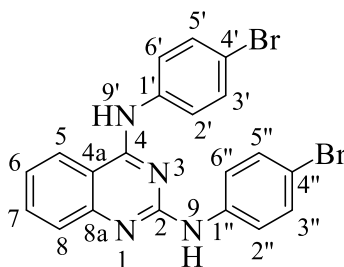
4-Bromoaniline (0.25 g, 1.4 mmol, 1.4 eq) was reacted with compound **3** (0.26 g, 1.0 mmol) for the synthesis of **10**. Compound **10** was purified by recrystallisation from boiling MeOH and obtained as a pale-brown solid (0.30 g, 78%) m.p. 161-162 °C, *R*_f=0.7 (EtOAc/hexane, 80:20). ¹H NMR (400 MHz, DMSO) δ_H 9.20 (1H, s, H-9), 8.58 (1H, t, *J* 5.6 Hz, H-9'), 8.12 (1H, dd, *J* 8.4, 1.2 Hz, H-5), 7.91 – 7.85 (2H, m, H-3'', 5''), 7.61 (1H, td, *J* 8.4, 1.2 Hz, H-7), 7.59 (1H, dd, *J* 1.8, 0.8 Hz, H-5'), 7.43 (1H, dd, *J* 8.4, 1.2 Hz, H-8), 7.42 – 7.37 (2H, m, H-2'', 6''), 7.19 (1H, td, *J* 8.4, 1.2 Hz, H-6), 6.40 (1H, dd, *J* 3.2, 1.8 Hz, H-4'), 6.37 (1H, dd, *J* 3.2, 0.8 Hz, H-3'), 4.78 (2H, d, *J* 5.6 Hz, H-11); ¹³C NMR (101 MHz, DMSO) δ_C 159.9 (C-q), 156.5 (C-q), 152.3 (C-q), 151.1 (C-q), 141.9 (C-5'), 140.8 (C-q), 132.7 (C-7), 130.9 (C-2'', 6''), 125.4 (C-8), 122.8 (C-5), 121.7 (C-6), 120.4 (C-3'', 5''), 111.7 (C-q), 111.7 (C-q), 110.5 (C-4'), 107.0 (C-3'), 37.2 (C-11); HRMS (ESI) *m/z*: Found 395.0506. Calculated 395.0507, C₁₉H₁₆BrN₄O [M+H]⁺; HPLC purity: 99%.

***N*², *N*⁴-Bis(furan-2-ylmethyl)quinazoline-2,4-diamine (11)**

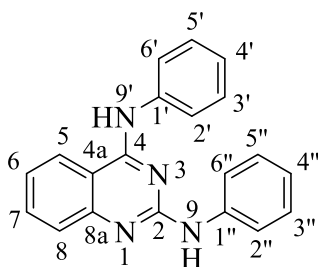
Furfurylamine (0.073 mL, 0.81 mmol, 1.1 eq) was reacted with compound **3** (0.19 g, 0.73 mmol) for the synthesis of **11**, which was purified by flash chromatography, *R_f* = 0.3 (MeOH/DCM, 10:90), and obtained as a pale-yellow solid (0.16 g, 66%), m.p. 116-117 °C. ¹H NMR (400 MHz, DMSO) δ_H 8.43 – 8.26 (1H, m, H-9/ 9'), 8.01 (1H, dd, *J* 8.4, 1.3 Hz, H-5), 7.55 (1H, d, *J* 1.8 Hz, H-5'/ 5''), 7.52 (1H, d, *J* 1.8 Hz, H-5'/ 5''), 7.48 (1H, td, *J* 8.4, 1.3 Hz, H-7), 7.27 (1H, dd, *J* 8.4, 1.3 Hz, H-8), 7.04 (1H, td, *J* 8.4, 8.4, 1.3 Hz, H-6), 7.00 – 6.89 (1H, m, H-9/ 9'), 6.38 (1H, dd, *J* 3.2, 1.8 Hz, H-4'/4''), 6.35 (1H, dd, *J* 3.2, 1.8 Hz, H-4'/4''), 6.32 (1H, dd, *J* 3.2, 0.8 Hz, H-3'/3''), 6.22 (1H, dd, *J* 3.2, 0.8 Hz, H-3'/3''), 4.70 (2H, d, *J* 5.5 Hz, H-10/10'), 4.54 (2H, d, *J* 5.5 Hz, H-10/10'); ¹³C NMR (101 MHz, DMSO) δ_C 159.8 (C-q), 158.8 (C-q), 154.1 (C-q), 152.6 (C-q), 151.7 (C-q), 141.8 (C-Ar), 141.4 (C-Ar), 132.3 (C-7), 124.7 (C-8), 122.7 (C-5), 120.3 (C-6), 111.1 (C-q), 110.4 (C-Ar), 110.3 (C-Ar), 107.1 (C-Ar), 106.2 (C-Ar), 37.6 (CH₂), 36.8 (CH₂); HRMS (ESI) *m/z*: Found 321.1342. Calculated 321.1352, C₁₈H₁₇N₄O₂ [M+H]⁺; HPLC purity: 97%.

***N*⁴-(Furan-2-ylmethyl)quinazoline-2,4-diamine (**12**)**

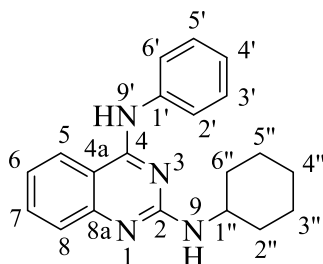
33% Methylamine in ethanol (0.079 mL, 0.62 mmol, 1.1 eq) was reacted with compound **3** (0.15 g, 0.58 mmol) for the synthesis of **12**, which was purified by flash chromatography, R_f = 0.3 (MeOH/DCM, 8:92), and obtained as a pale-yellow solid (0.076 g, 51%), m.p. 203-204 °C (Lit ⁸²: 205 °C). ¹H NMR (400 MHz, DMSO) δ_H 8.39 – 8.31 (1H, m, H-9'), 8.01 (1H, dd, J 7.9, 1.3 Hz, H-5), 7.56 (1H, dd, J 1.8, 0.8 Hz, H-5'), 7.49 (1H, td, J 7.9, 1.3 Hz, H-7), 7.28 (1H, dd, J 7.9, 1.3 Hz, H-8), 7.03 (1H, td, J 7.9, 1.3 Hz, H-6), 6.58 (1H, q, J 4.1 Hz, H-9), 6.39 (1H, dd, J 3.2, 1.8 Hz, H-4'), 6.33 (1H, dd, J 3.2, 0.8 Hz, H-3'), 4.69 (2H, d, J 5.4 Hz, H-10), 2.84 (3H, d, J 4.1 Hz, H-11); ¹³C NMR (101 MHz, DMSO-*d*₆) δ_C 159.5 (C-q), 159.2 (C-q), 152.6 (C-q), 151.1 (C-q), 141.8 (C-5'), 132.2 (C-7), 124.1 (C-8), 122.8 (C-5), 120.1 (C-6), 110.9 (C-q), 110.4 (C-4'), 107.1 (C-3'), 36.9 (C-10), 27.8 (C-12); HRMS (ESI) m/z : Found 255.1245. Calculated 255.1246, C₁₄H₁₅N₄O [M+H]⁺; HPLC purity: 95%.

***N*², *N*⁴-Bis(4-bromophenyl)quinazoline-2,4-diamine (13)**

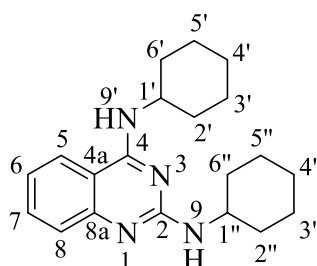
4-Bromoaniline (0.17 g, 1.0 mmol, 1.3 eq) was reacted with compound **5** (0.25 g, 0.75 mmol) for the synthesis of **13**, which was purified by recrystallisation from boiling MeOH and obtained as a light-brown solid (0.29 g, 82%), m.p. 183-184 °C, *R*_f = 0.6 (EtOAc/hexane, 50:50). ¹H NMR (400 MHz, DMSO) δ_H 9.69 (1H, s, H-9/9'), 9.31 (1H, s, H-9/9'), 8.38 (1H, dd, *J* 7.5, 1.2 Hz, H-5), 7.92 – 7.88 (4H, m, H-2', 2'', 6', 6''), 7.69 (1H, td, *J* 7.5, 1.2 Hz, H-7), 7.57 (2H, d, *J* 8.9 Hz, H-3', 5'/3'', 5''), 7.52 (1H, dd, *J* 7.5, 1.2 Hz, H-8), 7.41 (2H, d, *J* 8.9 Hz, H-3', 5'/3'', 5''), 7.31 (1H, td, *J* 7.5, 1.2 Hz, H-6); ¹³C NMR (101 MHz, DMSO) δ_C 158.2 (C-q), 155.9 (C-q), 151.4 (C-q), 140.5 (C-q), 138.8 (C-q), 133.1 (C-7), 131.2 (C-Ar ×2), 130.9 (C-Ar ×2), 125.7 (C-8), 124.4 (C-Ar ×2), 123.1 (C-5), 122.2 (C-6), 120.7 (C-Ar ×2), 115.2 (C-q), 112.1 (C-q), 111.8 (C-q); HRMS (ESI) *m/z*: Found 468.9663. Calculated 468.9663, C₂₀H₁₅Br₂N₄ [M+H]⁺; HPLC purity: 98%.

***N*², *N*⁴-Diphenylquinazoline-2,4-diamine (14)**

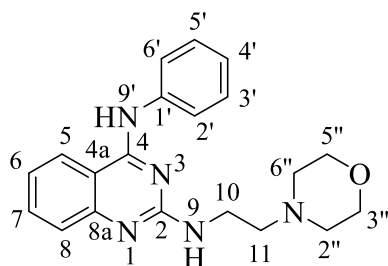
Aniline (0.064 mL, 0.70 mmol, 1.2 eq) was reacted with compound **6** (0.15 g, 0.59 mmol) for the synthesis of **14**, which was purified by recrystallisation from boiling MeOH and obtained as a white solid (0.092 g, 52%), m.p. 70-71 °C (Lit ⁹⁹: 75 °C), *R*_f = 0.4 (MeOH/DCM, 8:92). ¹H NMR (400 MHz, DMSO) δ_H 9.57 (1H, s, H-9/ 9'), 9.12 (1H, s, H-9/ 9'), 8.40 (1H, dd, *J* 8.2, 1.3 Hz, H-5), 7.94 (2H, d, *J* 7.7 Hz, H-2', 6'/ 2'', 6'') 7.89 (2H, d, *J* 7.7 Hz, H-2', 6'/ 2'', 6''), 7.67 (1H, td, *J* 8.2, 1.3 Hz, H-7), 7.51 (1H, dd, *J* 8.2, 1.3 Hz, H-8), 7.45 – 7.37 (2H, m, H-3', 5'/ 3'', 5''), 7.29 (1H, td, *J* 8.2, 1.3 Hz, H-6), 7.26 – 7.22 (2H, m, H-3', 5'/ 3'', 5''), 7.15 (1H, t, *J* 7.4 Hz, H-4'/ 4''), 6.91 (1H, t, *J* 7.4 Hz, H-4'/ 4''); ¹³C NMR (101 MHz, DMSO) δ_C 158.4 (C-q), 156.4 (C-q), 151.7 (C-q), 141.1 (C-q), 139.4 (C-q), 132.9 (C-7), 128.4 (C-Ar ×2), 128.2 (C-Ar ×2), 125.6 (C-8), 123.4 (C-Ar), 123.1 (C-5), 122.4 (C-Ar ×2), 121.8 (C-6), 120.8 (C-Ar), 118.9 (C-Ar ×2), 111.8 (C-q); HRMS (ESI) *m/z*: Found 313.1441. Calculated 313.1453 C₂₀H₁₇N₄ [M+H]⁺; HPLC purity: 99%.

***N*²-Cyclohexyl-*N*⁴-phenylquinazoline-2,4-diamine (**15**)**

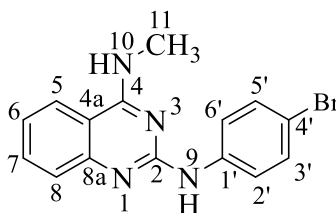
Cyclohexylamine (0.11 mL, 0.89 mmol, 1.2 eq) was reacted with compound **6** (0.20 g, 0.78 mmol) for the synthesis of **15**, which was purified by flash chromatography, $R_f = 0.3$ (EtOAc/Hexane, 30:70) as a white solid (0.18 g, 72%), m.p. 133-134 °C. ¹H NMR (400 MHz, DMSO) δ_H 9.35 (1H, s, H-9/ 9'), 8.28 (1H, dd, J 8.0, 1.2 Hz, H-5), 7.96 (2H, d, J 7.9 Hz, H-2', 6'), 7.54 (1H, td, J 8.0, 1.2 Hz, H-7), 7.35 (2H, t, J 7.9 Hz, H-3', 5'), 7.30 (1H, dd, J 8.0, 1.2 Hz, H-8), 7.15 – 7.03 (2H, m, H-4', 6), 6.57 (1H, s, H-9/ 9'), 3.79 (1H, s, H-1''), 1.94 – 1.29 (8H, m, H-2'', 3'', 5'', 6''), 1.61 – 1.58 (1H, m, H-4''), 1.21 – 1.17 (1H, m, H-4''); ¹³C NMR (101 MHz, DMSO) δ_C 158.1 (C-q), 158.0 (C-q), 152.4 (C-q), 139.8 (C-q), 132.5 (C-7), 128.2 (C-3', 5'), 124.6 (C-8), 123.0 (C-6), 122.8 (C-5), 121.5 (C-2', 6'), 120.1 (C-4'), 110.9 (C-q), 49.2 (C-q), 32.8 (CH₂ ×2), 25.4 (C-4''), 25.0 (CH₂ ×2); HRMS (ESI) m/z : Found 319.1917. Calculated 319.1923, C₂₀H₂₃N₄ [M+H]⁺; HPLC purity: 99%.

***N*², *N*⁴-Dicyclohexylquinazoline-2,4-diamine (16)**

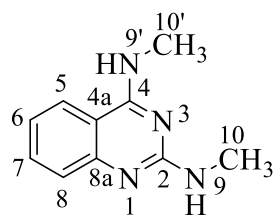
Cyclohexylamine (0.073 mL, 0.63 mmol, 1.1 eq) was reacted with compound **10** (0.15 g, 0.57 mmol) for the synthesis of **16**, which was purified by flash chromatography, $R_f = 0.3$ (EtOAc/Hexane, 30:70), and obtained as a white solid (0.13 g, 69%), m.p. 148-149 °C. ¹H NMR (400 MHz, DMSO) δ_H 8.02 (1H, dd, J 8.2, 1.1 Hz, H-5), 7.44 (1H, td, J 8.2, 1.1 Hz, H-7), 7.19 (1H, dd, J 8.2, 1.1 Hz, H-8), 6.98 (1H, td, J 8.2, 1.1 Hz, H-6), 6.50 – 6.09 (1H, m, H-9/9'), 4.19 – 3.99 (1H, m, H-1'/1''), 3.87 – 3.69 (1H, m, H-1'/1''), 2.03 – 0.98 (20H, m, 2'-6', 2''-6''); ¹³C NMR (101 MHz, DMSO) δ_C 159.0 (C-q), 158.5 (C-q), 151.6 (C-q), 132.0 (C-7), 124.0 (C-8), 122.9 (C-5), 119.4 (C-6), 110.8 (C-q), 49.2 (C-1'/1''), 32.8 (CH₂ × 2), 32.2 (CH₂ × 2), 25.5 (CH₂), 25.4 (CH₂), 25.2 (CH₂ × 2), 25.0 (CH₂ × 2); HRMS (ESI) m/z : Found 325.2388. Calculated 325.2392, C₂₀H₂₉N₄ [M+H]⁺; HPLC purity: 98%.

***N*²-(2-Morpholinoethyl)-*N*⁴-phenylquinazoline-2,4-diamine (**17**)**

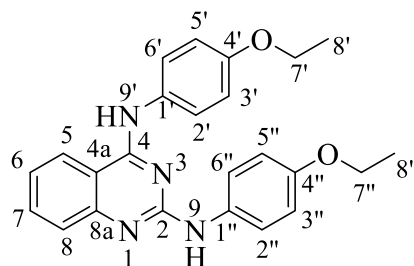
4-(2-Aminoethyl)morpholine (0.071 mL, 0.52 mmol, 1.1 eq) was reacted with compound **6** (0.12 g, 0.46 mmol) for the synthesis of **17**, which was purified by flash chromatography, $R_f = 0.25$ (MeOH/DCM, 10:90), and obtained as a pale-yellow solid (0.12 g, 71%), m.p. 145-146 °C. ¹H NMR (400 MHz, CDCl₃) δ_H 7.79 – 7.71 (3H, m, H-5, 2', 6'), 7.57 (1H, td, J 8.2, 1.3 Hz, H-7), 7.49 (1H, dd, J 8.2, 1.3 Hz, H-8), 7.42 – 7.36 (2H, m, H-3', 5'), 7.19 – 7.11 (2H, m, H-6, 4'), 6.32 – 5.61 (1H, m, H-9/9'), 3.73 – 3.67 (4H, m, H-2'', 5''/3'', 6''), 3.59 (2H, dd, J 10.7, 5.8 Hz, H-10), 3.45 – 3.12 (1H, m, H-9/9'), 2.58 (2H, t, J 5.8 Hz, H-11), 2.50 – 2.44 (4H, m, H-2'', 5''/3'', 6''); ¹³C NMR (101 MHz, CDCl₃) δ_C 158.7 (C-q), 158.3 (C-q), 151.2 (C-q), 138.7 (C-q), 133.4 (C-7), 129.0 (C-3', 5'), 125.1 (C-8), 124.3 (C-6/4'), 122.0 (C-6/4'), 121.8 (C-2', 6'), 121.0 (C-5), 111.0 (C-q), 67.1 (CH₂ × 2), 57.8 (C-11), 53.6 (CH₂ × 2), 38.1 (C-10); HRMS (ESI) m/z : Found 250.1979. Calculated 250.1981, C₂₀H₂₄N₅O [M+H]⁺; HPLC purity: 95%.

***N*²-(4-Bromophenyl)-*N*⁴-methylquinazoline-2,4-diamine (**18**)**

4-Bromoaniline (0.11 g, 0.64 mmol, 1.3 eq) was reacted with compound **4** (0.10 g, 0.51 mmol) for the synthesis of **18**, which was purified by recrystallisation from boiling MeOH and obtained as a white solid (0.11 g, 64%), m.p. 150-151 °C, R_f = 0.65 (MeOH/DCM, 8:92). ¹H NMR (400 MHz, DMSO) δ_H 9.22 (1H, s, H-9), 8.18 (1H, q, *J* 4.4 Hz, H-10), 8.03 (1H, dd, *J* 8.4, 1.2 Hz, H-5), 7.97 – 7.88 (2H, m, H-3', 5'), 7.59 (1H, td, *J* 8.3, 1.3 Hz, H-7), 7.48 – 7.38 (3H, m, H-2', 6', 8), 7.19 (1H, td, *J* 8.3, 1.3 Hz, H-6), 3.04 (3H, d, *J* 4.4 Hz, H-11); ¹³C NMR (101 MHz, DMSO) δ_C 160.6 (C-q), 156.5 (C-q), 150.2 (C-q), 140.8 (C-q), 132.5 (C-7), 130.9 (C-2', 6'), 125.0 (C-8), 122.6 (C-5), 121.7 (C-6), 120.5 (C-3', 5'), 111.8 (C-q), 27.8 (C-11); HRMS (ESI) *m/z*: Found 329.0392. Calculated 329.0402, C₁₅H₁₄BrN₄ [M+H]⁺; HPLC purity: 99%.

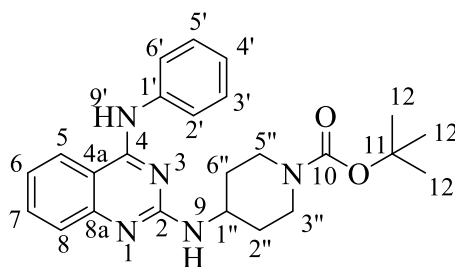
***N*², *N*⁴-Dimethylquinazoline-2,4-diamine (19)**

33% Methylamine in ethanol (0.11 mL, 0.85 mmol, 1.1 eq) was reacted with compound **4** (0.15 g, 0.78 mmol) for the synthesis of **19**, which was purified by flash chromatography, $R_f = 0.5$ (MeOH/DCM, 12:88), and obtained as a white solid (0.13 g, 92%), m.p. 124-125 °C. ¹H NMR (400 MHz, DMSO) δ_H 7.90 (1H, dd, J 8.1, 1.0 Hz, H-5), 7.74 – 7.66 (1H, m, H-9'), 7.46 (1H, td, J 8.1, 1.0 Hz, H-7), 7.27 (1H, dd, J 8.1, 1.0 Hz, H-8), 7.01 (1H, td, J 8.1, 1.0 Hz, H-6), 6.28 – 6.15 (1H, m, H-9), 2.97 (3H, d, J 3.8 Hz, H-10'), 2.88 (3H, d, J 3.8 Hz, H-10); ¹³C NMR (101 MHz, DMSO) δ_C 160.2 (C-q), 159.5 (C-q), 151.0 (C-q), 131.6 (C-7), 124.1 (C-8), 122.2 (C-5), 119.5 (C-6), 111.0 (C-q), 27.5 (C-CH₃), 27.1 (C-CH₃); HRMS (ESI) m/z : Found 189.1131. Calculated 189.1140, C₁₀H₁₃N₄ [M+H]⁺; HPLC purity: 99%.

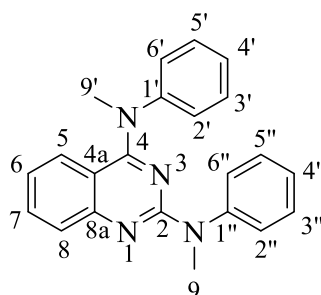
***N*², *N*⁴-Bis(4-ethoxyphenyl)quinazoline-2,4-diamine (20)**

4-Ethoxy aniline (0.13 mL, 1.0 mmol, 2 eq) was reacted with compound **2** (0.10 g, 0.50 mmol, 1 eq) for the synthesis of **20**. Compound **20** was purified by flash column chromatography, $R_f = 0.4$ (MeOH/DCM, 8:92), recrystallised from boiling methanol and obtained as a light brown solid (0.205 g, 64%), m.p. 69-70 °C. ^1H NMR (400 MHz, DMSO) δ_{H} 9.41 (1H, s, H-9/ 9'), 8.83 (1H, s, H-9/ 9'), 8.32 (1H, dd, J 8.3, 1.3 Hz, H-5), 7.72 – 7.69 (4H, m, H-Ar), 7.61 (1H, td, J 8.3, 1.3 Hz, H-7), 7.41 (1H, dd, J 8.3, 1.3 Hz, H-8), 7.21 (1H, td, J 8.3, 1.3 Hz, H-6), 6.99 – 6.89 (2H, m, H-Ar), 6.85 – 6.75 (2H, m, H-Ar), 4.05 (2H, q, J 7.0 Hz, H-7'/7''), 3.98 (2H, q, J 7.0 Hz, H-7'/7''), 1.35 (3H, t, J 7.0 Hz, H-8'/8''), 1.31 (3H, t, J 7.0 Hz, H-8'/8''); ^{13}C NMR (400 MHz, DMSO) δ_{C} 158.4 (C-q), 156.7 (C-q), 154.9 (C-q), 153.0 (C-q), 151.8 (C-q), 134.3 (C-q), 132.6 (C-7), 132.3 (C-q), 125.3 (C-8), 124.3 (C-Ar \times 2), 122.9 (C-5), 121.2 (C-6), 120.5 (C-Ar \times 2), 114.2 (C-Ar \times 2), 114.1 (C-Ar \times 2), 111.6 (C-q), 63.1 (C-CH₂), 63.0 (C-CH₂), 14.7 (C-CH₃), 14.7 (C-CH₃); HRMS (ESI) m/z : Found 401.1980. Calculated 401.1978, C₂₄H₂₅N₄O₂ [M+H]⁺; HPLC purity: 96%.

***Tert*-butyl 4-((4-(phenylamino)quinazolin-2-yl)amino)piperidine-1-carboxylate**
(21)



4-amino-1-boc-piperidine (0.23 g, 1.2 mmol, 1 eq) was reacted with compound **6** (0.30 g, 1.2 mmol) for the synthesis **21**, which was purified by flash chromatography, $R_f = 0.7$ (EtOAc/Hexane, 30:70), followed by recrystallisation from boiling methanol and obtained as a white solid (0.28 g, 85%), m.p. 106-107 °C. (400 MHz, DMSO) δ_H 9.34 (1H, s, H-9'), 8.28 (1H, dd, J 7.9, 1.1 Hz, H-5), 7.93 (2H, d, J 8.1 Hz, H-2', 6'), 7.55 (1H, td, J 7.9, 1.1 Hz, H-7), 7.36 (2H, t, J 8.1 Hz, H-3', 5'), 7.31 (1H, dd, J 7.9, 1.1 Hz, H-8), 7.13 (1H, td, J 7.9, 1.1 Hz, H-6), 7.08 (1H, t, J 8.1 Hz, H-4'), 6.78 – 6.56 (1H, m, H-9), 4.03 – 3.95 (3H, m, H-1'', H-CH₂), 2.92 – 2.86 (2H, m, H-CH₂), 1.94 – 1.80 (2H, m, H-CH₂), 1.41 (9H, s, H-12), 1.39 – 1.32 (2H, m, H-CH₂); ^{13}C NMR (101 MHz, DMSO) δ_C 158.1 (C-q), 153.9 (C-q), 152.5 (C-q), 139.7 (C-q), 132.5 (C-7), 128.3 (C-3', 5'), 124.9 (C-8), 123.0 (C-4'/5), 122.9 (C-4'/5), 121.6 (C-2', 6'), 120.3 (C-6), 78.5 (C-q), 47.5 (C-1''), 42.5 (CH₂ × 2), 31.7 (CH₂ × 2), 28.1 (C-12); HRMS (ESI) m/z : Found 420.2402. Calculated 240.2400, C₂₄H₃₀N₅O₂ [M+H]⁺; HPLC purity: 96%.

***N*²,*N*⁴-Dimethyl-*N*²,*N*⁴-diphenylquinazoline-2,4-diamine (22)**

N-Methylaniline (0.060 mL, 0.55 mmol, 1 eq) was reacted with compound **7** (0.15 g, 0.56 mmol) for the synthesis **22**, which was purified by flash chromatography, $R_f = 0.4$ (EtOAc/Hexane, 30:70), followed by recrystallisation from boiling methanol and obtained as a white solid (0.14 g, 73%), m.p. 112–113 °C. ¹H NMR (400 MHz, DMSO) δ_H 7.48 – 7.43 (2H, m, H-2', 6'), 7.42 – 7.35 (6H, m, H-3', 3'', 5, 5', 5'', 7), 7.30 – 7.24 (1H, m, H-4''), 7.21 – 7.14 (3H, m, H-2'', 4', 6''), 6.85 – 6.80 (1H, m, H-8), 6.74 – 6.68 (1H, m, H-6), 3.60 (3H, s, H-9/9'), 3.32 (3H, s, H-9/9'); ¹³C NMR (101 MHz, DMSO) δ_C 161.3 (C-q), 157.5 (C-q), 153.4 (C-q), 147.9 (C-q), 145.6 (C-q), 131.6 (C-5), 129.5 (C-3'', 5''), 127.9 (C-3', 5'), 125.9 (C-7), 125.8 (C-2', 6'), 125.7 (C-4''), 125.7 (C-8), 125.3 (C-2'', 6''), 124.1 (C-4'), 120.1 (C-6), 111.8 (C-q), 41.4 (C-9'), 37.5 (C-9); HRMS (ESI) m/z : Found 341.1768. Calculated 341.1766, C₂₂H₂₁N₄ [M+H]⁺; HPLC purity: 99%.



References

Stefan J. Benjamin

M.Sc. Dissertation

- 1 R. Nehgina, A. M. Neghina, I. Marincu and I. Lacobicciu, *Am. J. Med. Sci.*, 2010, **340**, 492–498.
- 2 B. H. Kean, K. E. Mott and J. Adair, *Rev. Infect. Dis.* 1982, **4**, 908–911.
- 3 P. B. Bloland, *Drug resistance in malaria*, Centers for Disease Control and Prevention, 2004, vol. 41, 45–53
- 4 The World Health Organisation, *World Malaria Report*, 2015.
- 5 D. Gollin and C. Zimmermann, *Sci. Expr.*, 2007, 1–6.
- 6 B. L. Rice, M. M. Acosta, M. A. Pacheco, J. M. Carlton, J. W. Barnwell and A. A. Escalante, *Mol. Phylogen. Evo.*, 2014, **78**, 172–184.
- 7 S. M. Rich and F. J. Ayala, *Adv. Parasitol.*, 2003, **54**, 255–280.
- 8 A. Kantele and T. S. Jokiranta, *Clin. Infect. Dis.*, 2011, **52**, 1356–1362.
- 9 J. Cox-Singh, J. Hiu, S. B. Lucas, P. C. Divis, M. Zulkarnaen, P. Chandran, K. T. Wong, P. Adem, S. R. Zaki, B. Singh and S. Krishna, *Malaria J.*, 2010, **9**, 10.
- 10 F. Cowman, D. Berryl and J. Baum, *J. Cell Biol.*, 2012, **198**, 961–971.
- 11 L. H. Bannister, J. M. Hopkins, R. E. Fowler, S. Krishna and G. H. Mitchell, *Parasitol. Today*, 2000, **16**, 427–433.
- 12 L. Florens, M. P. Washburn, J. D. Raine, R. M. Anthony, M. Grainger, J. D. Haynes, J. K. Moch, N. Muster, J. B. Sacci, D. L. Tabb, A. A. Witney, D. Wolters, Y. Wu, M. J. Gardner, A. A. Holder, R. E. Sinden, J. R. Yates and D. J. Carucci, *Nature*, 2002, **419**, 520–526.
- 13 M. Delves, D. Plouffe, C. Scheurer, S. Meister, S. Wittlin, E. A. Winzeler, R. E. Sinden and D. Leroy, *PLoS Med.*, 2012, **9**.
- 14 A. Saifi, M. A. Saifi, T. Beg, A. H. Harrath, F. Suleman, H. Altayalan and S. Al Quraishy, *Afr. J. Pharm. Pharmacol.*, 2013, **7**, 148–156.
- 15 P. Oliaro, *Pharmacol. Ther.*, 2001, **89**, 207–219.
- 16 G. Padmanaban, V. A. Nagaraj and P. N. Rangarajan, *Curr. Sci.*, 2007, **92**, 1545–1555.
- 17 A. Shandilya, S. Chacko, B. Jayaram and I. Ghosh, *Sci. Rep.*, 2013, **3**, 2513.
- 18 S. Percário, D. R. Moreira, B. A. Q. Gomes, M. E. S. Ferreira, A. C. M. Gonçalves, P. S. O. C. Laurindo, T. C. Vilhena, M. F. Dolabela and M. D. Green, *Int. J. Mol. Sci.*, 2012, **13**, 16346–16372.
- 19 M. Anthea, J. Hopkins, C. Laughlin, S. Johnson, M. Warner, D. Lahart and J. D. Wright, *Human Biology and Health*, Prentice Hall, New Jersey, USA, 1993.
- 20 T. J. Egan, J. M. Combrinck, J. Egan, G. R. Hearne, H. M. Marques, S. Ntenti, B. T. Sewell, P. J. Smith, D. Taylor, D. A. van Schalkwyk and J. C. Walden, *Biochem. J.*, 2002, **365**, 343–347.
- 21 P. J. Rosenthal, *Int. J. Parasitol.*, 2004, **34**, 1489–1499.
- 22 K. K. Eggleston, K. L. Duffin and D. E. Goldberg, *J. Biol. Chem.*, 1999, **274**, 32411–32417.
- 23 S. Q. Toh, A. Glanfield, G. N. Gobert and M. K. Jones, *Parasites & Vectors*, 2010, **3**, 108–118.
- 24 D. A. Elliott, M. T. McIntosh, H. D. Hosgood, S. Chen, G. Zhang, P. Baevova and K. A. Joiner, *PNAS*, 2008, **105**, 2463–8.
- 25 L. Kořený, M. Oborník and J. Lukeš, *PLoS Pathog.*, 2013, **9**.
- 26 A. Butykai, A. Orbán, V. Kocsis, D. Szaller, S. Bordács, E. Tátrai-Szekeres, L. F. Kiss, A. Bóta, B. G. Vértessy, T. Zelles and I. Kézsmárki, *Sci. Rep.*, 2013, **3**, 1431–1442.
- 27 J. M. Pisciotto and D. Sullivan, *Parasitol. Int.*, 2008, **57**, 89–96.
- 28 D. Jani, R. Nagarkatti, W. Beatty, R. Angel, C. Slebodnick, J. Andersen, S. Kumar and D. Rathore,

- PLoS Pathog.*, 2008, **4**.
- 29 M. Chugh, V. Sundararaman, S. Kumar, V. S. Reddy and W. A. Siddiqui, *PNAS*, 2013, **110**, 1–6.
 - 30 K. Nakatani, H. Ishikawa, S. Aono and Y. Mizutani, *Biochem. Biophys. Res. Commun.*, 2013, **439**, 477–480.
 - 31 K. Nakatani, H. Ishikawa, S. Aono and Y. Mizutani, *Sci. Rep.*, 2014, **4**, 6137.
 - 32 A. Soni, M. Goyal, K. Prakash, J. Bhardwaj, A. J. Siddiqui and S. K. Puri, *Gene*, 2015, **566**, 109–119.
 - 33 N. T. Huy, Y. Shima, A. Maeda, T. T. Men, K. Hirayama, A. Hirase, A. Miyazawa and K. Kamei, *PLoS ONE*, 2013, **8**.
 - 34 A. N. Hoang, K. K. Ncokazi, K. A. de Villiers, D. W. Wright and T. J. Egan, *Dalton Trans.*, 2010, **39**, 1235–44.
 - 35 T. J. Egan, *J. Inorg. Biochem.*, 2008, **102**, 1288–1299.
 - 36 A. Dorn, S. R. Vippagunta, H. Matile, A. Bubendorf, J. L. Vennerstrom and R. G. Ridley, *Biochem. Pharmacol.*, 1998, **55**, 737–747.
 - 37 R. D. Sandlin, K. Y. Fong, R. Stiebler, C. P. Gulka, J. E. Nesbitt, M. P. Oliveira, M. F. Oliveira and D. W. Wright, *Cryst. Growth & Design*, 2016, **16**, 2542–2551.
 - 38 K. Cohen, S. Yielding and K. Phifer, *Nature*, 1964, **202**, 805–806.
 - 39 P. B. Macomber and H. Sprinz, *Nature*, 1967, **214**, 937–939.
 - 40 P. M. O'Neill, B. K. Park, A. E. Shone, J. L. Maggs, P. Roberts, P. A. Stocks, G. A. Biagini, P. G. Bray, P. Gibbons, N. Berry, P. A. Winstanley, A. Mukhtar, R. Bonar-Law, S. Hindley, R. B. Bambal, C. B. Davis, M. Bates, T. K. Hart, S. L. Gresham, R. M. Lawrence, R. A. Brigandi, F. M. Gomez-Delas-Heras, D. V. Gargallo and S. A. Ward, *J. Med. Chem.*, 2009, **52**, 1408–1415.
 - 41 T. J. Egan and K. K. Ncokazi, *J. Inorg. Biochem.*, 2004, **98**, 144–152.
 - 42 T. J. Egan and K. K. Ncokazi, *J. Inorg. Biochem.*, 2005, **99**, 1532–1539.
 - 43 K. A. de Villiers, H. M. Marques and T. J. Egan, *J. Inorg. Biochem.*, 2008, **102**, 1660–1667.
 - 44 K. Y. Fong and D. W. Wright, *Future Med. Chem.*, 2013, **5**, 1437–1450.
 - 45 K. A. de Villiers, J. Gildenhuis and T. Le Roex, *ACS Chem. Biol.*, 2012, **7**, 666–671.
 - 46 A. P. Gorka, A. De Dios and P. D. Roepe, *J. Med. Chem.*, 2013, **56**, 5231–5246.
 - 47 J. N. Alumasa, A. P. Gorka, L. B. Casabianca, E. Comstock, A. C. De Dios and P. D. Roepe, *J. Inorg. Biochem.*, 2011, **105**, 467–475.
 - 48 I. Weissbuch and L. Leiserowitz, *Chem. Rev.*, 2008, **108**, 4899–4914.
 - 49 J. Gildenhuis, T. le Roex, T. J. Egan and K. A. de Villiers, *J. Am. Chem. Soc.*, 2013, **135**, 1037–1047.
 - 50 K. N. Olafson, M. A. Ketchum, J. D. Rimer and P. G. Vekilov, *PNAS*, 2015, **112**, 4946–4951.
 - 51 R. Thomsen and M. H. Christensen, *J. Med. Chem.*, 2006, **49**, 3315–3321.
 - 52 A. C. C. de Sousa, N. C. Diaz, A. M. T. de Souza, L. M. Cabral, H. C. Castro, M. G. Albuquerque and C. R. Rodrigues, *Med. Chem. Res.*, 2015, **24**, 3529–3536.
 - 53 R. M. Packard, *New Eng. J. Med.*, 2000, **78**, 397–399.
 - 54 <http://irmapperjavascriptwcfservice.cloudapp.net/>, Date Accessed: 2016-08-23.
 - 55 A. Ecker, A. M. Lehane, J. Clain and D. A. Fidock, *Trends Parasitol.*, 2013, **28**, 504–514.
 - 56 C. Setthaudom, P. Tan-Ariya, N. Sitthichot, R. Khositnithikul, N. Suwandittakul, S. Leelayoova and M. Mungthin, *Am. J. Trop. Med. & Hyg.*, 2011, **85**, 606–611.

- 57 S. Pulcini, H. M. Staines, A. H. Lee, S. H. Shafik, G. Bouyer, C. M. Moore, D. A. Daley, M. J. Hoke, L. M. Altenhofen, H. J. Painter, J. Mu, D. J. P. Ferguson, M. Llinás, R. E. Martin, D. A. Fidock, R. A. Cooper and S. Krishna, *Sci. Rep.*, 2015, **5**, 14552–14568.
- 58 R. A. Cooper, C. L. Hartwig and M. T. Ferdig, *Acta Trop.*, 2005, **94**, 170–180.
- 59 Z. A. Knight, B. Gonzalez, M. E. Feldman, E. R. Zunder, D. David, O. Williams, R. Loewith, D. Stokoe, A. Balla, T. Balla, W. A. Weiss, R. L. Williams and K. M. Shokat, *Cell*, 2010, **125**, 733–747.
- 60 A. Mbengue, S. Bhattacharjee, T. Pandharkar, H. Liu, G. Estiu, R. V. Stahelin, S. S. Rizk, D. L. Njimoh, Y. Ryan, K. Chotivanich, C. Nguon, M. Ghorbal, J. J. Lopez-Rubio, M. Pfrender, S. Emrich, N. Mohandas, A. M. Dondorp, O. Wiest and K. Haldar, *Nature*, 2015, **520**, 683–687.
- 61 M. V. Ignatushchenko, R. W. Winter, H. P. Bachinger, D. J. Hinrichs and M. K. Riscoe, *FEBS Lett.*, 1997, **409**, 67–73.
- 62 M. V. Ignatushchenko, R. W. Winter and M. Riscoe, *Am. J. Trop. Med. & Hyg.*, 2000, **62**, 77–81.
- 63 H. Fujioka, Y. Nishiyama, H. Furukawa and N. Kumada, *Antimicrob. Agents Chemother.*, 1989, **33**, 6–9.
- 64 J. K. Baird, *Antimicrob. Agents Chemother.*, 2011, **55**, 1827–1830.
- 65 J. X. Kelly, M. J. Smilkstein, R. Brun, S. Wittlin, R. A. Cooper, K. D. Lane, A. Janowsky, R. A. Johnson, R. A. Dodean, R. Winter, D. J. Hinrichs and M. K. Riscoe, *Nature*, 2009, **459**, 270–3.
- 66 Y. Kurosawa, A. Dorn, M. Kitsuji-Shirane, H. Shimada, T. Satoh, H. Matile, W. Hofheinz, R. Masciadri, M. Kansy and R. G. Ridley, *Antimicrob. Agents Chemother.*, 2000, **44**, 2638–2644.
- 67 M. A. Rush, M. L. Baniecki, R. Mazitschek, J. F. Cortese, R. Wiegand, J. Clardy and D. F. Wirth, *Antimicrob. Agents Chemother.*, 2009, **53**, 2564–2568.
- 68 F. J. Gamo, L. M. Sanz, J. Vidal, C. de Cozar, E. Alvarez, J. L. Lavandera, D. E. Vanderwall, D. V. S. Green, V. Kumar, S. Hasan, J. R. Brown, C. E. Peishoff, L. R. Cardon and J. F. Garcia-Bustos, *Nature*, 2010, **465**, 305–310.
- 69 W. A. Guiguemde, A. A. Shelat, D. Bouck, S. Duffy, G. J. Crowther, P. H. Davis, D. C. Smithson, M. Connelly, J. Clark, F. Zhu, M. B. Jiménez-Díaz, M. S. Martinez, E. B. Wilson, A. K. Tripathi, J. Gut, E. R. Sharlow, I. Bathurst, F. El Mazouni, J. W. Fowble, I. Forquer, P. L. McGinley, S. Castro, I. Angulo-Barturen, S. Ferrer, P. J. Rosenthal, J. L. DeRisi, D. J. Sullivan, J. S. Lazo, D. S. Roos, M. K. Riscoe, M. A. Phillips, P. K. Rathod, W. C. Van Voorhis, V. M. Avery and R. K. Guy, *Nature*, 2010, **465**, 311–315.
- 70 R. D. Sandlin, K. Y. Fong, K. J. Wicht, H. M. Carrell, T. J. Egan and D. W. Wright, *Int. J. Parasitol.*, 2014, **4**, 316–325.
- 71 M. Asif, *J. Med. Chem.*, 2014, **2014**, 1–27.
- 72 T. P. Selvam, P. V. Kumar and P. Vijayaraj, *Research in Pharmacy*, 2011, **1**, 1–21.
- 73 M. H. Nelson and C. R. Dolder, *Ann. Pharmacother.*, 2006, **40**, 261–269.
- 74 A. W. Hensbergen, V. R. Mills, I. Collins and A. M. Jones, *Tetrahedron Lett.*, 2015, **56**, 6478–6483.
- 75 D. Wang and F. Gao, *Chem. Cent. J.*, 2013, **7**, 95–110.
- 76 M. A. McGowan, J. L. Henderson and S. L. Buchwald, *Org. Lett.*, 2012, 4–7.
- 77 P. He, Y. B. Nie, J. Wu and M. W. Ding, *Org. Biomol. Chem.*, 2011, **9**, 1429–1436.
- 78 N. -C. Cho, J. -H. Cha, H. Kim, J. Kwak, D. Kim, S. -H. Seo, J. -S. Shin, T. Kim, K. -D. Park, J. Lee, K. -T. No, Y. -K. Kim, K. -T. Lee and A. -N. Pae, *Bioorg. Med. Chem.*, 2015, **23**, 7717–7727.
- 79 K. S. Bhat, *Int. J. Pharm. Pharm. Sci.*, 2014, **6**, 3–7.
- 80 J. Odingo, T. O'Malley, E. A. Kesicki, T. Alling, M. A. Bailey, J. Early, J. Ollinger, S. Dalai, N. Kumar, R. V. Singh, P. A. Hipkind, J. W. Cramer, T. Ioerger, J. Sacchettini, R. Vickers and T. Parish, *Bioorg. Med. Chem.*, 2014, **22**, 6965–6979.

-
- 81 K. Yoshida and M. Taguchi, *J. Chem. Soc., Perkin Trans. I*, 1992, 5–8.
- 82 K. S. van Horn, X. Zhu, T. Pandharkar, S. Yang, B. Vesely, M. Vanaerschot, J. C. Dujardin, S. Rijal, D. E. Kyle, M. Z. Wang, K. A. Werbovets and R. Manetsch, *J. Med. Chem.*, 2014, **57**, 5141–5156.
- 83 J. Alsenz and M. Kansy, *Adv. Drug Delivery Rev.*, 2007, **59**, 546–567.
- 84 C. D. Bevan and R. S. Lloyd, *Anal. Chem.*, 2000, **72**, 1781–1787.
- 85 K. K. Ncokazi and T. J. Egan, *Anal. Biochem.*, 2005, **338**, 306–319.
- 86 M. Delves, D. Plouffe, C. Scheurer, S. Meister, S. Wittlin, E. A. Winzeler, R. E. Sinden and D. Leroy, *PLoS Med.*, 2012, **9**.
- 87 J. M. Combrinck, T. E. Mabotha, K. K. Ncokazi, M. A. Ambele, D. Taylor, P. J. Smith, H. C. Hoppe and T. J. Egan, *ACS Chem. Biol.*, 2013, **8**, 133–137.
- 88 P. Leeson, *Nature*, 2012, **481**, 455–456.
- 89 W. Trager and J. B. Jensen, *J. Parasitol.*, 2005, **91**, 484–486.
- 90 M. T. Makler, J. M. Ries, J. A. Williams, J. E. Bancroft, R. C. Piper, B. L. Gibbins and D. J. Hinrichs, *Am. J. Trop. Med. & Hyg.*, 1993, **48**, 739–741.
- 91 T. Mosmann, *J. Immunol. Methods*, 1983, **65**, 55–63.
- 92 L. V. Rubinstein, R. H. Shoemaker, K. D. Paull, R. M. Simon, S. Tosini, P. Skehan, D. A. Scudiero, A. Monks and M. R. Boyd, *J. Natl. Cancer Inst.*, 1990, **82**, 1113–8.
- 93 H. E. Gottlieb, V. Kotlyar and A. Nudelman, *J. Org. Chem.*, 1997, **62**, 7512–7515.
- 94 M. H. P. Verheij, A. J. Thompson, J. E. van Muijlwijk-Koezen, S. C. R. Lummis, R. Leurs and I. J. P. De Esch, *J. Med. Chem.*, 2012, **55**, 8603–8614.
- 95 D. A. Thorat, M. R. Doddareddy, S. H. Seo, T. J. Hong, Y. S. Cho, J. S. Hahn and A. N. Pae, *Bioorg. Med. Chem. Lett.*, 2011, **21**, 1593–1597.
- 96 S. Molecolari and P. Vegetale, *J. Med. Chem.*, 2014, **57**, 8187–8192.
- 97 K. Kanuma, K. Omodera, M. Nishiguchi, T. Funakoshi, S. Chaki, Y. Nagase, I. Iida, J. I. Yamaguchi, G. Semple, T. A. Tran and Y. Sekiguchi, *Bioorg. Med. Chem.*, 2006, **14**, 3307–3319.
- 98 K. S. Van Horn, W. N. Burda, R. Fleeman, L. N. Shaw and R. Manetsch, *J. Med. Chem.*, 2014, **57**, 3075–3093.
- 99 N. A. Lange and F. E. Sheibley, *J. Am. Chem. Soc.*, 1931, **53**, 3867–75.



Supplementary Data

Stefan J. Benjamin

M.Sc. Dissertation

Appendix A

CheckCIF/PLATON report

Structure factors have been supplied for data block(s) c2c

THIS REPORT IS FOR GUIDANCE ONLY. IF USED AS PART OF A REVIEW PROCEDURE FOR PUBLICATION, IT SHOULD NOT REPLACE THE EXPERTISE OF AN EXPERIENCED CRYSTALLOGRAPHIC REFEREE.

No syntax errors found. CIF dictionary Interpreting this report

Data block: c2c

Bond precision:	C-C = 0.0035 Å	Wavelength=0.71073
Cell:	a=30.523(5) b=6.7975(12) c=19.261(3) alpha=90 beta=127.608(3) gamma=90	
Temperature:	173 K	
	Calculated	Reported
Volume	3165.9(9)	3165.8(9)
Space group	C 2/c	C 1 2/c 1
Hall group	-C 2yc	-C 2yc
Moiety formula	2(C14 H16 Cl N3), 2(C H4 O), H2 O	0.2(C14 H16 Cl N3), 0.1(H 2 O), 0.2(C H4 O)
Sum formula	C30 H42 Cl2 N6 O3	C3 H4.20 Cl0.20 N0.60
Mr	605.60	60.56
Dx, g cm ⁻³	1.271	1.271
Z	4	40
Mu (mm ⁻¹)	0.245	0.245
F000	1288.0	1288.0
F000'	1289.62	
h,k,lmax	40,9,25	40 ,9, 25
Nref	4073	4054
Tmin,Tmax	0.963,0.983	0.620,0.746
Tmin'	0.957	
Correction method= # Reported T Limits: Tmin=0.620 Tmax=0.746		
AbsCorr = MULTI-SCAN		

Data completeness= 0.995 Theta(max)= 28.667

R(reflections)= 0.0481(2938) wR2(reflections)= 0.1453(4054)

S = 1.039 Npar= 192

